CHARACTERIZATION AND MEASUREMENTS OF WIRE ANTENNAS IN MOCK MISSILE BULKHEADS

by

İsa Kocakarın

Submitted to Graduate School of Natural and Applied Sciences
in Partial Fulfillment of the Requirements
for the Degree of Master of Science in
Electrical and Electronics Engineering

Yeditepe University
2019

CHARACTERIZATION AND MEASUREMENTS OF WIRE ANTENNAS IN MOCK MISSILE BULKHEADS

APPROVED BY:

Prof. Dr. Duygun Erol Barkana ....
(Thesis Supervisor)
(Yeditepe University)

Prof. Dr. Korkut Yeğin ....
(Ege University)

Assist. Prof. Dr. Engin Maşazade ....
(Yeditepe University)

DATE OF APPROVAL: ..../..../2019

ACKNOWLEDGEMENTS

First of all, I would like to thank my family, especially my late mother for her endless moral support and encouragement to finish my thesis.

I am indebted to Professor Korkut Yeğin who has put up with me and provided great knowledge during my education.

I am truly grateful to Professor Duygun Erol Barkana who willingly accepted to helped me and expressed her support.

I express my gratitude towards İsmail Şişman who helped me with proofreading of this thesis and always supported me in tough times.

I am also grateful to Ozan İçin and Hilmi Kayhan Yılmaz who helped me with the formatting of this thesis, without their help I might not be able to finish it.

ABSTRACT

CHARACTERIZATION AND MEASUREMENTS OF WIRE ANTENNAS IN MOCK MISSILE BULKHEADS

Wire antennas are commonly used inside missiles for communication and sensing purposes. The amount of signal coupling into the missile bulkhead can be detected by short probes in the form of wire antennas. The behavior of wire antenna inside missile bulkhead differs completely compared to free-space counterparts. The characterization of such antennas is crucial in missile operation. It was shown in earlier works that the detection of very weak electromagnetic signal inside missile bulkhead was very difficult, and often, electromagnetic field solvers were unable to characterize the signal levels primarily due to subtractive cancellation in field computations. The goal of this study is to measure wire antenna performance within the bulkhead and compare the results with a well-known electromagnetic field solver. Various bulkhead geometries are manufactured and extensive measurements are carried out. The extent of corroboration between numerical and experimental results are shown in terms of input admittances.

ÖZET

TAKLİT FÜZE BAŞLARININ İÇİNDEKİ TEL ANTENLERİN NİTELENDİRİLMESİ VE ÖLÇÜLMESİ

Tel Antenler füzelerin içinde, haberleşme amacıyla ve yakınlık algılayıcı tetikleme mekanizması olarak sıklıkla kullanılmaktadır. Tel anten şeklindeki kısa problarla da füze bölmesinin içindeki sinyal kuplajının seviyesi algılanabilir. Füze bölmesi içindeki tel antenlerin davranışları, boş uzaydaki tel antenler ile karşılaştırıldığında tamamen farklıdır. Bu antenlerin nitelendirilmesi füze savunma sistemlerinde yüksek önem ihtiva eder. Daha önceki çalışmalardan da bilindiği üzere füzenin içerisindeki çok zayıf elektromanyetik sinyal değerinin bulunması çok zordur ve genellikle elektromanyetik alan çözücü programlar bu sinyal seviyesini, çıkartma hatasından dolayı karakterize etmekte zorlanmaktadır. Bu çalışma en başta füze bölmelerinin içindeki tel antenlerin, füze başlığı ve yan duvarlarda açıklık olması durumundaki giriş empedansının ve ışıma karakteristiklerinin çıkarılmasını hedefler. Aynı zamanda antenin eksen dışındaki durumları için de yapılmıştır. Füze-Anten yapısının üç boyutlu elektromanyetik benzetimleri yapılmış ve giriş empedansları ölçümlerle birlikte doğrulanmıştır.

TABLE OF CONTENTS

LIST OF FIGURES

LIST OF TABLES

LIST OF SYMBOLS/ABBREVIATIONS

c	Speed of light
d	Diameter of top aperture.
f	Frequency
f_{3cm}	Resonance frequency of 3 cm antenna
f_{5cm}	Resonance frequency of 5 cm antenna
$Y_{antenna}$	Admittance of antenna
Y_{short}	Admittance of shorted cable
Y_0	Admittance of 50-ohm matched line
Y_L	Admittance of load
$Z_{antenna}$	Impedance of antenna
Z_{short}	Impedance of shorted cable
$\Gamma_{antenna}$	Reflection coefficient of antenna
Γ_{short}	Reflection coefficient of shorted cable
λ	Wavelength of an electromagnetic wave
BOR	Body of revolution
CAD	Computer aided design
CEM	Computational electromagnetics
FEM	Finite element method
FEKO	Feldberechnung für Körper mit beliebiger Oberfläche
FDTD	Finite difference time domain
Hz	Hertz
MHz	Megahertz
MLFMM	Multi level fast multipole method
MoM	Method of moments
PEC	Perfect electric conductor
RF	Radio frequency
VNA	Vector network analyzer

1. INTRODUCTION

Electromagnetic penetration through small apertures on conductive surfaces has been studied by researchers for many years. The electrical size of aperture may become small at lower frequencies that the radiation out of the system or penetration from the aperture into the system can be minimal. The amount of coupled signal in to the aperture is relatively small which makes it harder to detect and there is no known analytical solution to solve this problem.

One way to solve this problem is to treat the cylindrical body as a scatterer and to calculate the total field in the body as a sum of incident and scattered field. If the aperture on the body is too small this approach can lead to very inaccurate results since incident fields and the scattered fields are very close to each other in magnitude. As an alternative there are other methods such as the short circuit current method and the equivalent current method. These alternate methods are considerably more accurate than scatterer method for coupling through the apertures but they are more prone to internal resonances of the structure. These two methods require more computational resources compared to the scatterer method [1-6]. Another way to approach this problem is to formulate the problem using reciprocity [7-11].

In this study, we carried out simulations of two different wire antennas in a scaled version of a mock missile which has been constructed as a body of revolution (BOR) model in the 3D electromagnetic simulator, FEKO [12]. FEKO uses method of moments (MoM) approach when solving electromagnetic problems. The antennas are placed on 3 different locations with 2 different bulkheads and 5 different apertures totaling to 70 different configurations. After the simulations, we measured input admittances of antennas in an anechoic chamber.

2. SUBTRACTIVE CANCELLATION AND ANTENNA IMPEDANCE CALIBRATION

2.1. SUBSTRACTIVE CANCELLATION

For many years researchers used Maxwell equations and their numerical simuations to calculate electromagnetic fields created or propagated in space. While these methods are relatively accurate for simple calculations such as calculating field values of an antenna in open space, they are limited in calculating relatively low electromagnetic field values. This is mainly due to subtractive cancellation.

Subtractive cancellation occurs when two nearly equal numbers substracted from each other [13]. When an electromagnetic field coupling out from a small aperture on a conductive enclosure is to be calculated, the field at the aperture are very small compared to excitation fields. Since the amount coupling in or out from the missile bulkhead is small and the scattered electromagnetic field is nearly equal to incident electromagnetic field, there is a difference between radiation patterns and resonnat frequencies of nthe structures. The scope of this thesis is to lay these difference out in a comperative study between numerical analysis results by using electromagnetic solvers using numerical simulation and measurement results.

2.2. ANTENNA IMPEDANCE CALIBRATION

The probe antennas are connected with a short coaxial cable for measurements. Calibration of the network analyzer can only be carried up to the end of short coaxial cable, also referred as pigtail. To get the actual antenna impedance the effect of pigtail must be removed by de-embedding of its effect from measurements. To achieve that, same length pigtail with short circuit on one end is made and measurements of this shorted pigtail are carried out first. Then probe antenna with pigtail measurements are carried out and the effect of pigtail are calibrated out using the following formulations:

$$\Gamma_{antenna} = \frac{Z_{antenna} - Z_0}{Z_{antenna} + Z_0} \tag{2.1}$$

$$\Gamma_{short} = \frac{Z_{short} - Z_o}{Z_{short} + Z_o} \tag{2.2}$$

$$Y_{antenna} = Y_o * \frac{\Gamma_{short} + \Gamma_{antenna}}{\Gamma_{short} - \Gamma_{antenna}} \tag{2.3}$$

where the impedance of a shorted pigtail, impedance of wire antenna, reflection coefficients of shorted coaxial cable, and reflected coefficient of wire antennas are denoted as Z_{short}, $Z_{antenna}$, Γ_{short}, and $\Gamma_{antenna}$, respectively. Also, the characteristic impedance and admittance of the transmission line are denoted as and Y_o, where Z_o is taken as 50 Ohm.

3. SIMULATIONS

Simulations have been carried by utilizing a commercially available software FEKO. FEKO is a comprehensive computational electromagnetics (CEM) software used widely in the telecommunications, automobile, aerospace and defence industries. FEKO has many different approaches to solving electromagnetic problems such as MoM, multilevel fast multipole method (MLFMM), and diffraction based solutions. In this thesis we used MoM solver of FEKO.

3.1. SIMULATION SETUP

Dimensions of the mock missile used in simulations is given in Figure 3.1. The top aperture can be changed between 5 different apertures values (diameter d=4mm, d=10mm, d=15 mm apertures, no aperture, open)

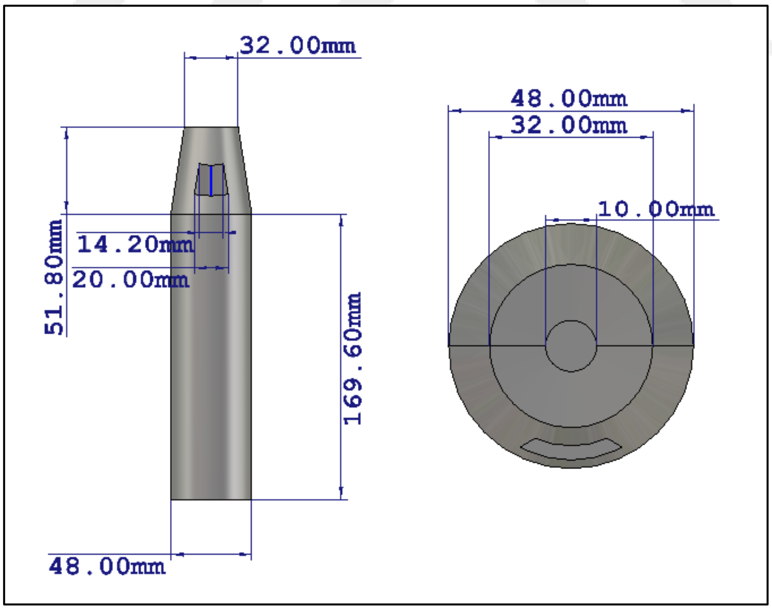

Figure 3.1. Dimensions of mock missile used in simulations

There are total of 70 configurations; 2 different wire antennas; 2 different bulkheads (one with a window one without), 5 different nose apertures (diameter d=4mm, d=10mm, d=15 mm apertures, no aperture, open), 3 different antenna positions (axial, +10 mm to side and

+15 mm to side) and an extra 1 set of antenna position for windowed bulkhead (-10 mm to window side);

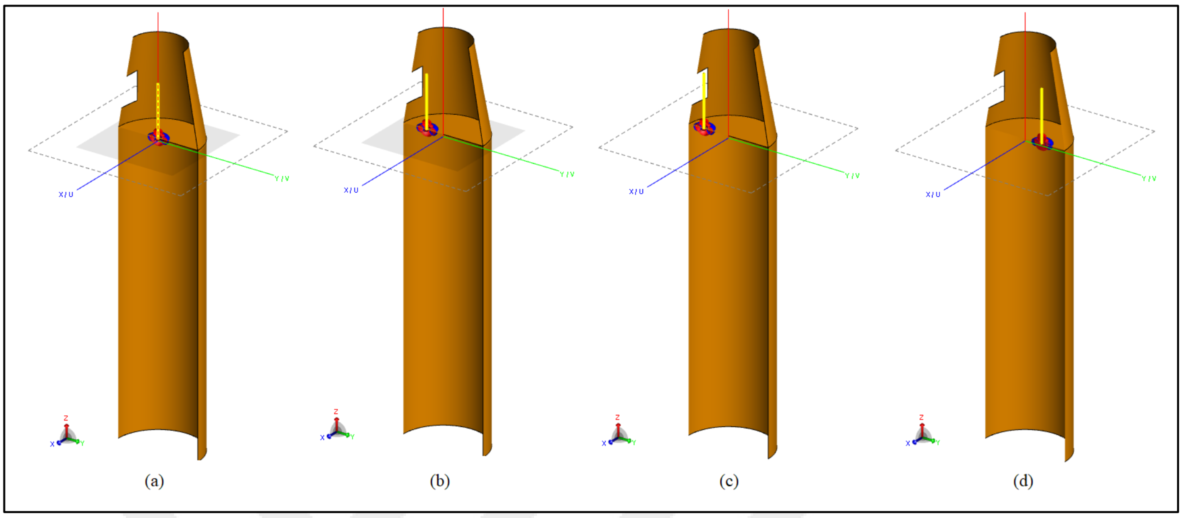

Figure 3.2. Positions of wire antenna. (a) Position 1, along z axis, (b) Position 2, 10 mm off-axis towards window, (c) Position 3 , 15 mm off-axis towards window, (d) Position 4, 10 mm off-axis away from window, only applicable to windowed bulkhead.

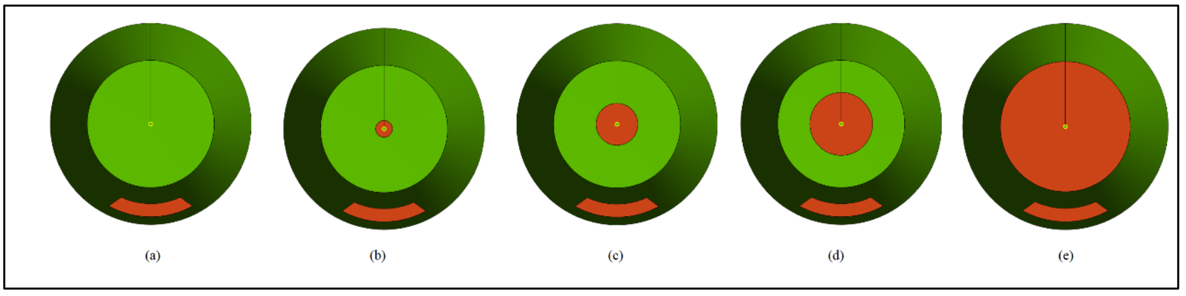

Figure 3.3. Aperture sizes on bulkhead top. (a) no aperture, (b) d=4 mm, (c) d=10 mm, (d) d=15 mm, (e) open

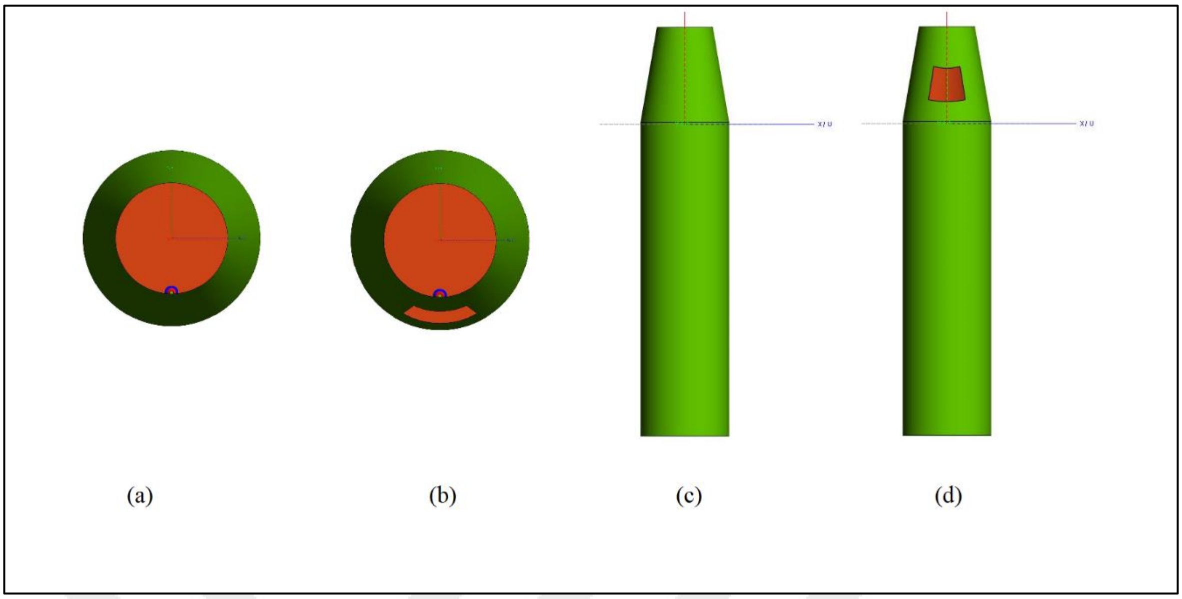

Figure 3.4. Bulkhead configurations. (a) Top view of windowless configuration, (b) Top view of windowed configuration, (c) Side view of windowless configuration, (d) Side view of windowed configuration

Wire antennas selected as 3 cm and 5 cm long as it should be able to fit inside the bulkhead which stands 51.25 mm long. From these lengths we can calculate the resonance frequencies using

$$\lambda = \frac{c}{f} \tag{3.1}$$

Since the monopoles are resonant at $\lambda/4$ for 5 cm long monopole we calculate the resonant frequency as

$$0.05m = \frac{\lambda_5}{4} \tag{3.2}$$

$$\lambda_{5cm} = 0.2m \tag{3.3}$$

$$f_{5cm} = \frac{c}{\lambda_{5cm}} = \frac{3 * 10^8}{0.2} = 1.5 * 10^9 \ Hz = 1.5 \ GHz \tag{3.4}$$

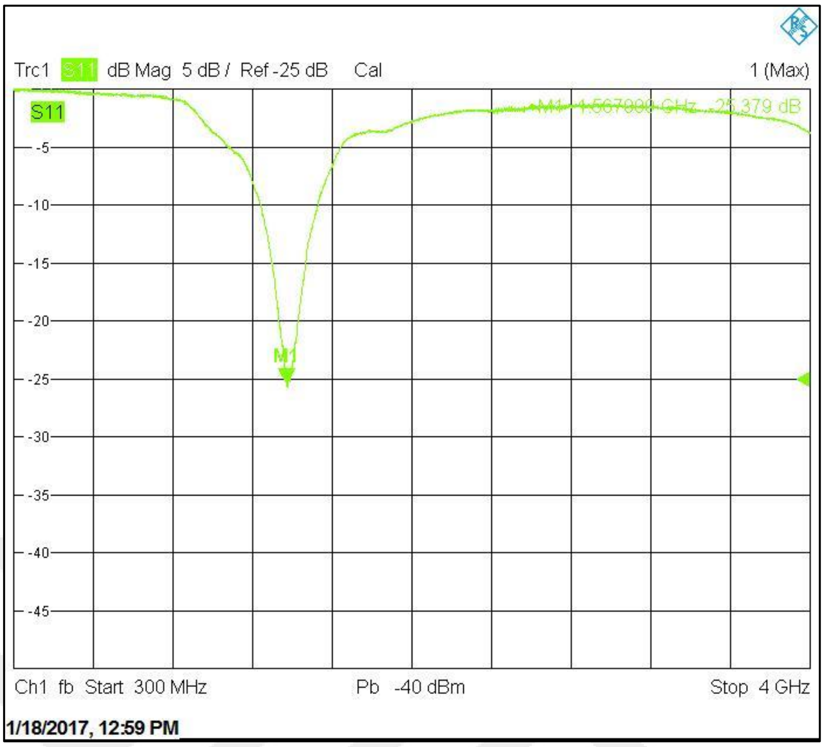

Figure 3.5. Measurement of S11 of 5 cm monopole antenna without a bulkhead

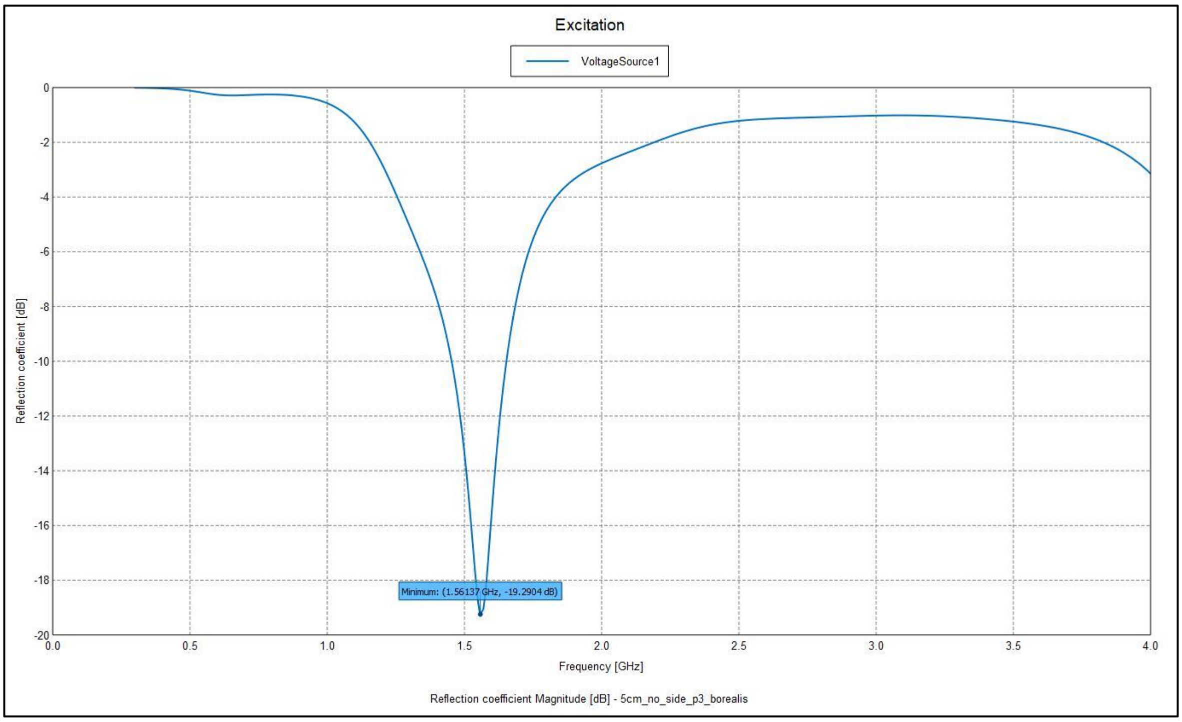

Figure 3.6. Simulation of S11 of 5 cm monopole antenna without a bulkhead

As can be seen in Figure 3.5 and Figure 3.6 simulation and measurement results are in agreement with each other, with only 6 MHz difference between simulation and the measurement.When we do the same calculations for the 3 cm long monopole, we get

$$f_{3cm} = \frac{c}{\lambda_{3cm}} = \frac{3 * 10^8}{\lambda_{3cm}} = \frac{3 * 10^8}{0.03 * 4} = 2.5 * 10^9\ Hz = 2.5\ GHz \qquad (3.5)$$

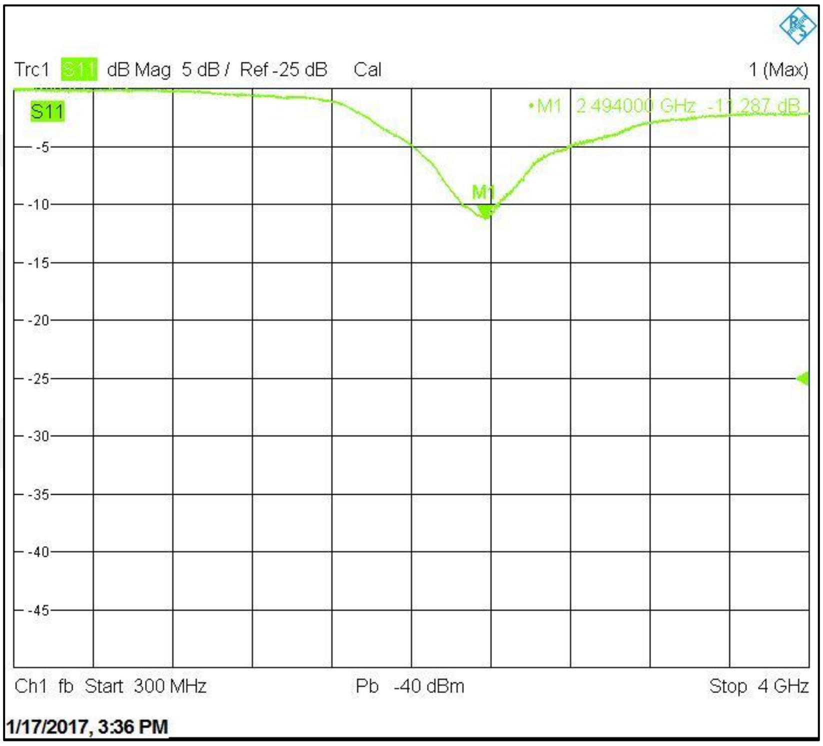

Figure 3.7. Measurement of S11 of 3 cm monopole antenna without a bulkhead

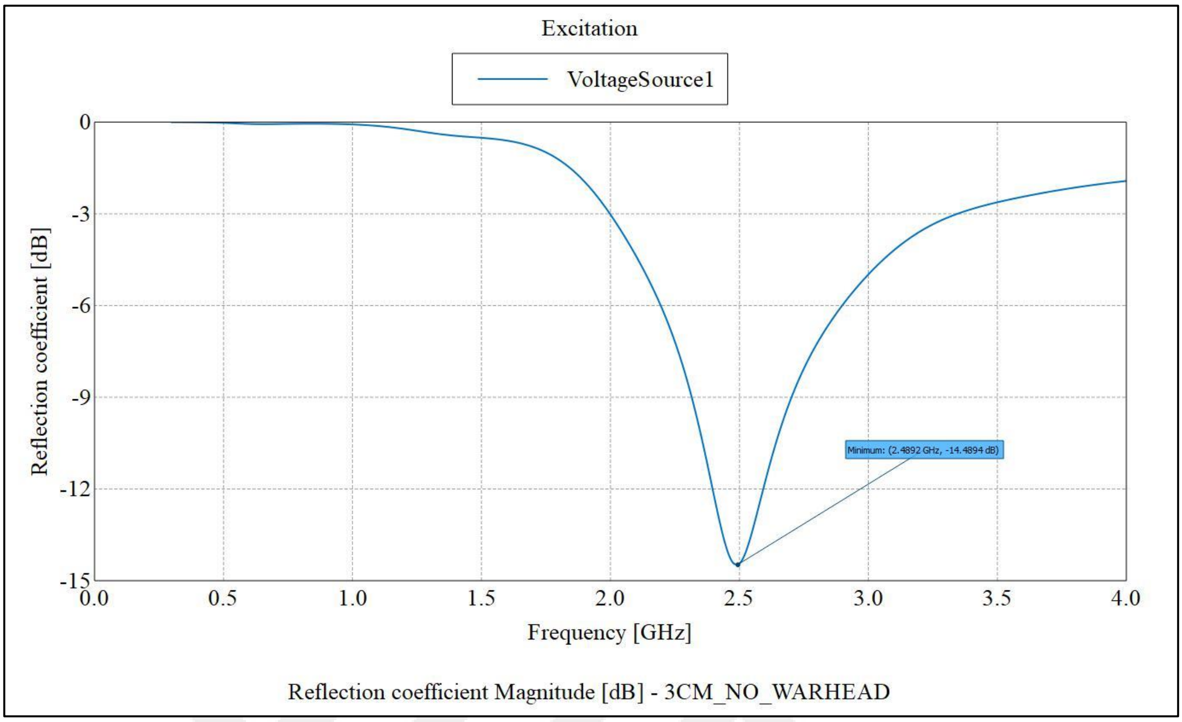

Figure 3.8. Simulation of S11 of 3 cm monopole antenna without bulkhead

From Figure 3.7 and Figure 3.8 we can observe that the S11 measurements of the 3 cm antenna in free space are in agreement with the calculations and simulations in with 22 MHz error.

These results hold true only when the antenna freely radiates into free space. Because we are studying wire antennas encapsulated by the bulkhead in its radiation zone, radiation characteristics of the antennas are affected by the bulkhead [5]. For 3cm antenna we can observe approximately 250 MHz frequency shift in the simulations from the calculated values in Figure 3.9 and Figure 3.10.

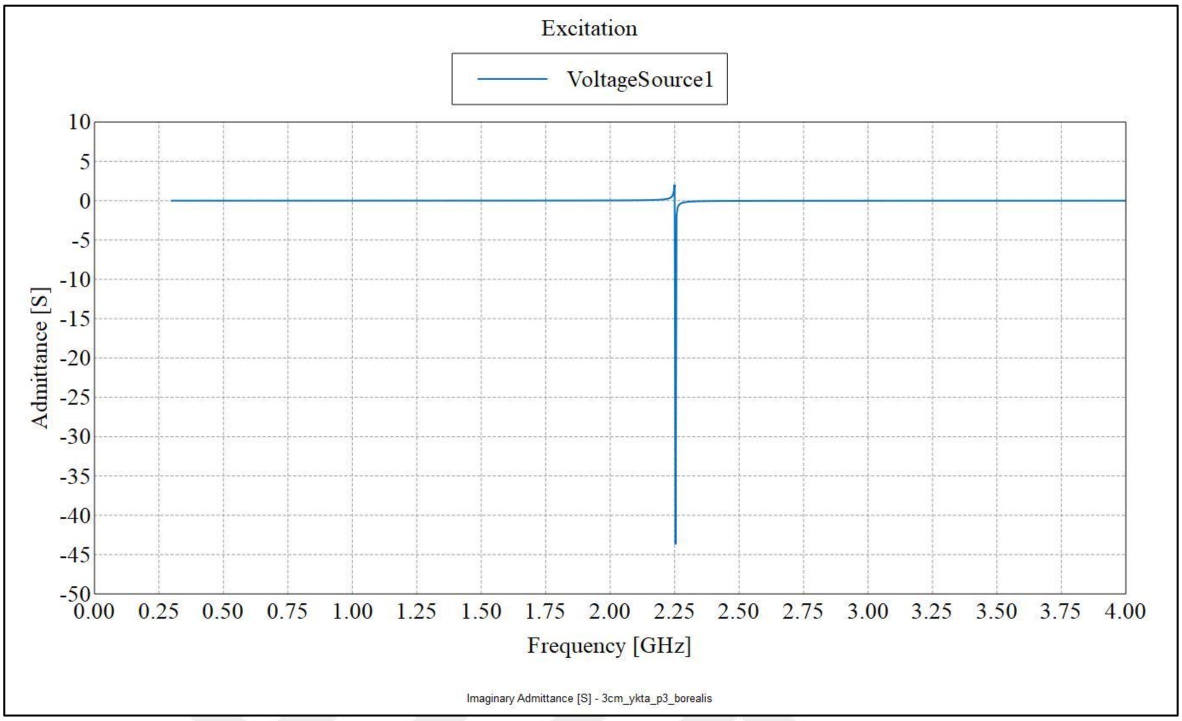

Figure 3.9. Imaginary admittance (Susceptance) plot for 15 mm off-axis, 3 cm long monopole, inside closed window, open top bulkhead.

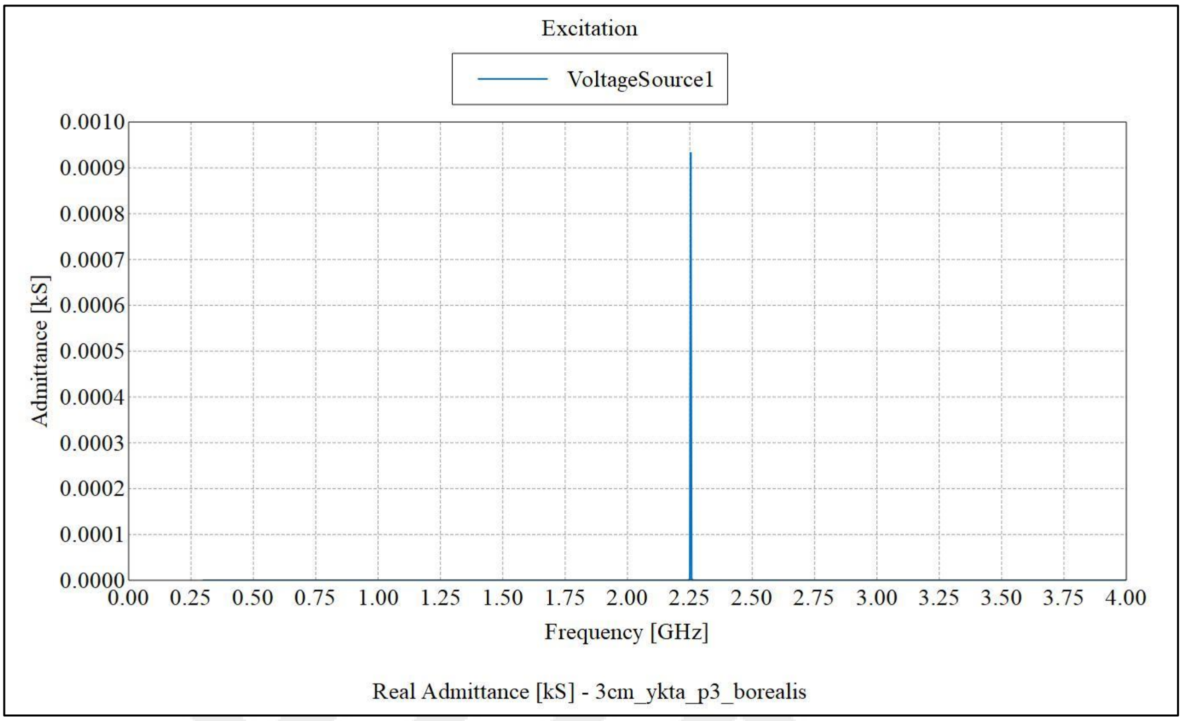

Figure 3.10. Real admittance (Conductance) plot for 15 mm off-axis, 3 cm long monopole, inside closed window, open top bulkhead.

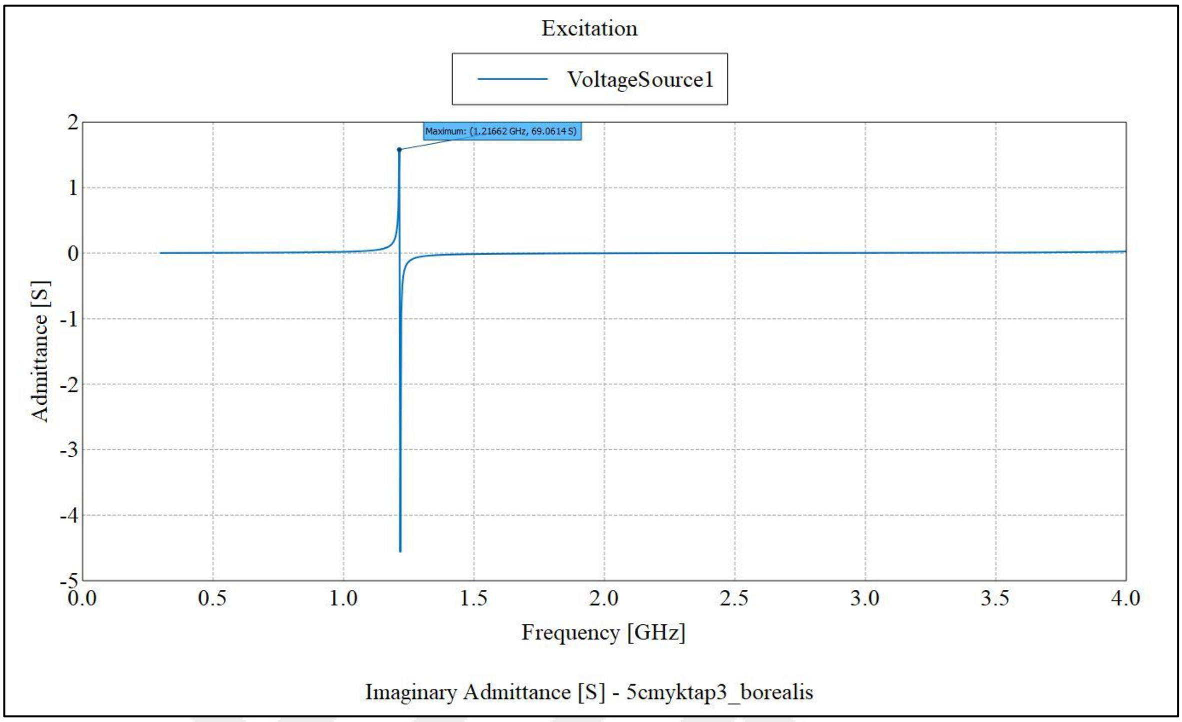

Figure 3.11. Imaginary admittance (Susceptance) plot for 15 mm off-axis, 5 cm long monopole, inside closed window, open top bulkhead.

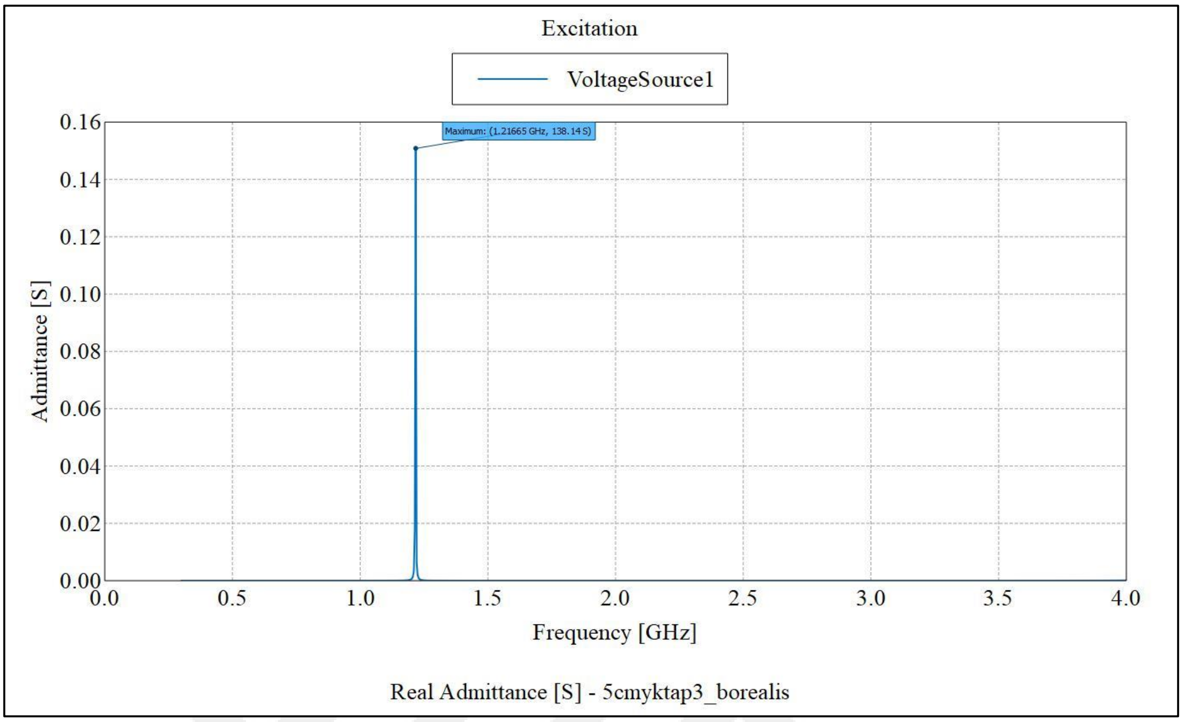

Figure 3.12.Real admittance (Conductance) plot for 15 mm off-axis, 5 cm long monopole, inside closed window, open top bulkhead

As in the case of 5 cm monopole antenna 283.3 MHz frequency shift is observed in simulations as in Figure 3.11 and Figure 3.12.

4. EXPERIMENTAL INVESTIGATION

The setup for measurements to analyze different situations of antenna placement and bulkhead apertures are explained in detail in this chapter. All measurements have been realized with real hardware.

4.1. MEASUREMENT SETUP

For the experimental setup RG402 semi-rigid cable are used. By removing the outer conductor shield and PTFE around the inner core 3 cm and 5 cm long monopoles made out of the exposed core as seen in Figure 4.1.

Dimensions of the mock missile model is same as in Figure 3.1.

Figure 4.1. 3 cm monopole antenna soldered on mock missile.

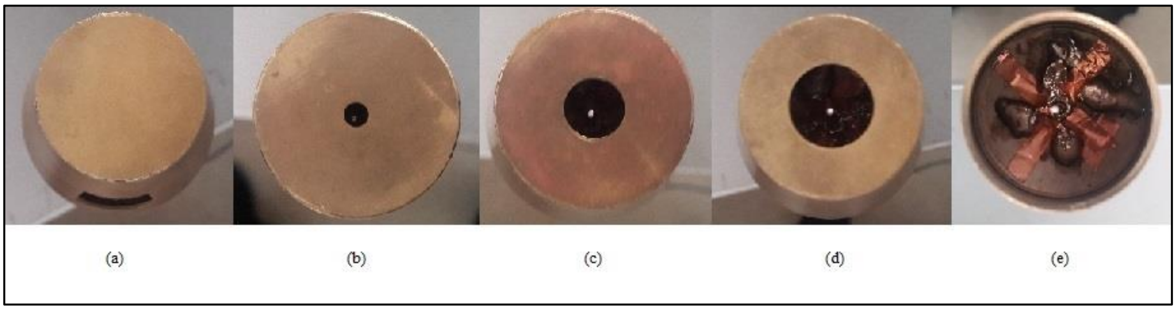

Figure 4.2. Aperture sizes on bulkhead top. (a) no aperture, (b) d=4 mm, (c) d=10 mm, (d) d=15 mm, (e) open

Figure 4.3. Bulkhead configurations. (a) Side view of windowless configuration, (b) Side view of windowed configuration

At the same time shorted wires of identical shielded cable length are cut and exposed cores are soldered to the body of the mock missile to obtain measurements of Zshort.

After both short and antenna impedance measurements are carried out using Rohde&Schwarz ZVA40 Vector Network Analyzer (VNA) these data sets are transferred to MATLAB in .dat format for further processing to obtain Susceptance and Conductance values. Measured values of $Z_{antenna}$ and Z_{short} are used to calculate Susceptance and Conductance values by using equations (2.1), (2.2), (2.3), (2.4) and (2.5). These calculated values are compared with the raw measurement data of the antennas.

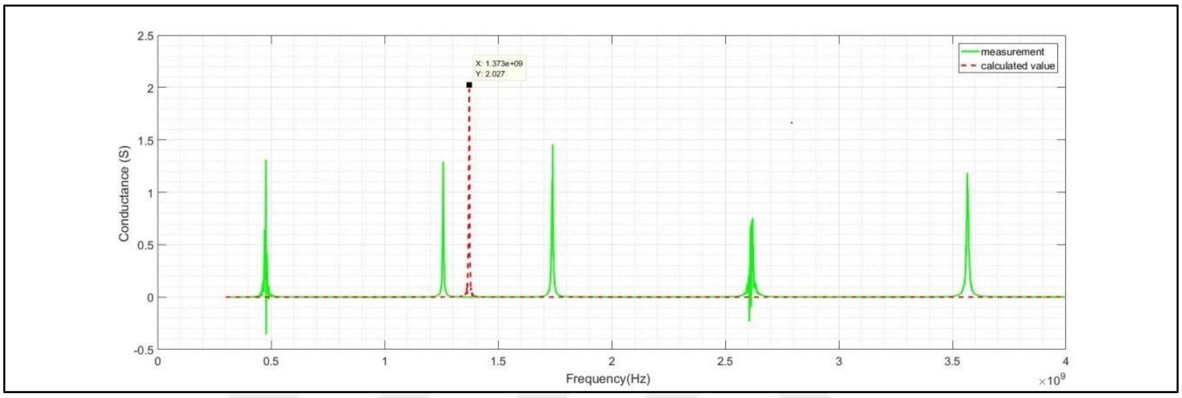

Figure 4.4. Comparision of direct measurements of the antenna conductance and calculated values

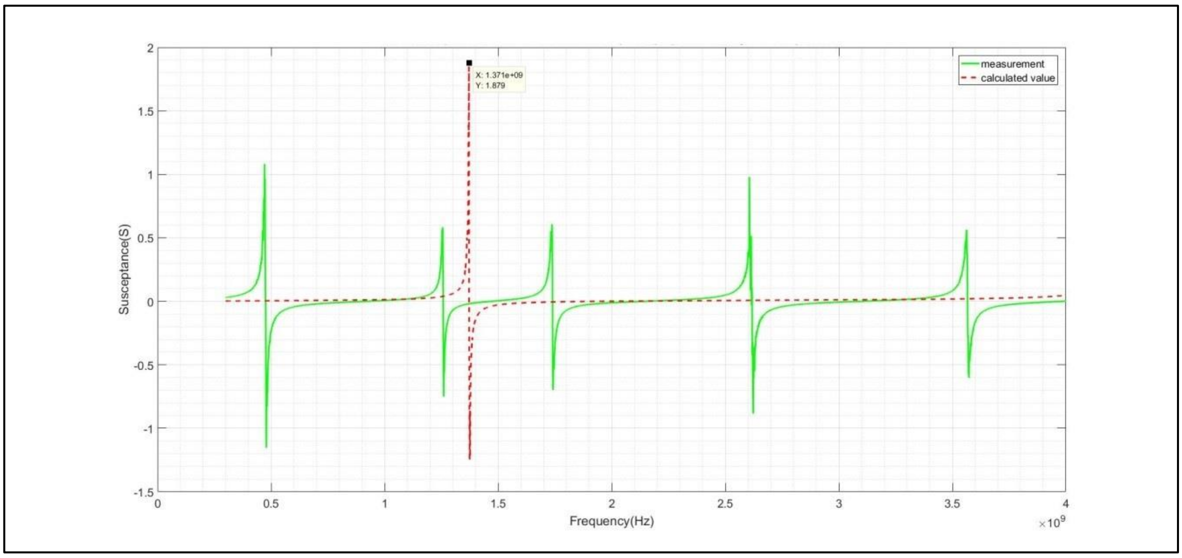

Figure 4.5. Comparision of direct measurements of the antenna susceptance and calculated values

As can be seen in Figure 4.4 and Figure 4.5 while the direct measurements of the antenna is useless for predicting the antenna characteristics, calculated values shows frequency drift similar to Figure 3.11 and Figure 3.12. All of the comparisons made between calculated values from measurements and the simulation results are shown in Chapter 5.

5. COMPARATIVE RESULTS OF SIMULATIONS AND MEASUREMENTS

In this Chapter comparisons of susceptance and conductance values of simulations and calculations from measurements are shown. Data plots are created in plotting tool Stanford Graphics. Positions of the Antennas are referred as same in Figure 3.2.

Results are first divided by their probe length then subdivided by aperture size and probe position.

5.1. 3 CM ANTENNA

5.1.1. Bulkhead with Window

For this comparision scenario from Figure 4.3(b) is used as bulkhead. All of the simulations and measurments made accordingly.

5.1.1.1. Open Top Aperture

Axisymmetric position (Position 1)

Figure 5.1 and Figure 5.2 show conductance and susceptance value plots for 3 cm monopole in windowed bulkhead, open top aperture, axisymmetric position. Some agreement can be seen in the measurements of susceptance plot.

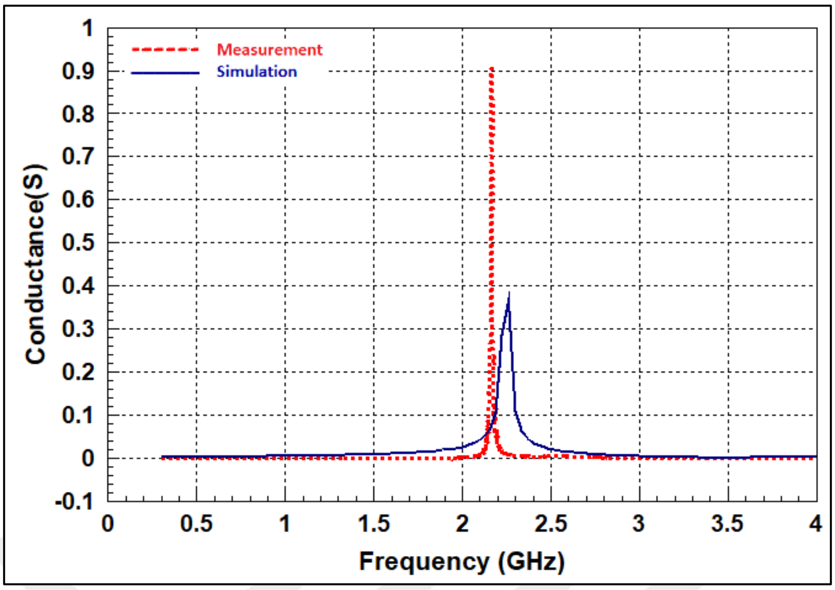

Figure 5.1. Conductance value plot for 3 cm monopole in windowed bulkhead, open top aperture, axisymmetric position.

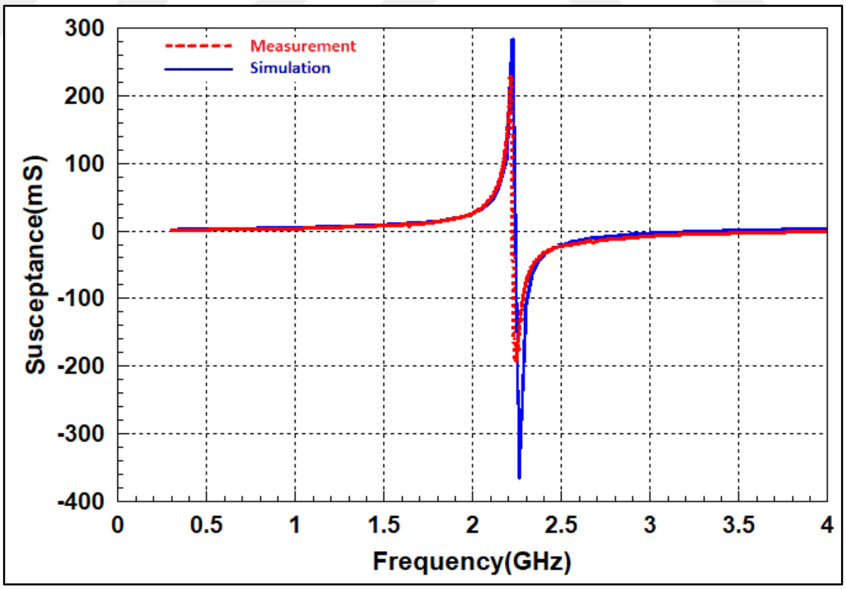

Figure 5.2. Susceptance value plot for 3 cm monopole in windowed bulkhead, open top aperture, axisymmetric position.

10 mm off-axis towards bulkhead window (Position 2)

Figure 5.3 and Figure 5.4 show conductance and susceptance value plots for 3 cm monopole in windowed bulkhead, open top aperture, 10 mm off-axis towards window. Some agreement can be seen in the measurements of susceptance plot.

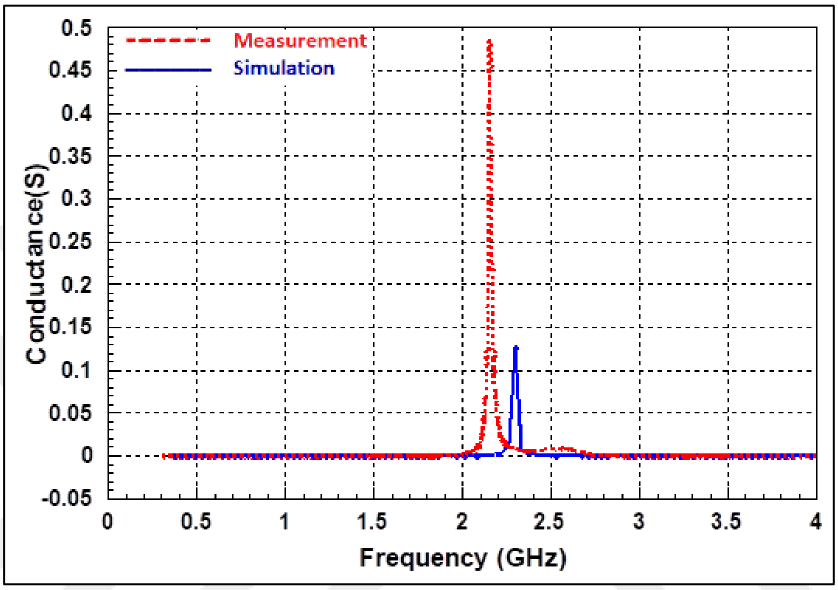

Figure 5.3. Conductance value plot for 3 cm monopole in windowed bulkhead, open top aperture, 10 mm off-axis towards window.

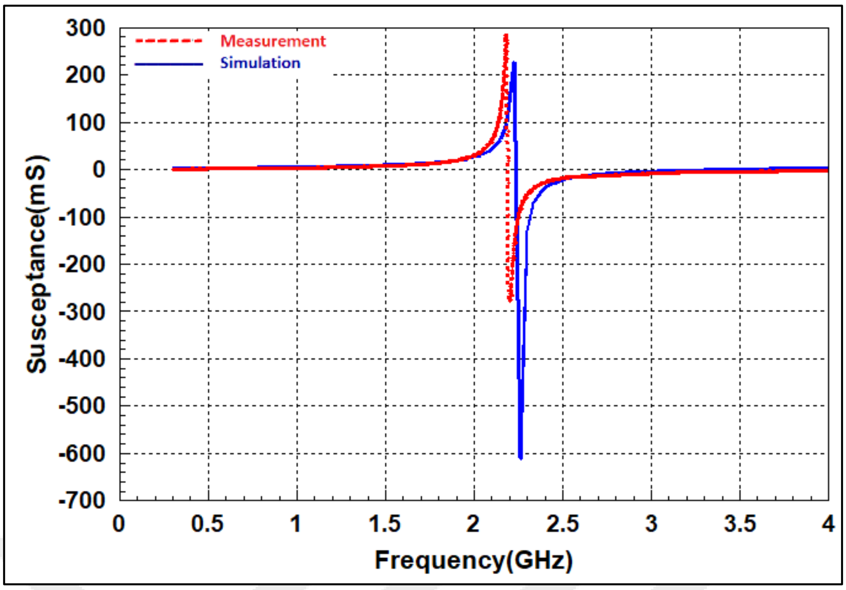

Figure 5.4. Susceptance value plot for 3 cm monopole in windowed bulkhead, open top aperture, 10 mm off-axis towards window.

15 mm off-axis towards bulkhead window (Position 3)

Figure 5.5 and Figure 5.6 show conductance and susceptance value plots for 3 cm monopole in windowed bulkhead, open top aperture, 15 mm off-axis towards window.Some agreement can be observed between simulations and measurements.

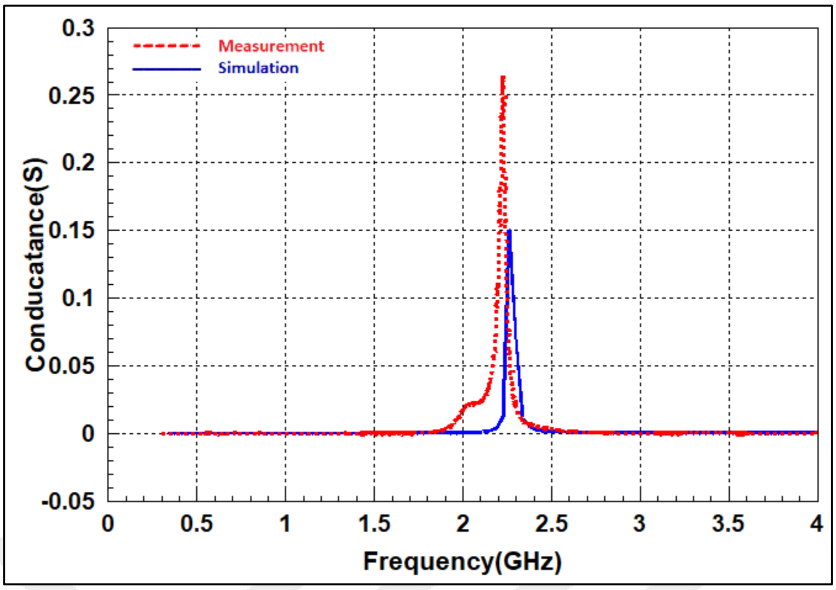

Figure 5.5. Conductance value plot for 3 cm monopole in windowed bulkhead, open top aperture, 15 mm off-axis towards window.

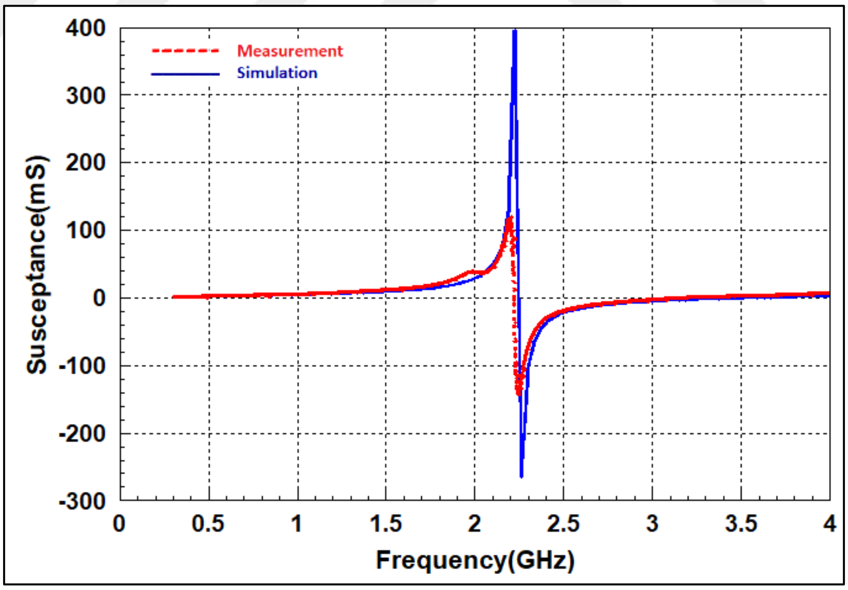

Figure 5.6. Susceptance value plot for 3 cm monopole in windowed bulkhead, open top aperture, 15 mm off-axis towards window.

10 mm off-axis away from window (Position 4)

Figure 5.7 and Figure 5.8 show conductance and susceptance value plots for 3 cm monopole in windowed bulkhead, open top aperture, 10 mm off-axis away from window.Some agreement can be observed between simulations and measurements.

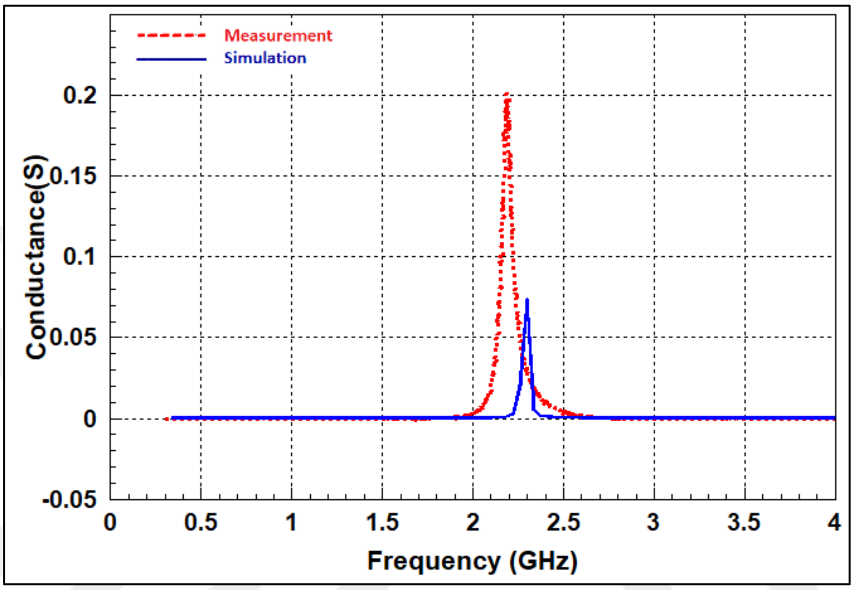

Figure 5.7. Conductance value plot for 3 cm monopole in windowed bulkhead, open top aperture, 10 mm off-axis away from window.

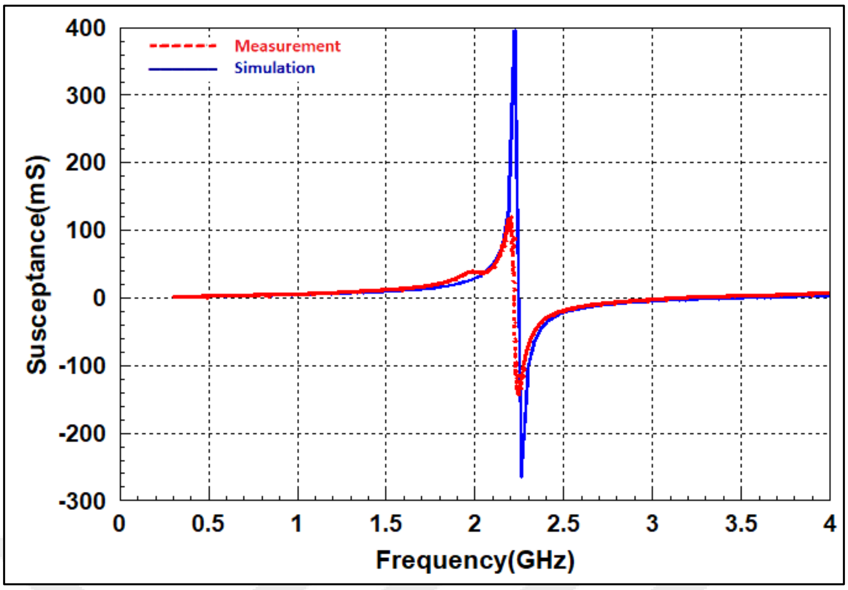

Figure 5.8. Susceptance value plot for 3 cm monopole in windowed bulkhead, open top aperture, 10 mm off-axis away from window.

5.1.1.2. Top with 15 mm Aperture

Axisymmetric position (Position 1)

Figure 5.9 and Figure 5.10 below show conductance and susceptance plots for 3 cm monopole in windowed bulkhead, 15 mm top aperture, axisymmetric position.Some agreement between the susceptance measurements and the simulations can be observed.

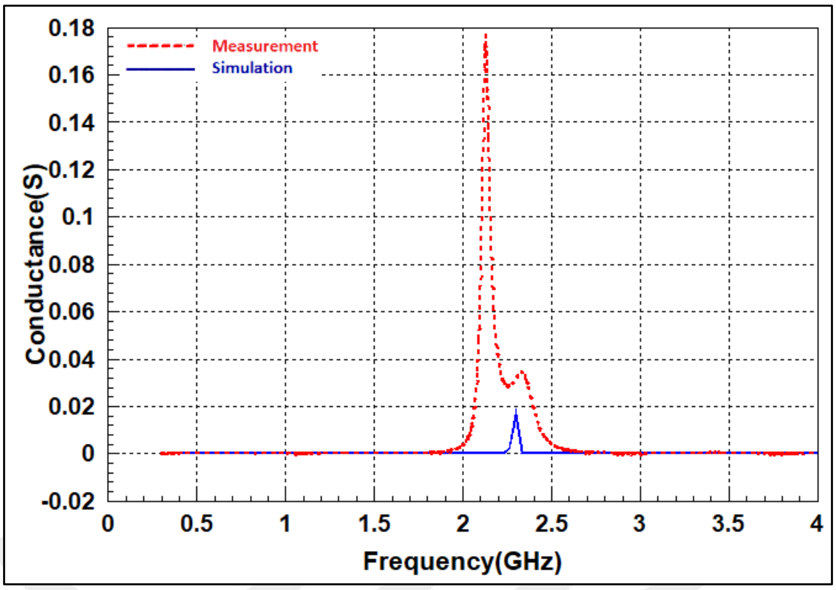

Figure 5.9. Conductance value plot for 3 cm monopole in windowed bulkhead, 15 mm top aperture, axisymmetric position.

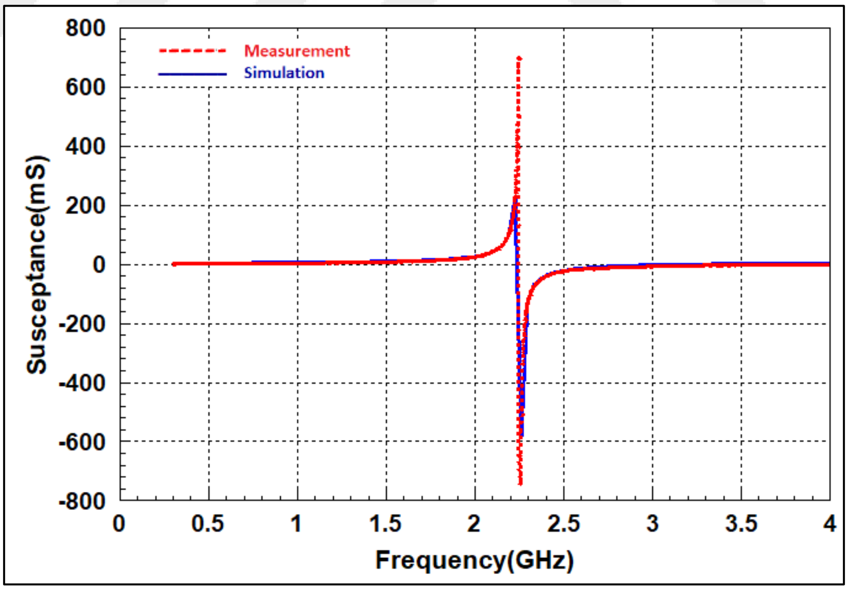

Figure 5.10. Susceptance value plot for 3 cm monopole in windowed bulkhead, 15 mm top aperture, axisymmetric position.

10 mm off-axis towards bulkhead window (Position 2)

Figure 5.11 and Figure 5.12 show conductance and susceptance value plots for 3 cm monopole in windowed bulkhead, 15 mm top aperture, 10 mm off-axis towards window. Some agreement between the susceptance measurements and the simulations can be observed.

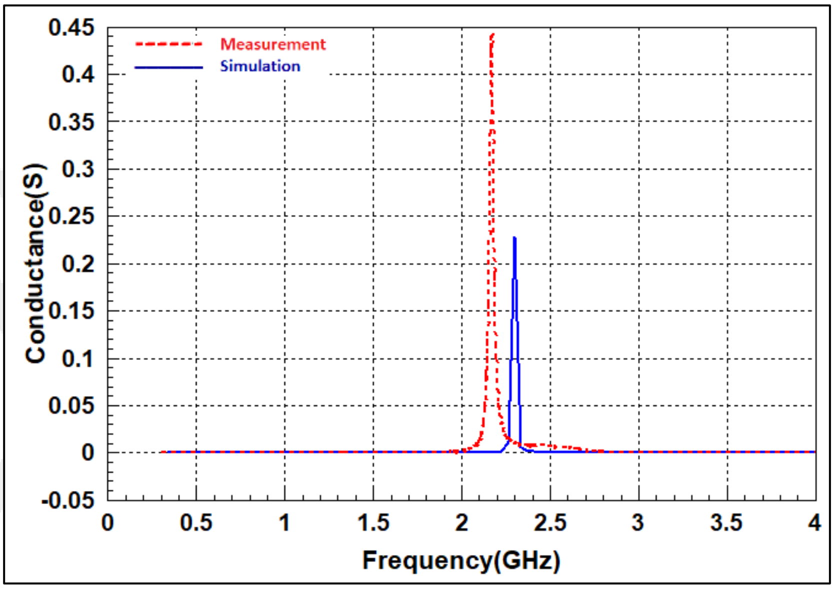

Figure 5.11. Conductance value plot for 3 cm monopole in windowed bulkhead, 15 mm top aperture, 10 mm off-axis towards window.

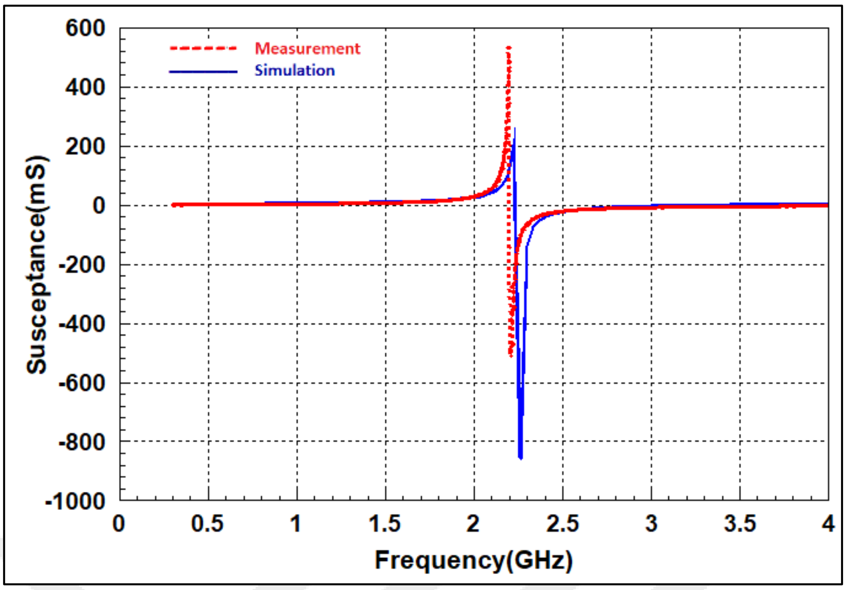

Figure 5.12. Susceptance value plot for 3 cm monopole in windowed bulkhead, 15 mm top aperture, 10 mm off-axis towards window.

15 mm off-axis towards bulkhead window (Position 3)

Figure 5.13 and Figure 5.14 show conductance and susceptance value plots for 3 cm monopole in windowed bulkhead, 15 mm top aperture, 15 mm off-axis towards window. Some agreement between the susceptance measurements and the simulations can be observed.

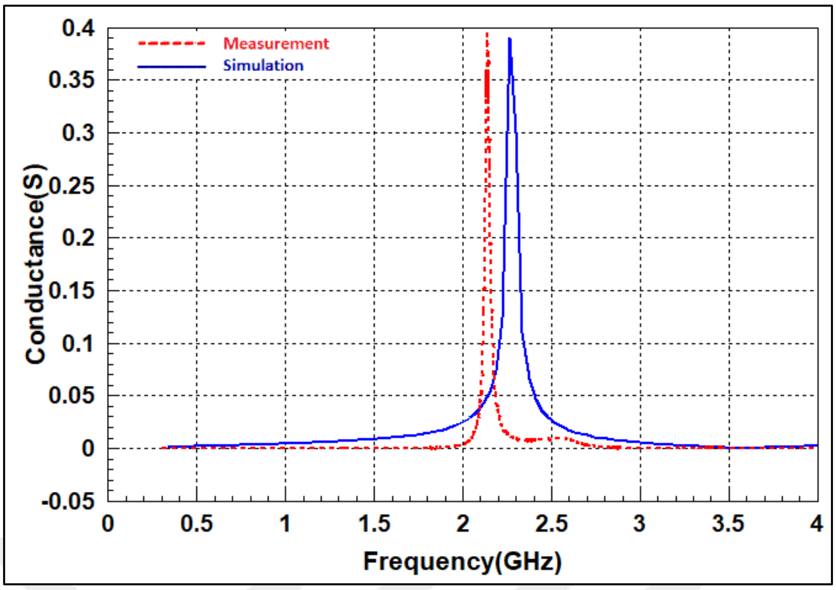

Figure 5.13. Conductance value plot for 3 cm monopole in windowed bulkhead, 15 mm top aperture, 15 mm off-axis towards window.

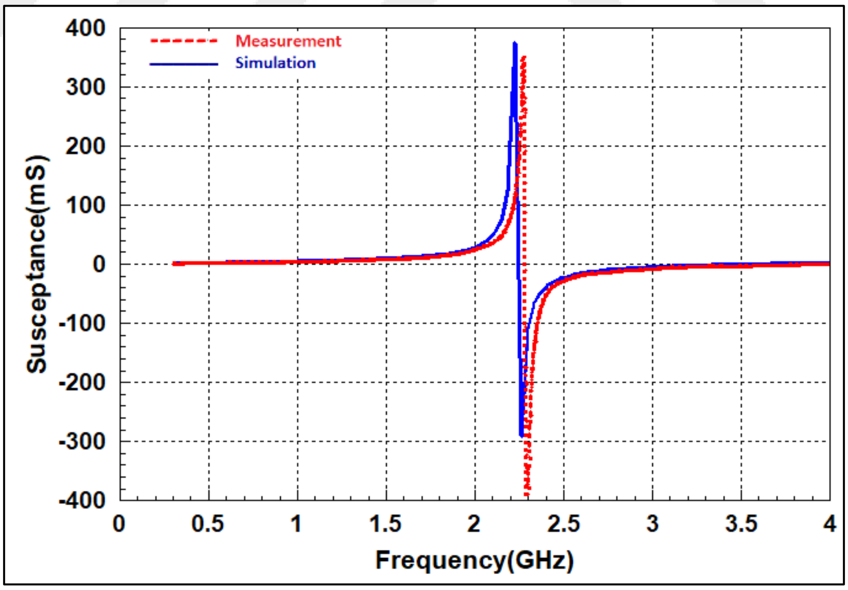

Figure 5.14. Susceptance value plot for 3 cm monopole in windowed bulkhead, 15 mm top aperture, 15 mm off-axis towards window.

10 mm off-axis away from bulkhead window (Position 4)

Figure 5.15 and Figure 5.16 show conductance and susceptance value plots for 3 cm monopole in windowed bulkhead, 15 mm top aperture, 10 mm off-axis away from window. Some agreement between the susceptance measurements and the simulations can be observed.

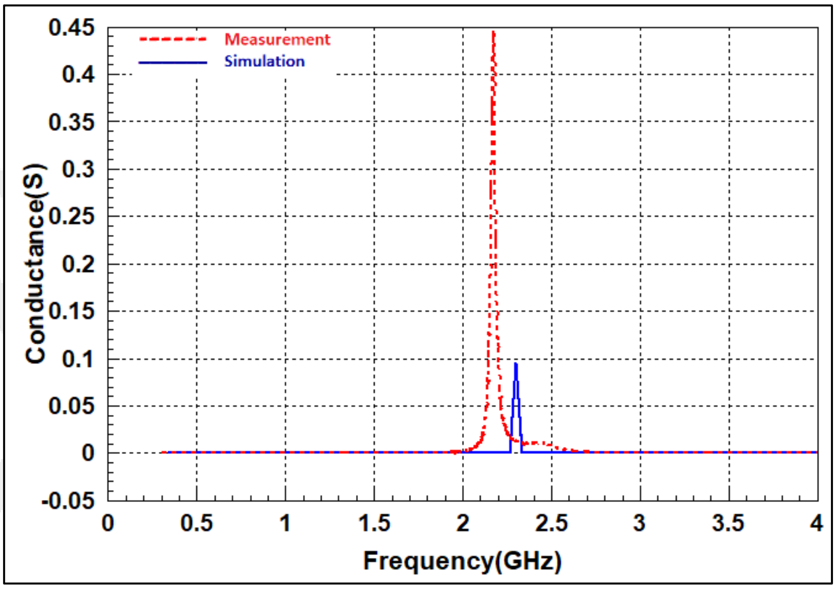

Figure 5.15. Conductance value plot for 3 cm monopole in windowed bulkhead, 15 mm top aperture, 10 mm off-axis away from window.

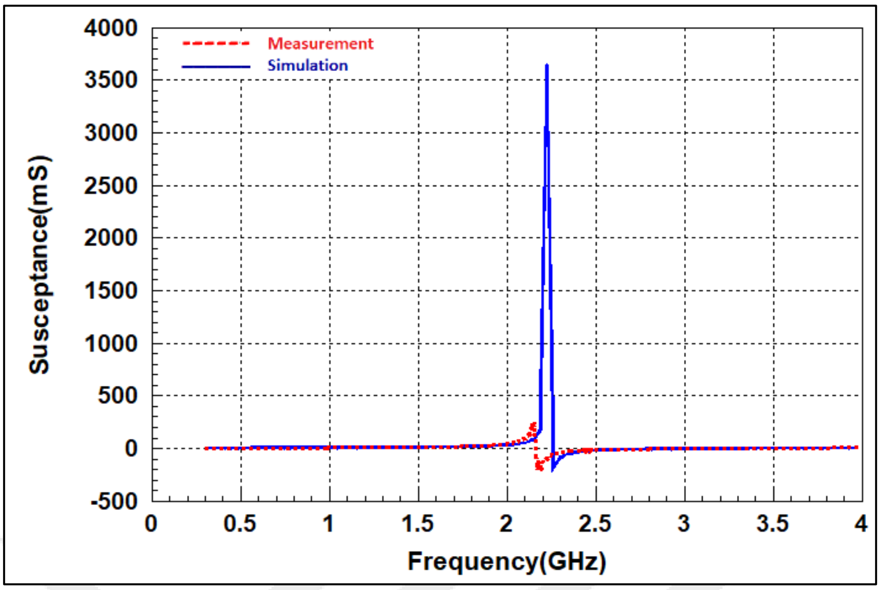

Figure 5.16.Susceptance value plot plot for 3 cm monopole in windowed bulkhead, 15 mm top aperture, 10 mm off-axis away from window.

5.1.1.3. Top with 10 mm Aperture

Axisymmetric position (Position 1)

Figure 5.17 and Figure 5.18 show conductance and susceptance value plots for 3 cm monopole in windowed bulkhead, 10 mm top aperture, axisymmetric position. Some agreement between measurements and the simulations can be observed.

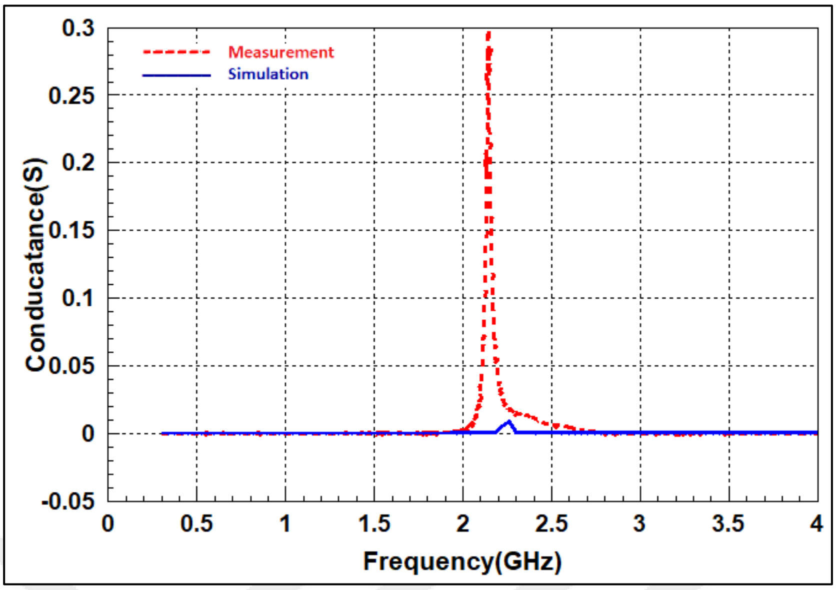

Figure 5.17. Conductance value plot for 3 cm monopole in windowed bulkhead, 10 mm top aperture, axisymmetric position.

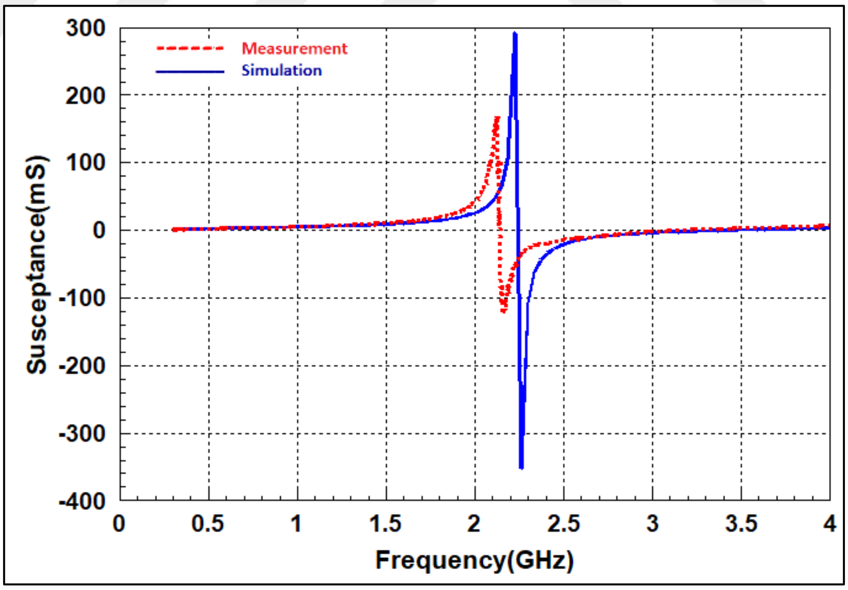

Figure 5.18. Susceptance value plot for 3 cm monopole in windowed bulkhead, 10 mm top aperture, axisymmetric position.

10 mm off-axis towards bulkhead window (Position 2)

Figure 5.19 and Figure 5.20 show conductance and susceptance value plots for 3 cm monopole in windowed bulkhead, 10 mm top aperture, 10 mm off-axis towards window.Some agreement between the susceptance measurements and the simulations can be observed.

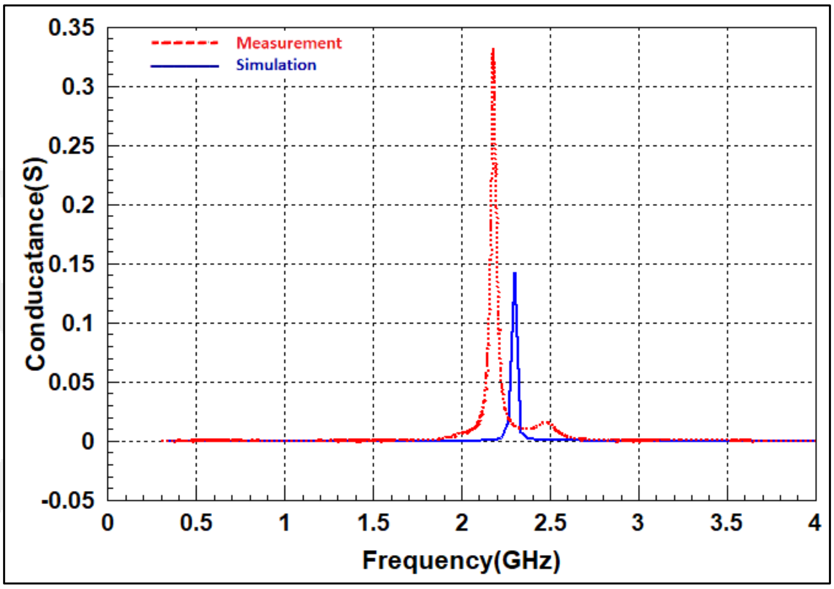

Figure 5.19. Conductance value plot for 3 cm monopole in windowed bulkhead, 10 mm top aperture, 10 mm off-axis towards window.

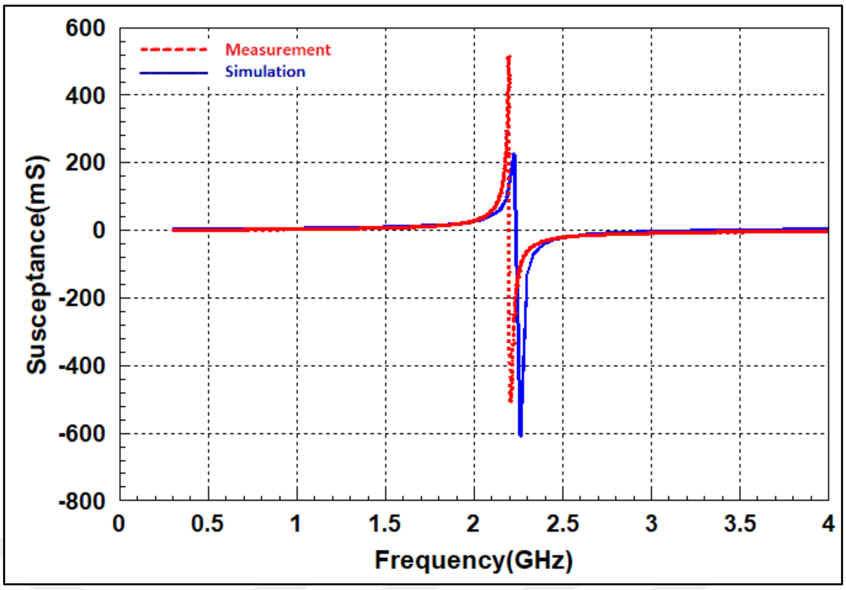

Figure 5.20. Susceptance value plot for 3 cm monopole in windowed bulkhead, 10 mm top aperture, 10 mm off-axis towards window.

15 mm off-axis towards bulkhead window (Position 3)

Figure 5.21 and Figure 5.22 show conductance and susceptance value plots for 3 cm monopole in windowed bulkhead, 10 mm top aperture, 15 mm off-axis towards window. Some agreement between the susceptance measurements and the simulations can be observed.

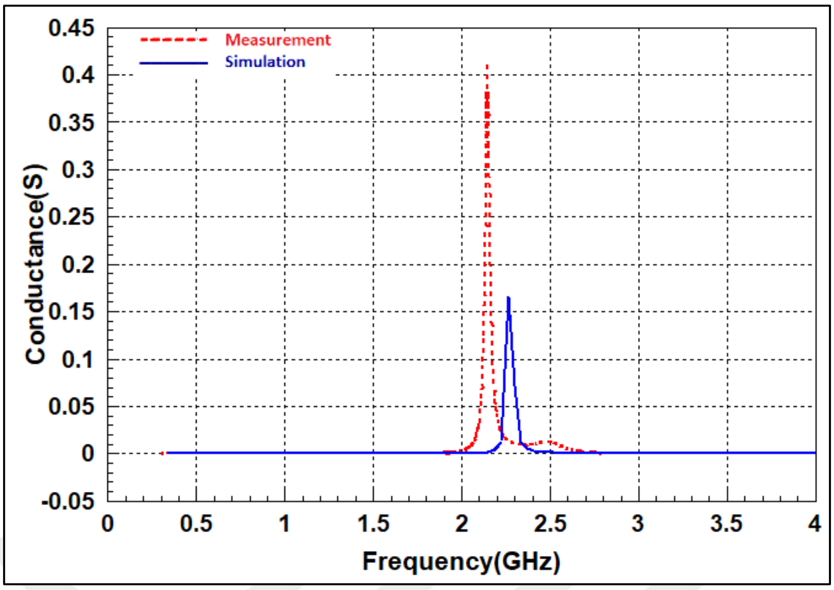

Figure 5.21. Conductance value plot for 3 cm monopole in windowed bulkhead, 10 mm top aperture, 15 mm off-axis towards window.

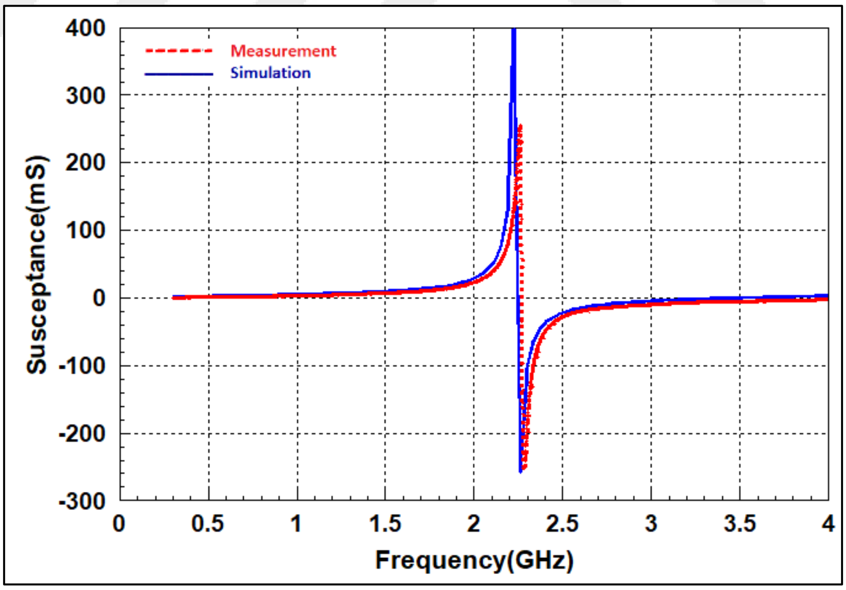

Figure 5.22. Susceptance value plot for 3 cm monopole in windowed bulkhead, 10 mm top aperture, 15 mm off-axis towards window.

10 mm off-axis away from bulkhead window (Position 4)

Figure 5.23 and Figure 5.24 show conductance and susceptance value plots for 3 cm monopole in windowed bulkhead, 10 mm top aperture, 10 mm off-axis away from window. Some agreement between the susceptance measurements and the simulations can be observed.

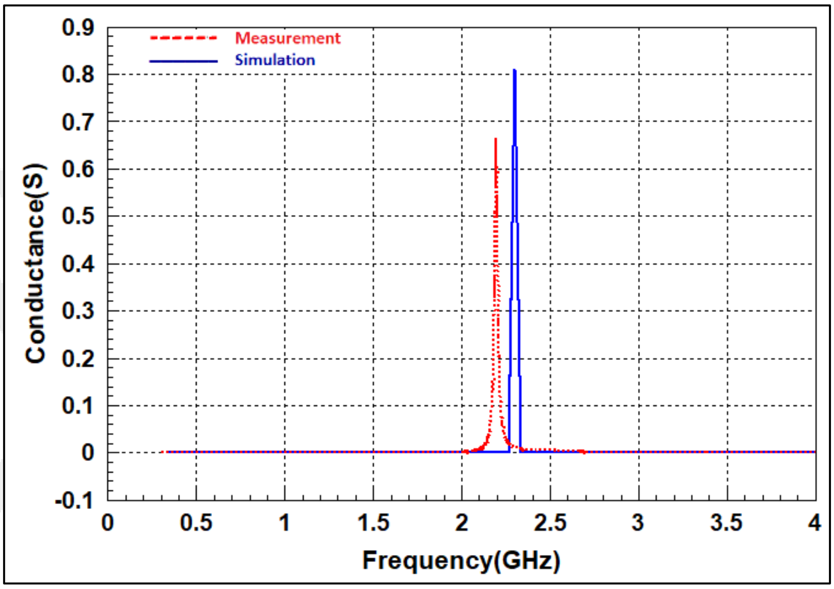

Figure 5.23. Conductance value plot for 3 cm monopole in windowed bulkhead, 10 mm top aperture, 10 mm off-axis away from window.

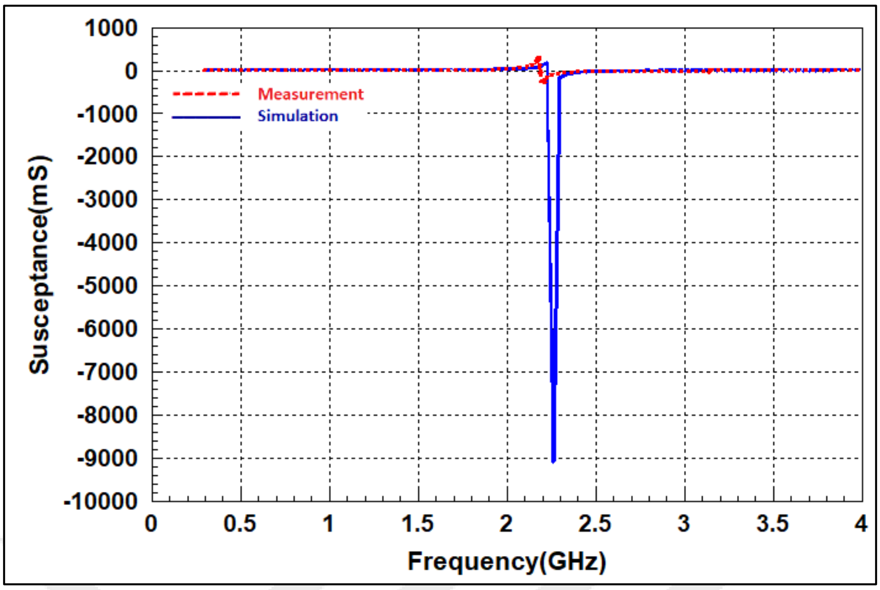

Figure 5.24. Susceptance value plot for 3 cm monopole in windowed bulkhead, 10 mm top aperture, 10 mm off-axis away from window.

5.1.1.4. Top with 4 mm Aperture

Axisymmetric position (Position 1)

Figure 5.26 and 5.27 show conductance and susceptance for 3 cm monopole in windowed bulkhead, 4 mm top aperture, axisymmetric position. Some agreement between measurements and the simulations can be observed.

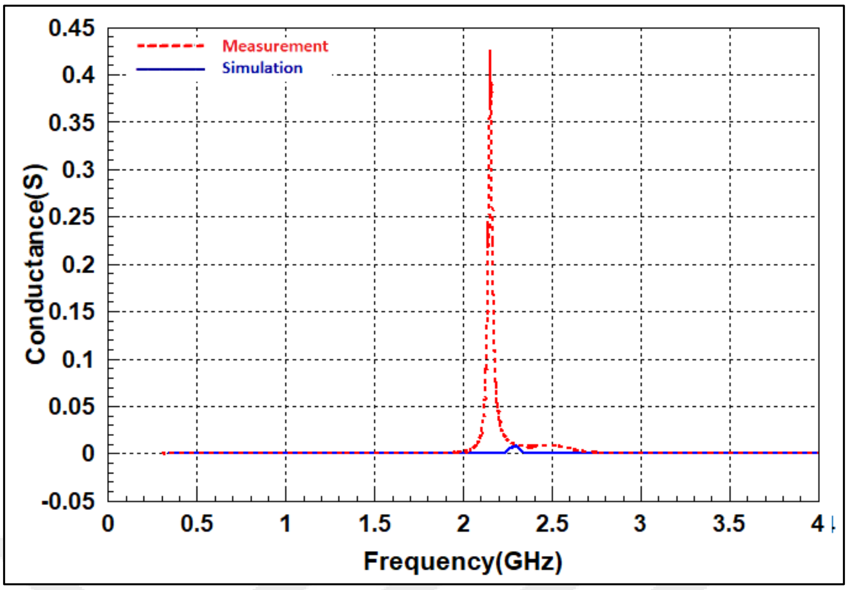

Figure 5.25. Conductance value plot for 3 cm monopole in windowed bulkhead, 4 mm top aperture, axisymmetric position.

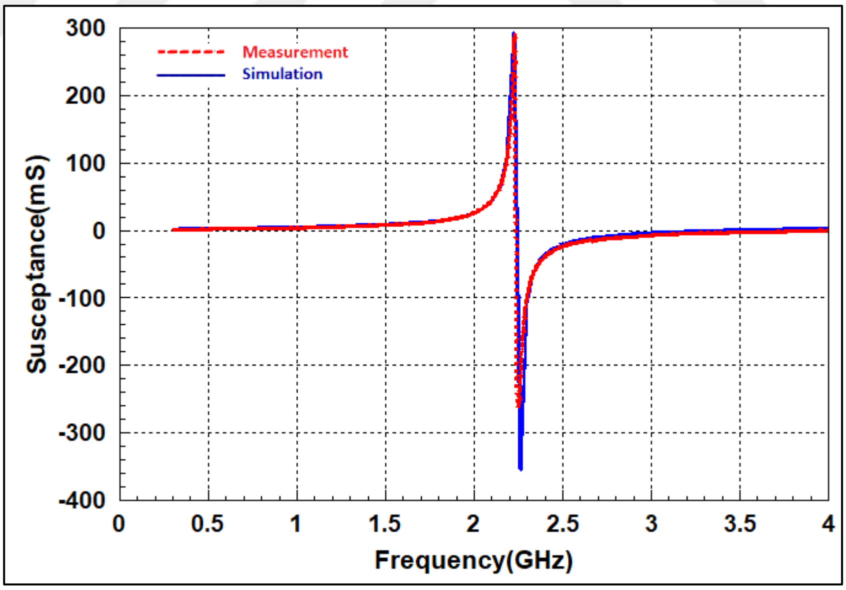

Figure 5.26. Susceptance value plot for 3 cm monopole in windowed bulkhead, 4 mm top aperture, axisymmetric position.

10 mm off-axis towards bulkhead window (Position 2)

Figure 5.27 and Figure 5.28 show conductance and susceptance value plots for 3 cm monopole in windowed bulkhead, 4 mm top aperture, 10 mm off-axis towards window.Some agreement between the susceptance measurements and the simulations can be observed.

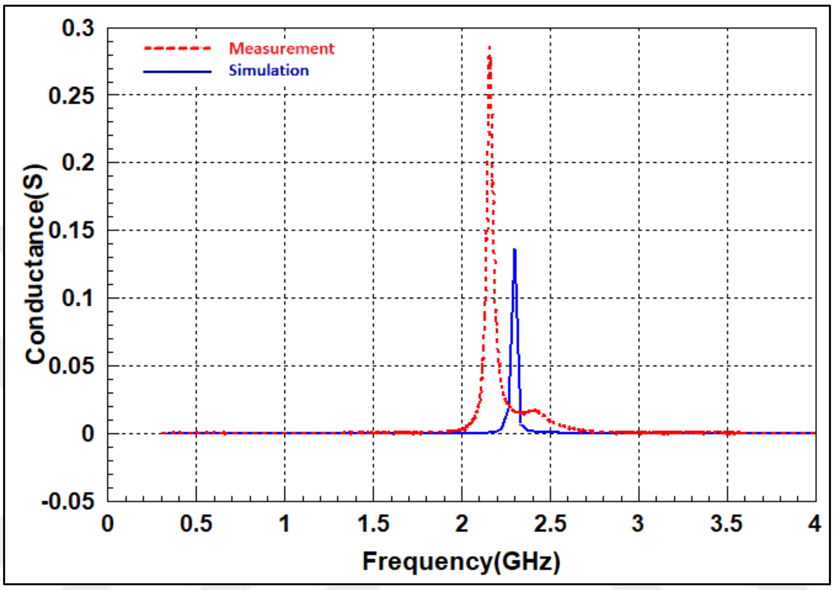

Figure 5.27. Conductance value plot for 3 cm monopole in windowed bulkhead, 4 mm top aperture, 10 mm off-axis towards window.

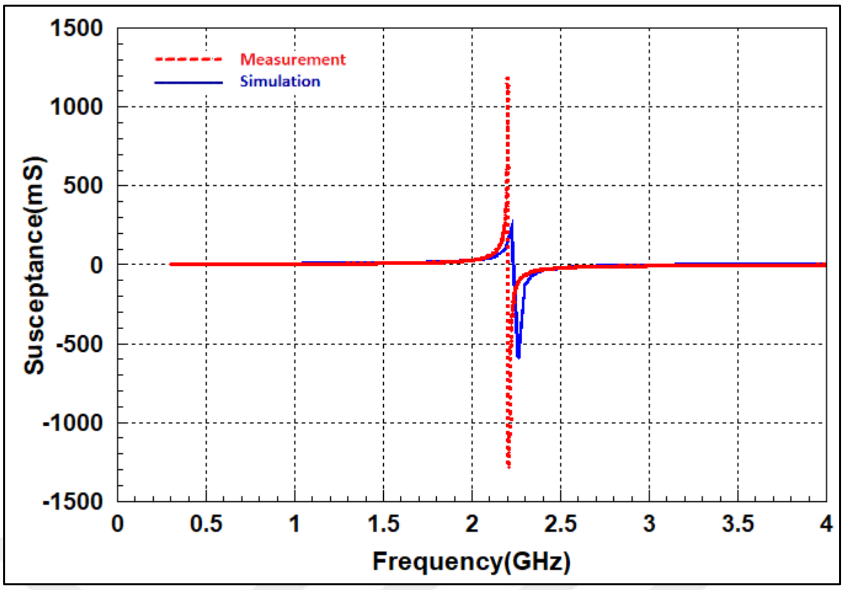

Figure 5.28. Susceptance value plot for 3 cm monopole in windowed bulkhead, 4 mm top aperture, 10 mm off-axis towards window.

15 mm off-axis towards bulkhead window (Position 3)

Figure 5.29 and Figure 5.30 show conductance and susceptance value plots for 3 cm monopole in windowed bulkhead, 4 mm top aperture, 10 mm off-axis towards window.A some agreement between the conductance measurements and the simulations can be observed.

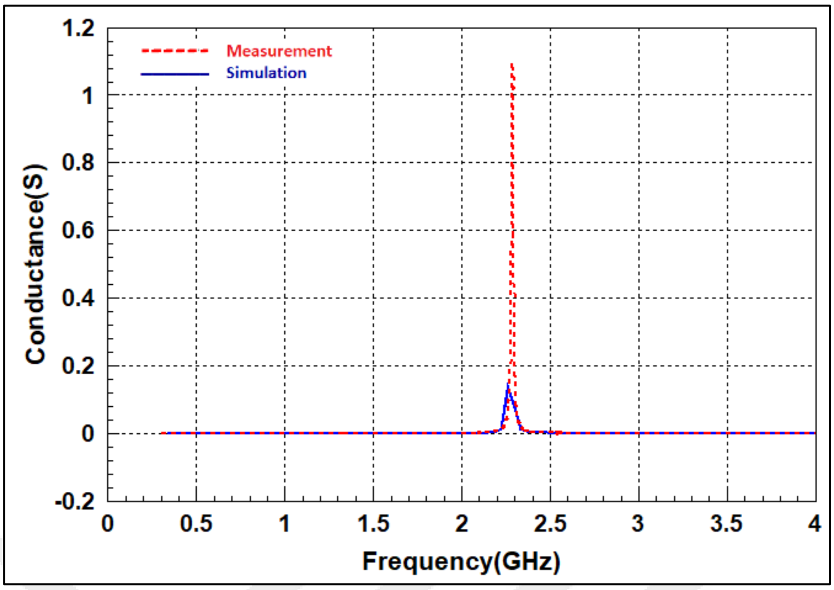

Figure 5.29. Conductance value plot for 3 cm monopole in windowed bulkhead, 4 mm top aperture, 15 mm off-axis towards window.

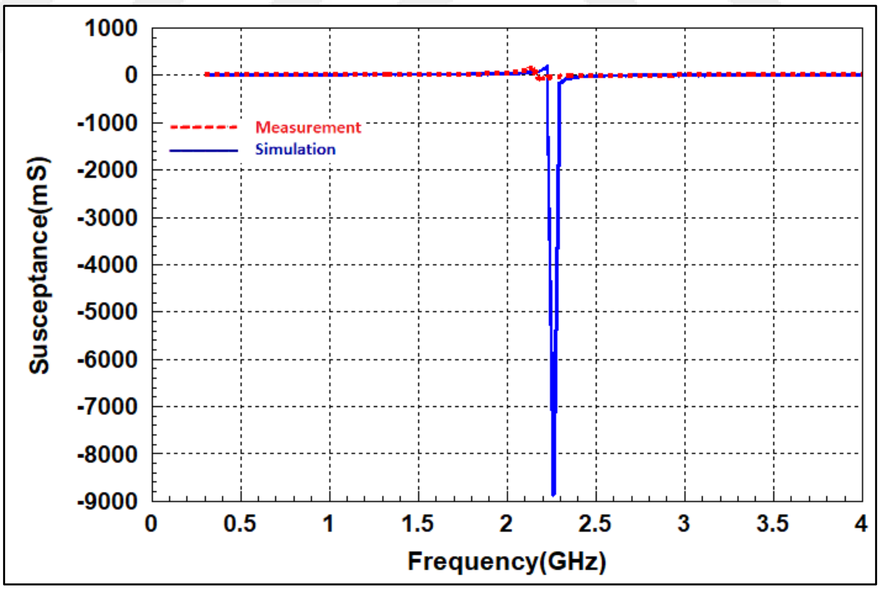

Figure 5.30. Susceptance value plot for 3 cm monopole in windowed bulkhead, 4 mm top aperture, 15 mm off-axis towards window.

10 mm off-axis away from bulkhead window (Position 4)

Figure 5.31 and Figure 5.32 show conductance and susceptance value plots for 3 cm monopole in windowed bulkhead, 4 mm top aperture, 10 mm off-axis away from window. Some agreement between the susceptance measurements and the simulations can be observed.

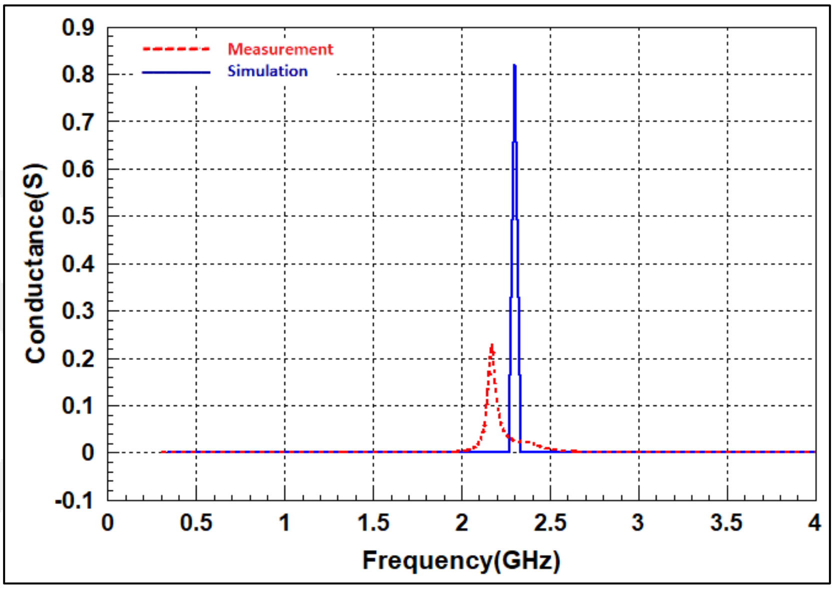

Figure 5.31. Conductance value plot for 3 cm monopole in windowed bulkhead, 4 mm top aperture, 10 mm off-axis away from window.

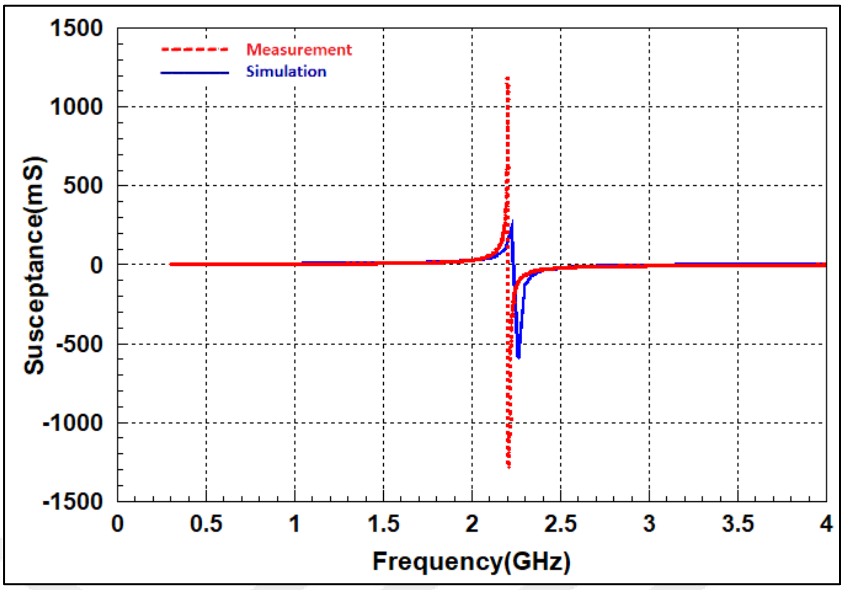

Figure 5.32. Susceptance value plot for 3 cm monopole in windowed bulkhead, 4 mm top aperture, 10 mm off-axis away from window.

5.1.1.5. Top with no Aperture

Axisymmetric position (Position 1)

Figure 5.33 and Figure 5.34 show conductance and susceptance value plots for 3 cm monopole in windowed bulkhead with no top aperture, at an axisymmetric position. Some agreement between susceptance measurements and the simulations can be observed.

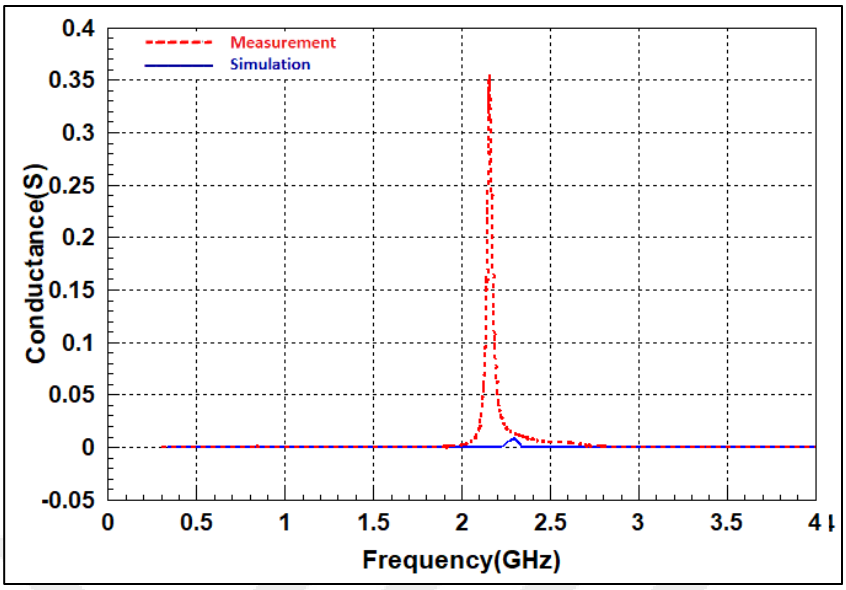

Figure 5.33. Conductance value plot for 3 cm monopole in windowed bulkhead, closed top aperture, axisymmetric position.

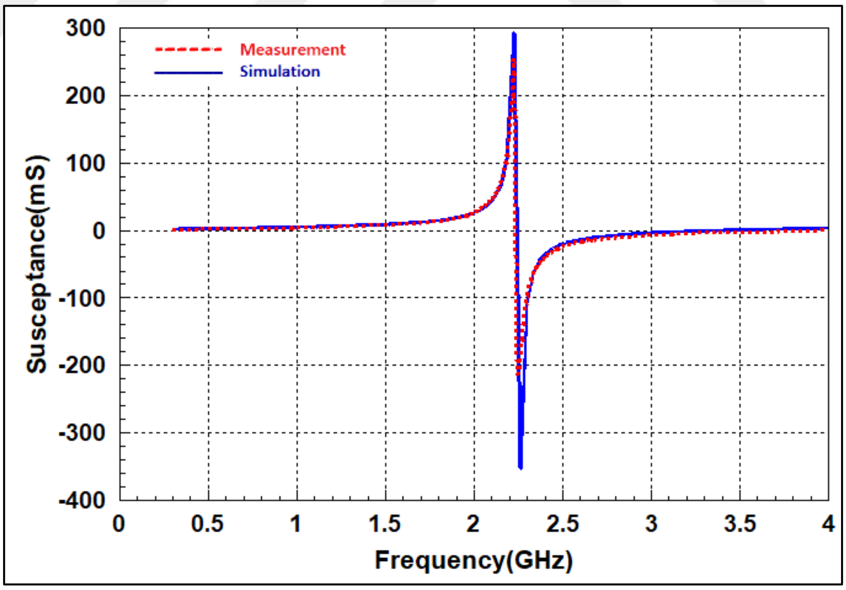

Figure 5.34. Susceptance value plot for 3 cm monopole in windowed bulkhead, closed top aperture, axisymmetric position.

10 mm off-axis towards bulkhead window (Position 2)

Figure 5.35 and Figure 5.36 show conductance and susceptance value plots for 3 cm monopole in windowed bulkhead with no top aperture, 10 mm off-axis towards window. Some agreement between susceptance measurements and the simulations can be observed.

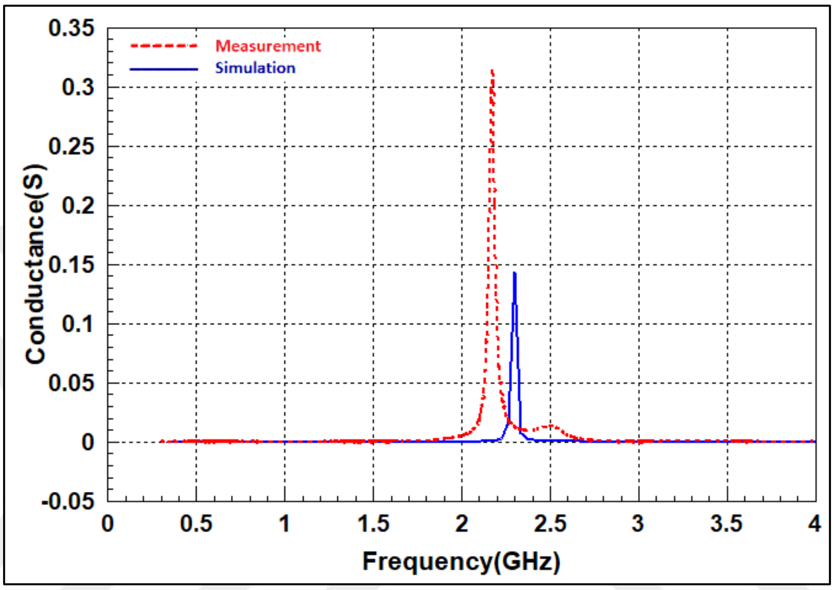

Figure 5.35. Conductance value plot for 3 cm monopole in windowed bulkhead, closed top aperture, 10 mm off-axis towards window.

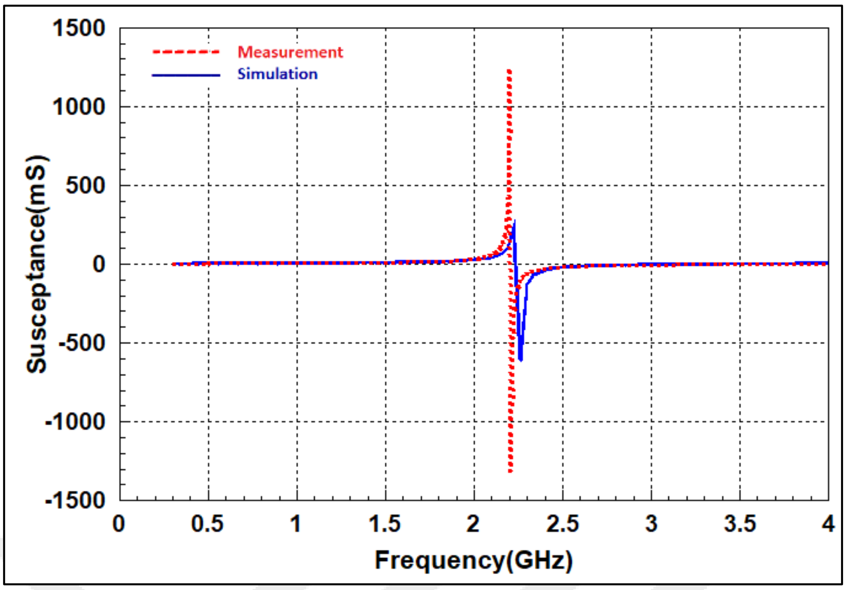

Figure 5.36. Susceptance value plot for 3 cm monopole in windowed bulkhead, closed top aperture, 10 mm off-axis towards window.

15 mm off-axis towards bulkhead window (Position 3)

Figure 5.37 and Figure 5.38 show conductance and susceptance value plots for 3 cm monopole in windowed bulkhead, 4 mm top aperture, 15 mm off-axis towards window.Some agreement between the susceptance measurements and the simulations can be observed.

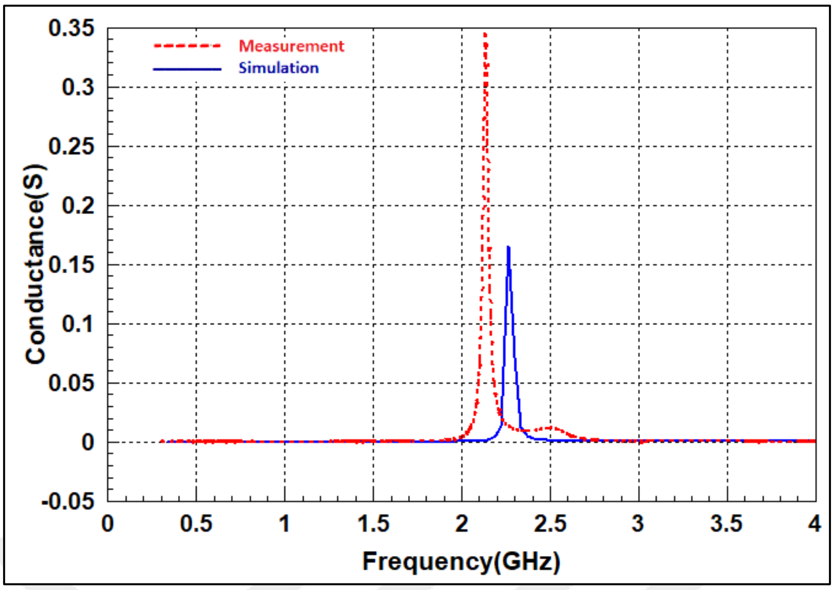

Figure 5.37. Conductance value plot for 3 cm monopole in windowed bulkhead, closed top aperture, 15 mm off-axis towards window.

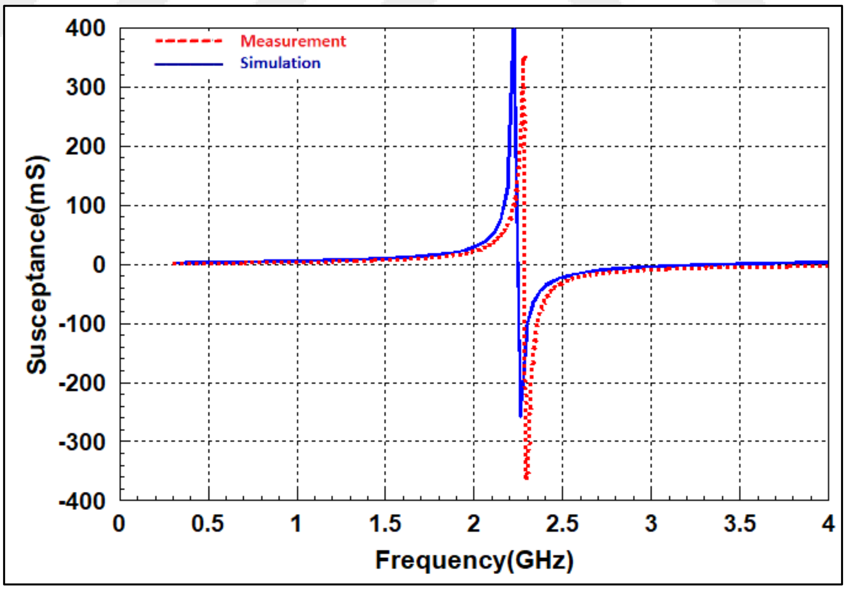

Figure 5.38. Susceptance value plot for 3 cm monopole in windowed bulkhead, closed top aperture, 15 mm off-axis towards window.

10 mm off-axis away from bulkhead window (Position 4)

Figure 5.39 and Figure 5.40 show conductance and susceptance value plots for 3 cm monopole in windowed bulkhead, 4 mm top aperture, 10 mm off-axis away from window. There is 84 MHz difference between both the conductance and susceptance measurements and the simulations.

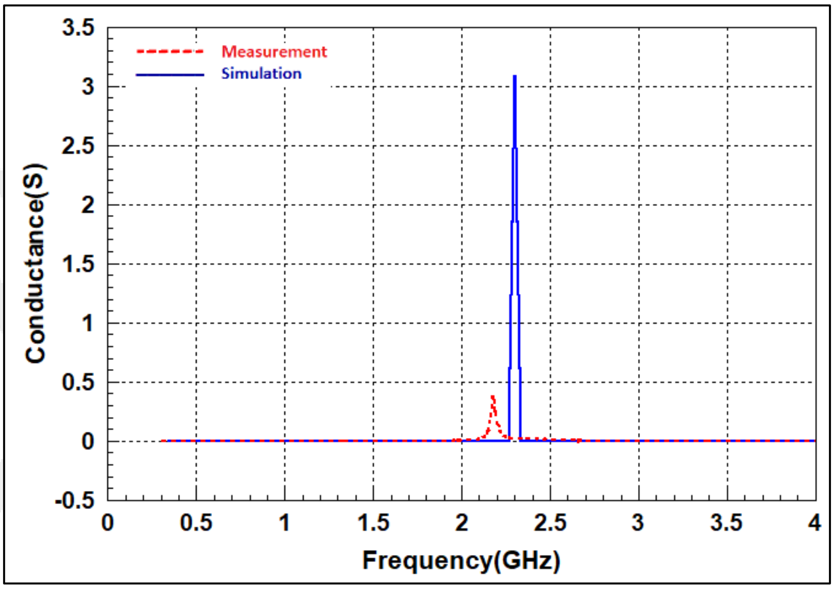

Figure 5.39. Conductance value plot for 3 cm monopole in windowed bulkhead, closed top aperture, 10 mm off-axis away from window.

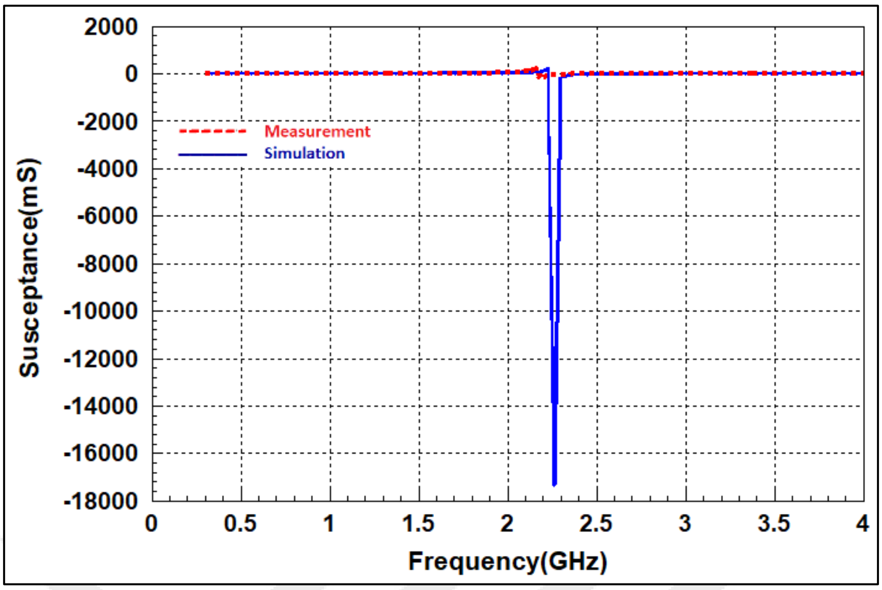

Figure 5.40. Susceptance value plot for 3 cm monopole in windowed bulkhead, closed top aperture, 10 mm off-axis away from window.

5.1.2. Bulkhead Without Window

For this comparision scenario from Figure 4.3(a) is used as bulkhead. All of the simulations and measurments made accordingly.

5.1.2.1. Open Top Aperture

Axisymmetric position (Position 1)

Figures 5.42 and 5.43 show conductance and susceptance values for 3 cm monopole in windowless bulkhead, open top aperture, axisymmetric position. While there is 76 MHz difference between the conductance measurements and the simulations, some agreement can be observed between susceptance simulations and measurments.

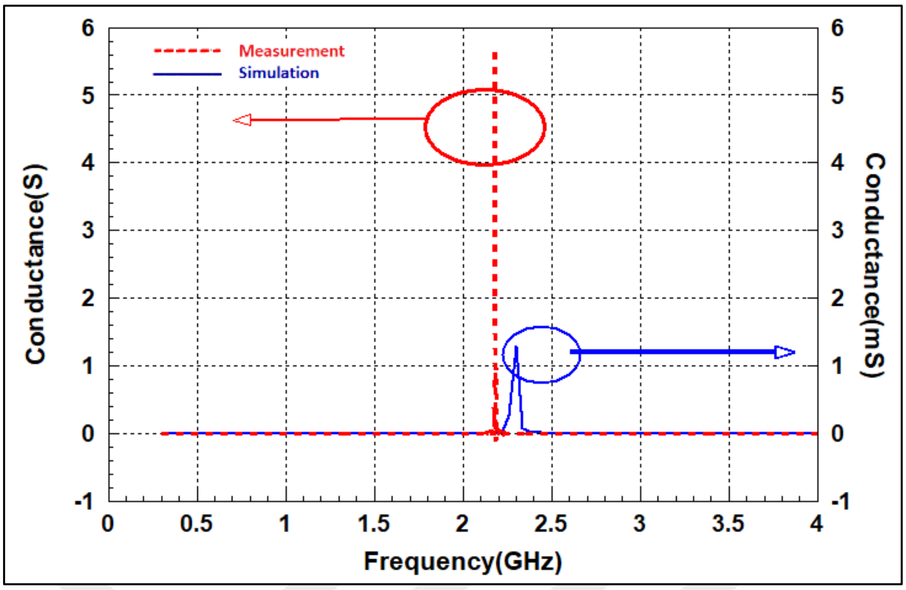

Figure 5.41. Conductance value plot for 3 cm monopole in windowless bulkhead, open top aperture, axisymmetric position.

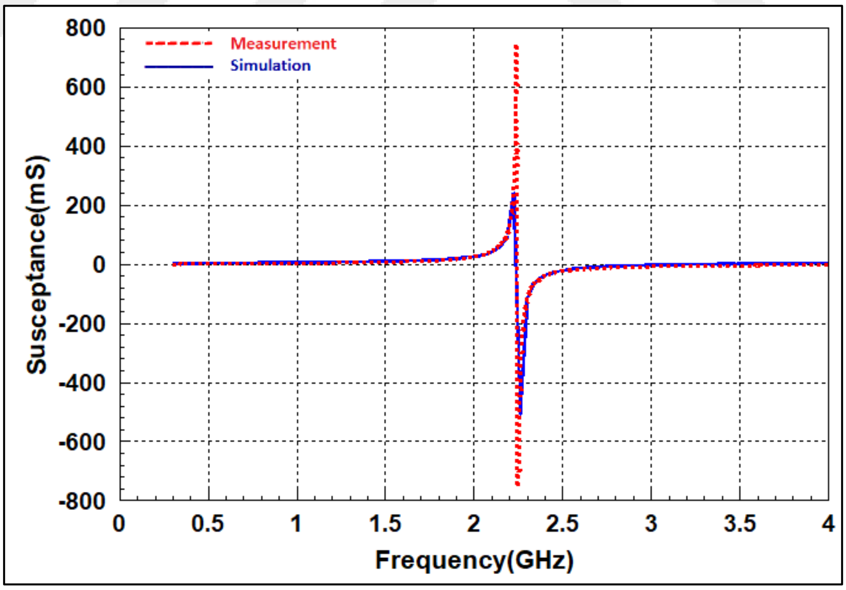

Figure 5.42. Susceptance value plot for 3 cm monopole in windowless bulkhead, open top aperture, axisymmetric position.

10 mm off-axis (Position 2)

Figure 5.43 and Figure 5.44 show conductance and susceptance value plots for 3 cm monopole in windowless bulkhead, open top aperture and 10 mm off-axis position. 63 MHz difference between susceptance measurements and the simulations can be observed.

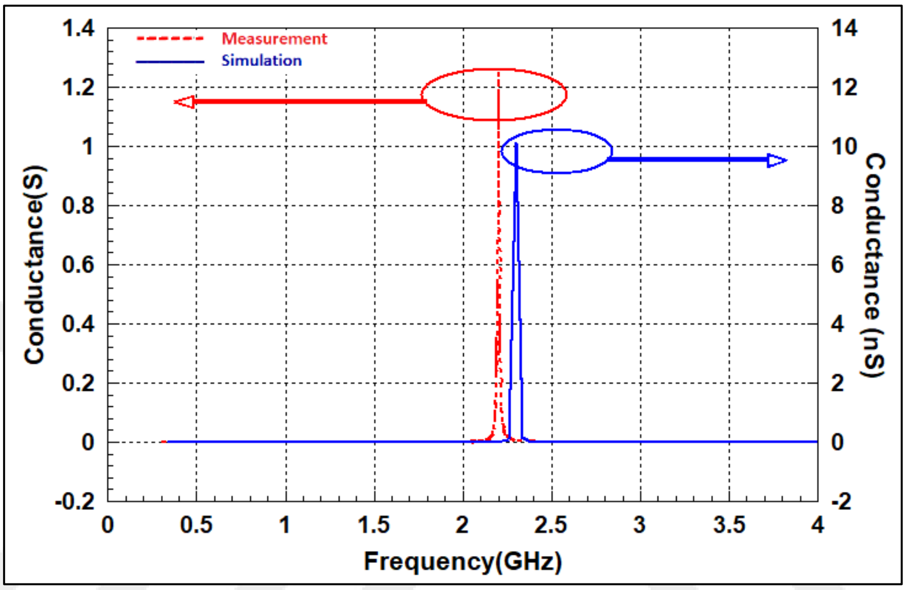

Figure 5.43. Conductance value plot for 3 cm monopole in windowless bulkhead, open top aperture, 10 mm off-axis.

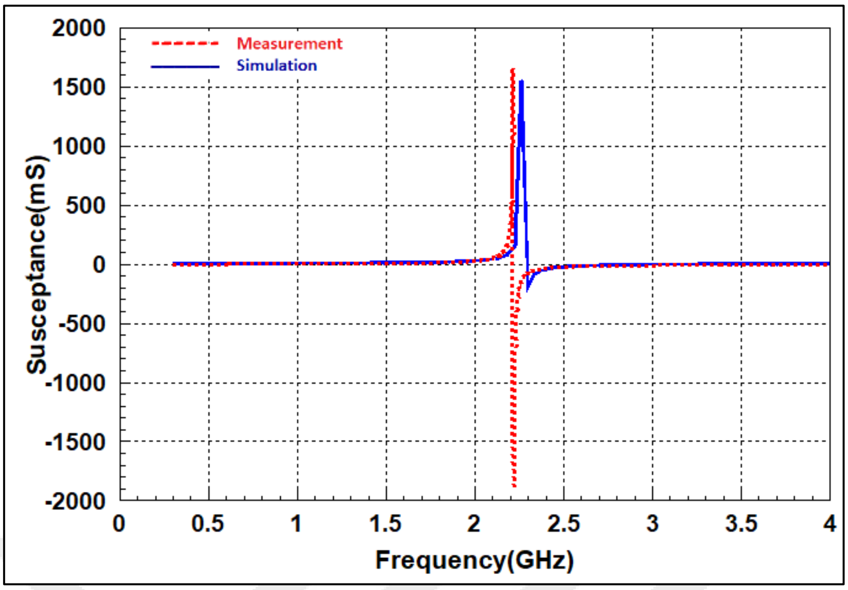

Figure 5.44. Susceptance value plot for 3 cm monopole in windowless bulkhead, open top aperture, 10 mm off-axis.

15 mm off-axis (Position 3)

Figure 5.45 and Figure 5.46 show conductance and susceptance value plots for 3 cm monopole in windowless bulkhead, open top aperture and 15 mm off-axis position. 67 MHz difference between the conductance measurements and the simulations can be observed while susceptance values agrees with each other.

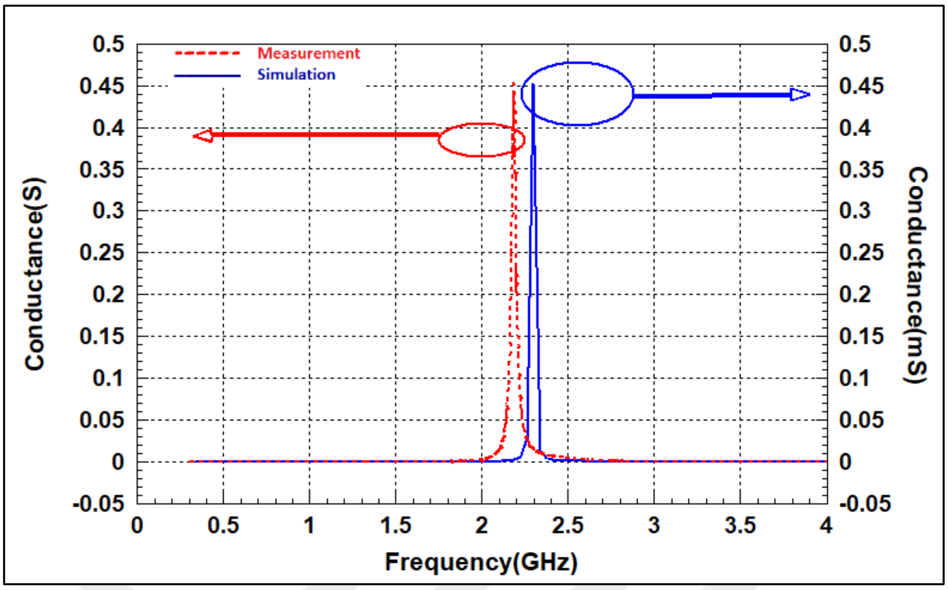

Figure 5.45. Conductance value plot for 3 cm monopole in windowless bulkhead, open top aperture, 15 mm off-axis.

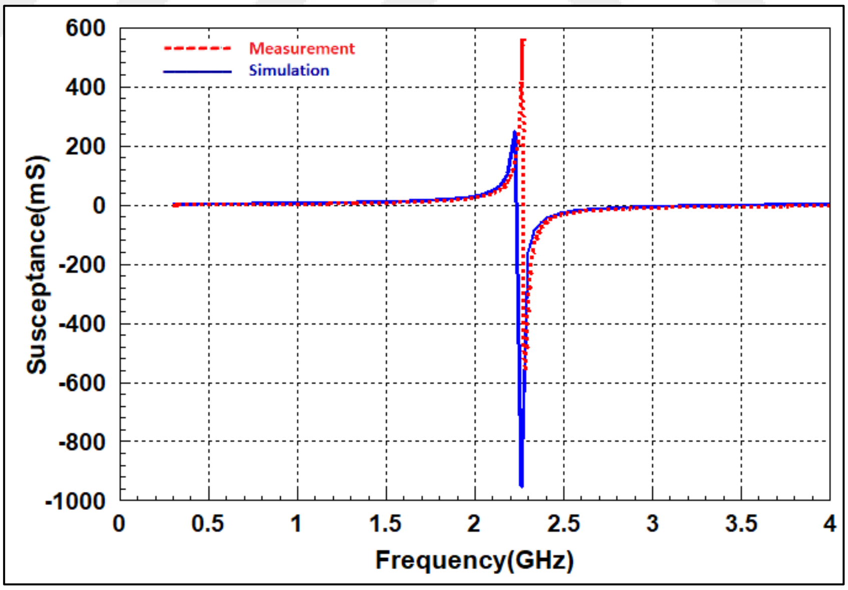

Figure 5.46. Susceptance value plot for 3 cm monopole in win4dowless bulkhead, open top aperture, 15 mm off-axis.

5.1.2.2. Top with 15 mm Aperture

Axisymmetric position (Position 1)

Figure 5.47 and Figure 5.48 show conductance and susceptance value plots for 3 cm monopole in windowless bulkhead, 15 mm top aperture, axisymmetric position.

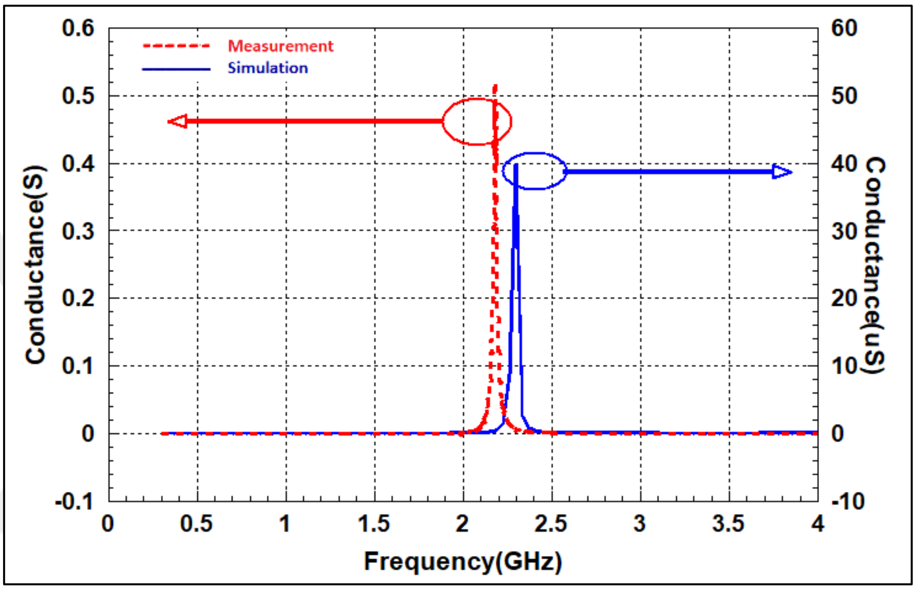

Figure 5.47. Conductance value plot for 3 cm monopole in windowless bulkhead, 15 mm top aperture, axisymmetric position.

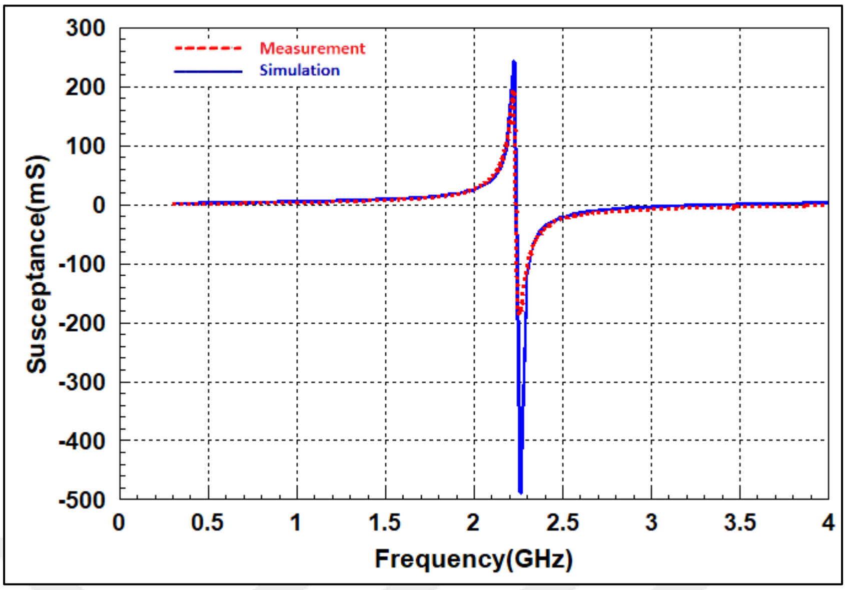

Figure 5.48. Susceptance value plot for 3 cm monopole in windowless bulkhead, 15 mm top aperture, axisymmetric position.

10 mm off-axis (Position 2)

Figure 5.49 and Figure 5.50 show conductance and susceptance value plots for 3 cm monopole in windowless bulkhead, 15 mm top aperture, 10 mm off-axis position. Small discrepancy between the simulation and measurements can be observed.

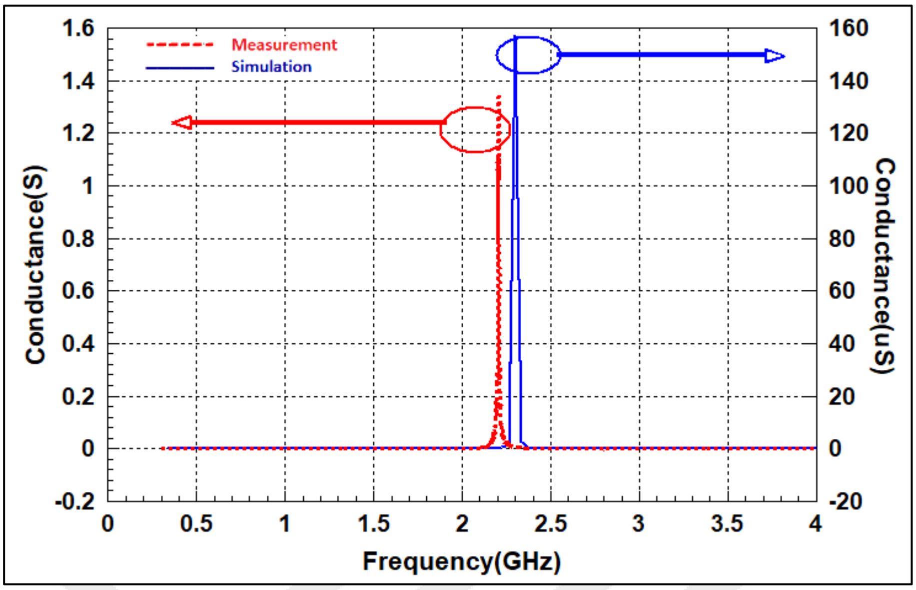

Figure 5.49. Conductance value plot for 3 cm monopole in windowless bulkhead, 15 mm top aperture, 10 mm off-axis.

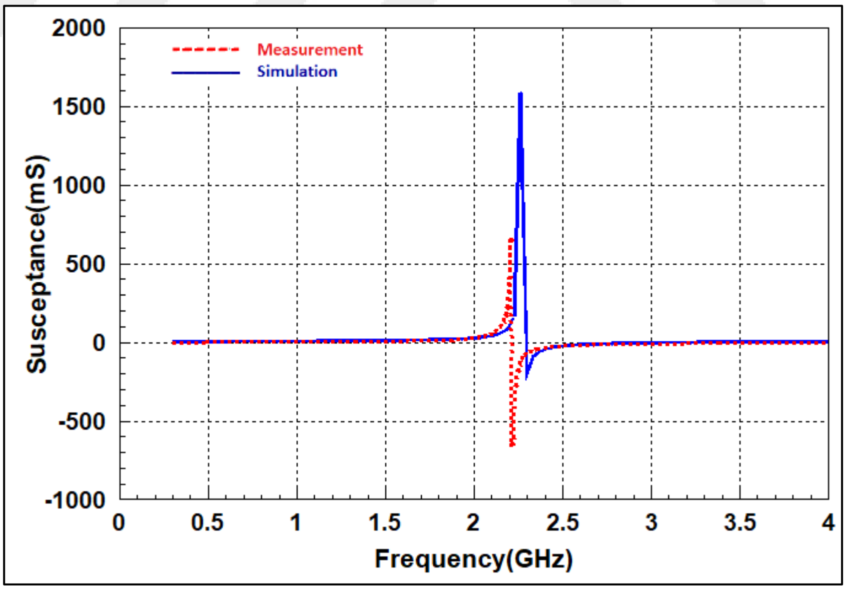

Figure 5.50. Susceptance value plot for 3 cm monopole in windowless bulkhead, 15 mm top aperture,10 mm off-axis.

15 mm off-axis (Position 3)

Figure 5.51 and Figure 5.52 show conductance and susceptance value plots for 3 cm monopole in windowless bulkhead, 15 mm top aperture, 15 mm off-axis position. Small discrepancy between the simulation and measurements can be observed.

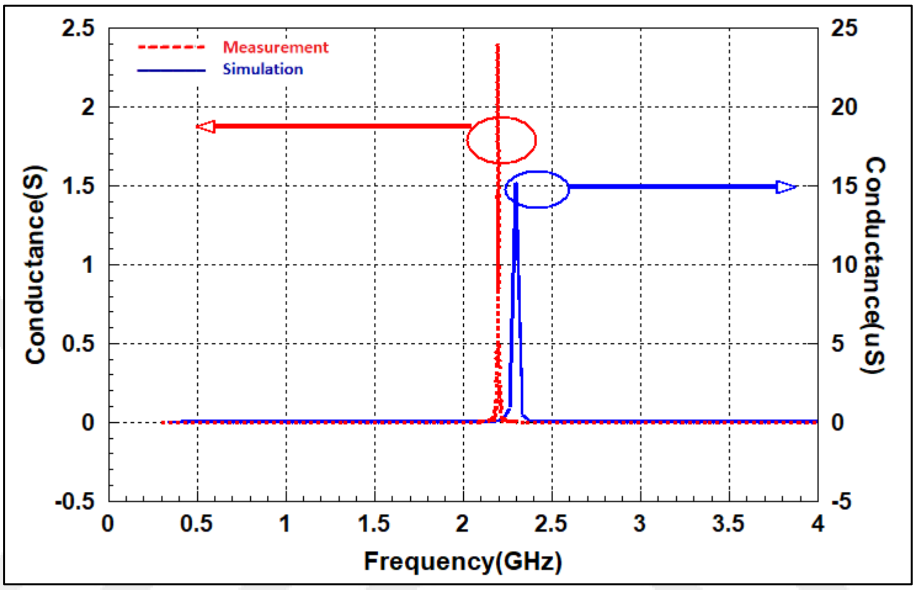

Figure 5.51. Conductance value plot for 3 cm monopole in windowless bulkhead, 15 mm top aperture, 15 mm off-axis.

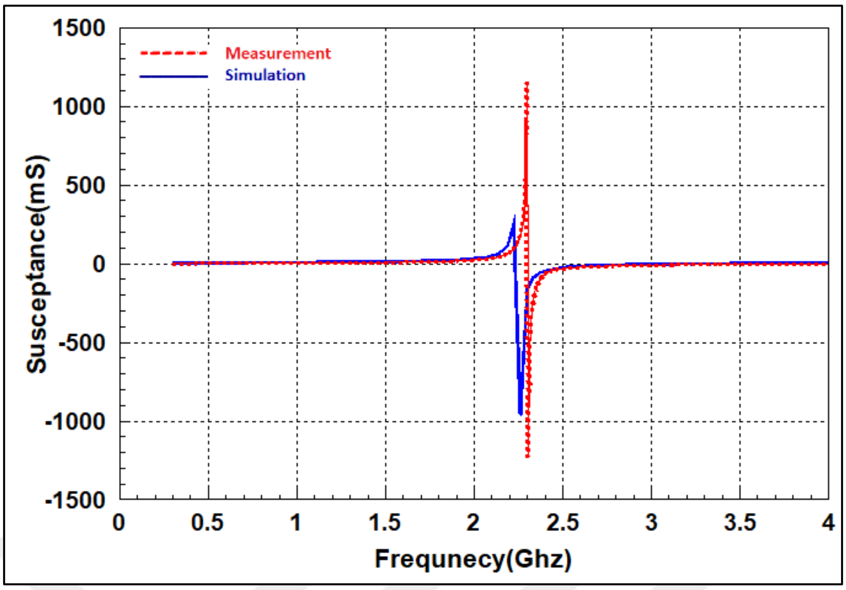

Figure 5.52. Susceptance value plot for 3 cm monopole in windowless bulkhead, 15 mm top aperture,15 mm off-axis.

5.1.2.3. Top with 10 mm Aperture

Axisymmetric position (Position 1)

Figure 5.53 and Figure 5.54 show conductance and susceptance value plots for 3 cm monopole in windowless bulkhead, 10 mm top aperture, axisymmetric position. Some agreement between susceptance values is observed.

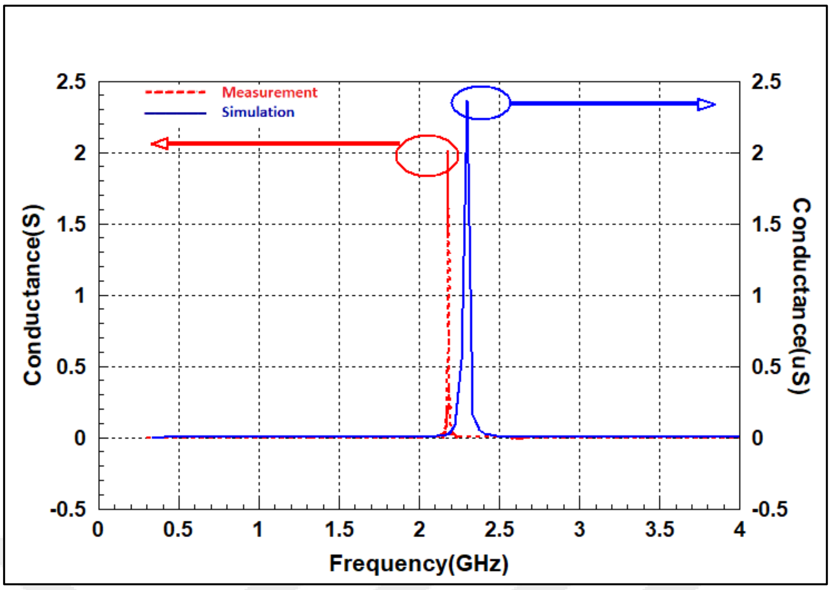

Figure 5.53. Conductance value plot for 3 cm monopole in windowless bulkhead, 10 mm top aperture, axisymmetric position.

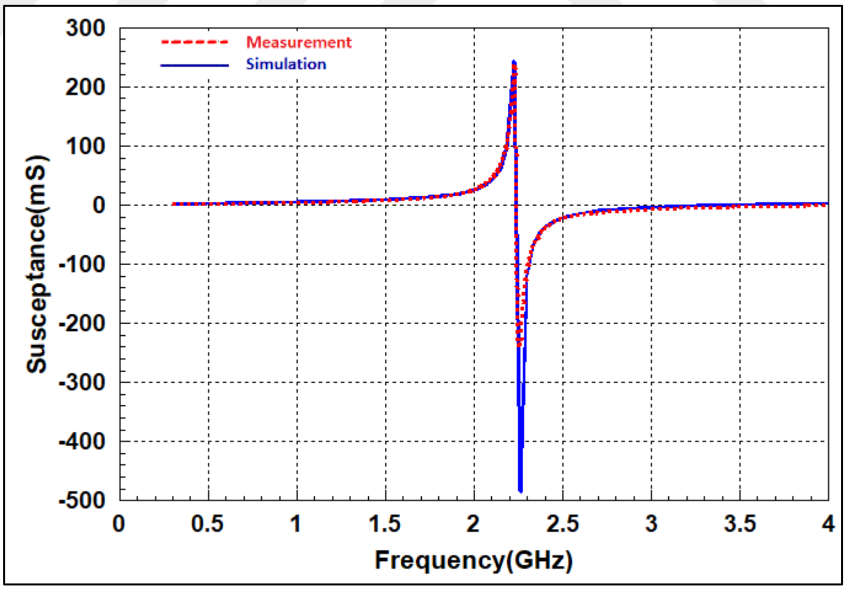

Figure 5.54. Susceptance value plot for 3 cm monopole in windowless bulkhead, 10 mm top aperture, axisymmetric position.

10 mm off-axis (Position 2)

Figure 5.55 and Figure 5.56 show conductance and susceptance value plots for 3 cm monopole in windowless bulkhead, 10 mm top aperture, 10 mm off-axis position. Some agreement between susceptance values is observed.

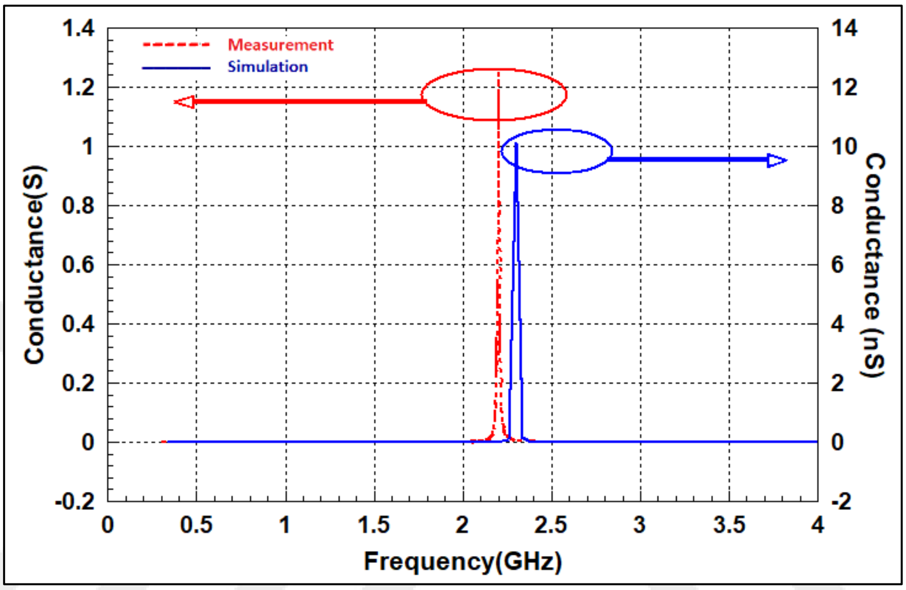

Figure 5.55. Conductance value plot for 3 cm monopole in windowless bulkhead, 10 mm top aperture, 10 mm off-axis.

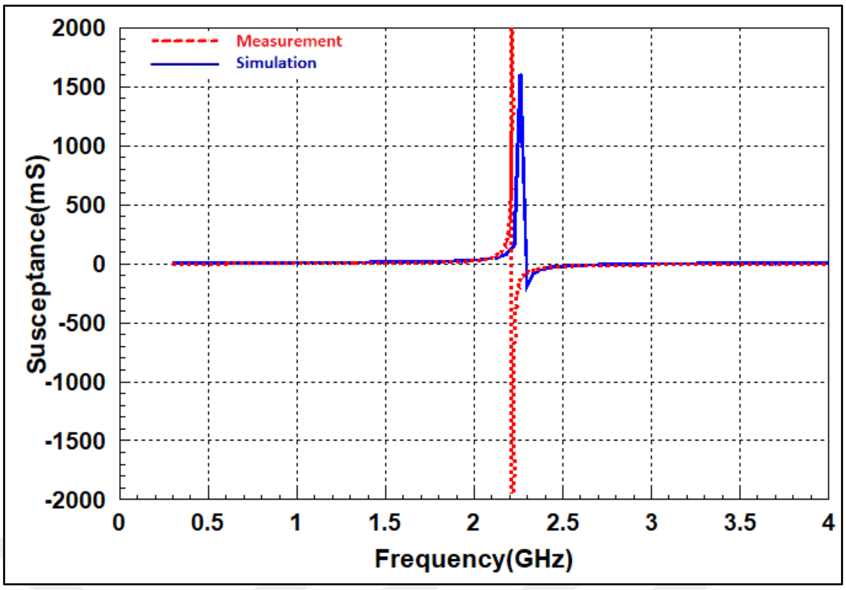

Figure 5.56. Susceptance value plot for 3 cm monopole in windowless bulkhead, 10 mm top aperture, 10 mm off-axis.

15 mm off-axis (Position 3)

Figure 5.57 and Figure 5.58 show conductance and susceptance value plots for 3 cm monopole in windowless bulkhead, 10 mm top aperture, 15 mm off-axis position. A small discrepancy between measurements and simulation values is observed.

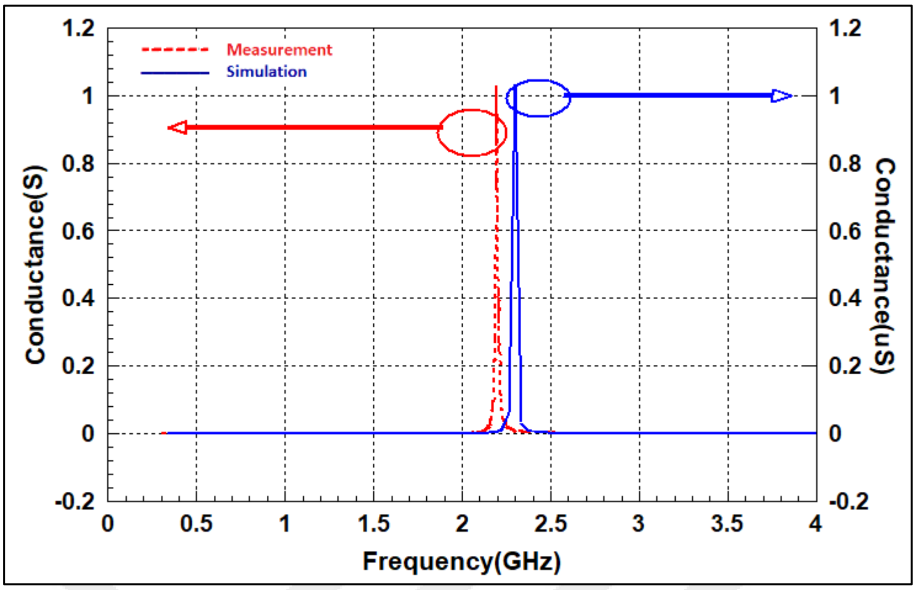

Figure 5.57. Conductance value plot for 3 cm monopole in windowless bulkhead, 10 mm top aperture, 15 mm off-axis.

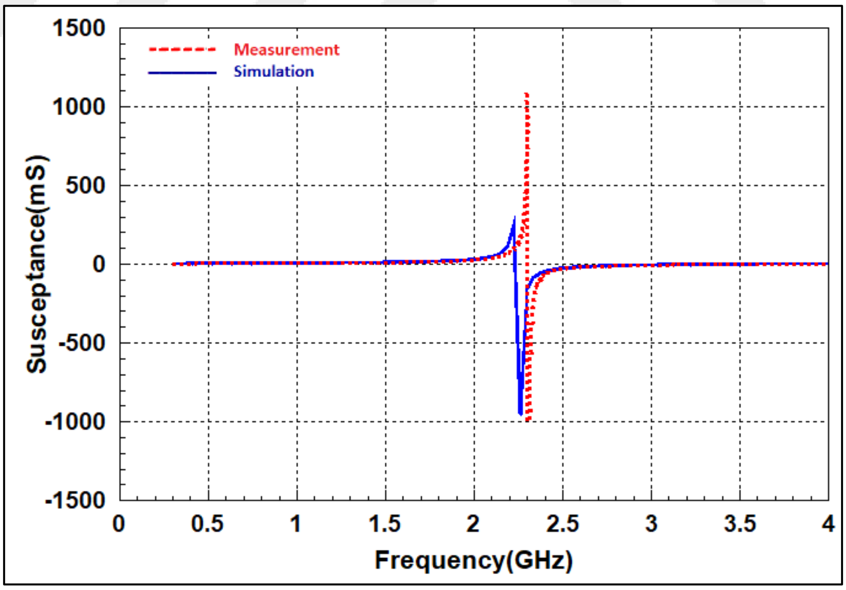

Figure 5.58. Susceptance value plot for 3 cm monopole in windowless bulkhead, 10 mm top aperture, 15 mm off-axis.

5.1.2.4. Top with 4 mm Aperture

Axisymmetric position (Position 1)

Figure 5.59 and Figure 5.60 show conductance and susceptance value plots for 3 cm monopole in windowless bulkhead, 4 mm top aperture, axisymmetric position. Some agreement between susceptance values is observed.

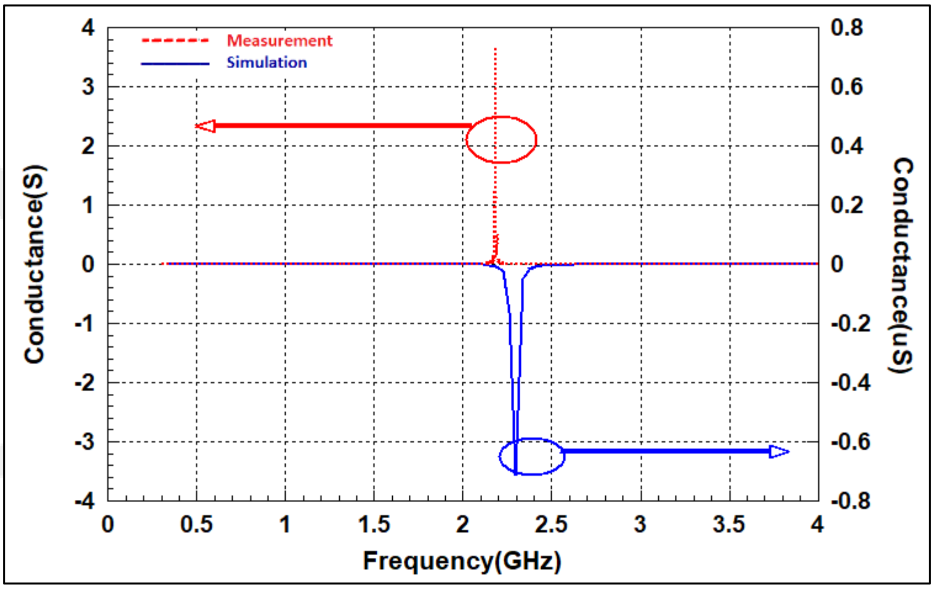

Figure 5.59. Conductance value plot for 3 cm monopole in windowless bulkhead, 4 mm top aperture, axisymmetric position.

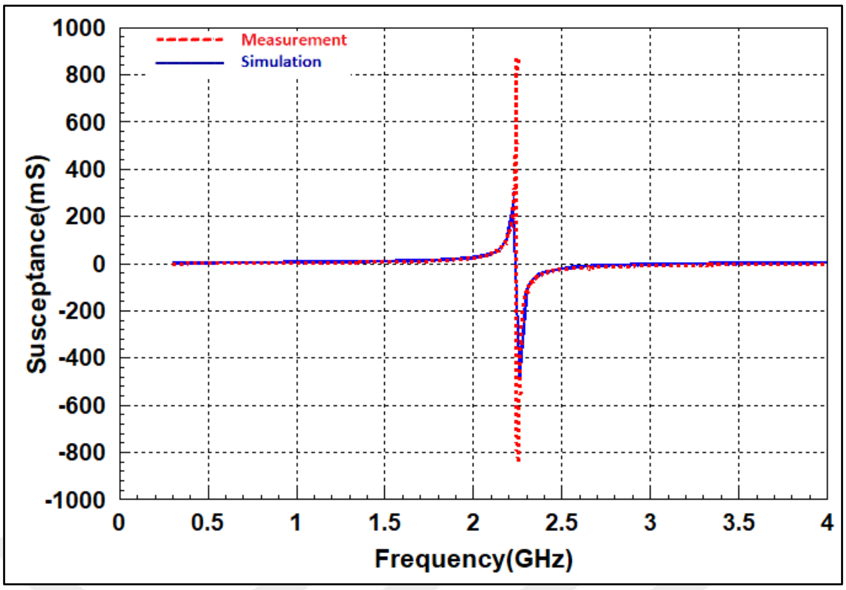

Figure 5.60. Susceptance value plot for 3 cm monopole in windowless bulkhead, 4 mm top aperture, axisymmetric position.

10 mm off-axis (Position 2)

Figure 5.61 and Figure 5.62 show conductance and susceptance value plots for 3 cm monopole in windowless bulkhead, 4 mm top aperture, 10 mm off-axis position. A small discrepancy between measurements and simulation values is observed.

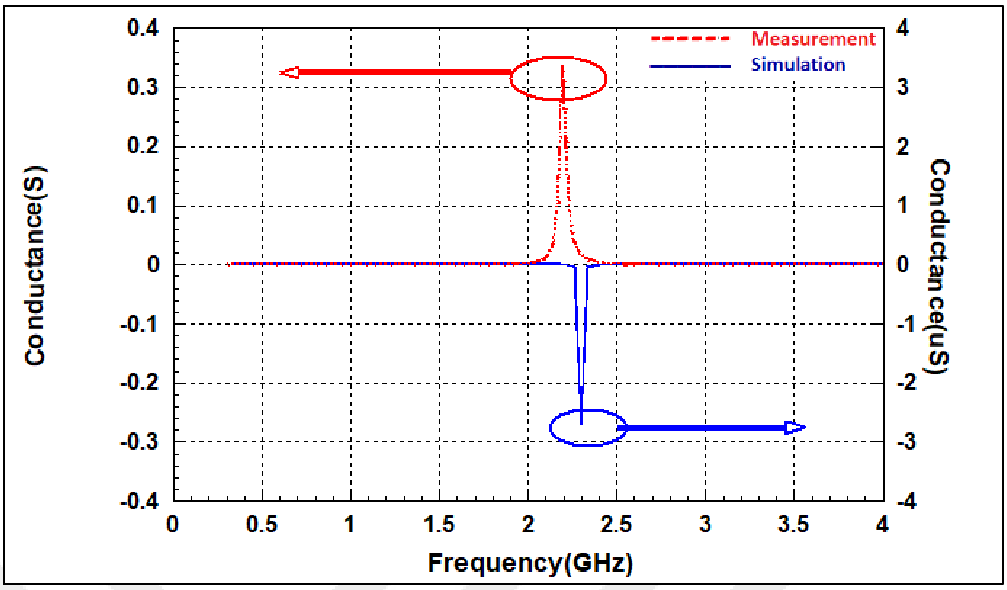

Figure 5.61. Conductance value plot for 3 cm monopole in windowless bulkhead, 4 mm top aperture,10 mm off-axis.

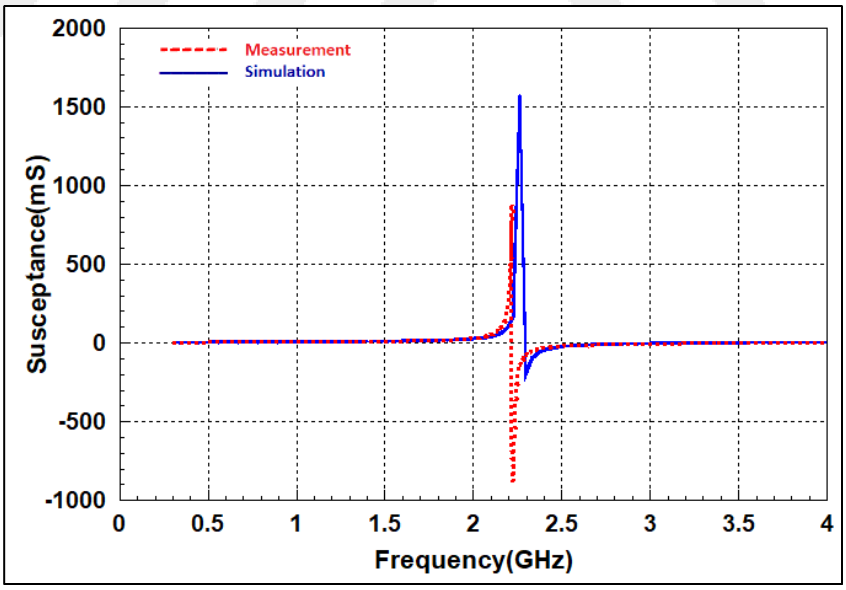

Figure 5.62. Susceptance value plot for 3 cm monopole in windowless bulkhead, 4 mm top aperture, 10 mm off-axis.

15 mm off-axis (Position 3)

Figure 5.63 and Figure 5.64 show conductance and susceptance value plots for 3 cm monopole in windowless bulkhead, 4 mm top aperture, 15 mm off-axis position. A small discrepancy between measurements and simulation values is observed.

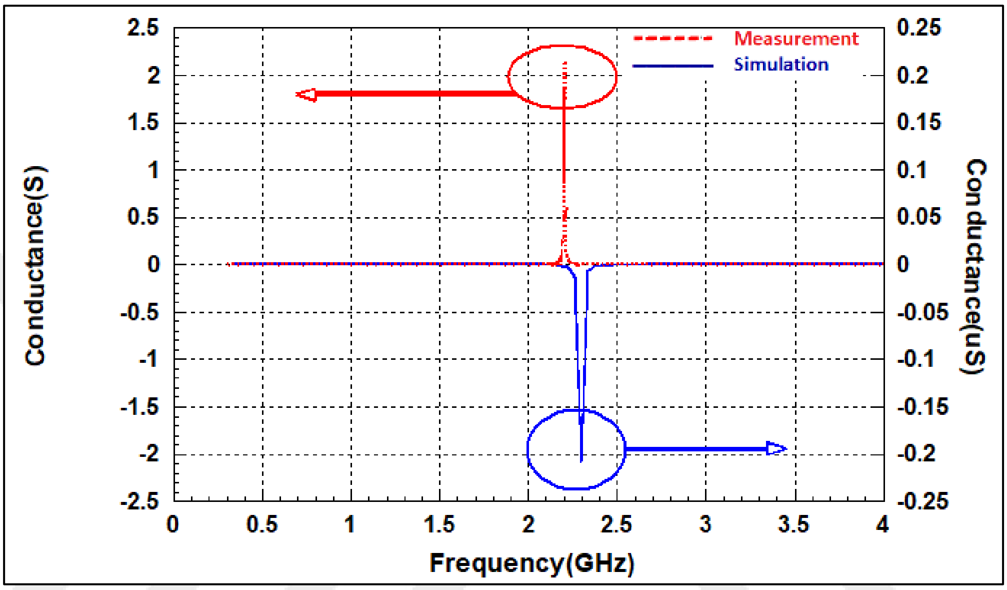

Figure 5.63. Conductance value plot for 3 cm monopole in windowless bulkhead, 4 mm top aperture,15 mm off-axis.

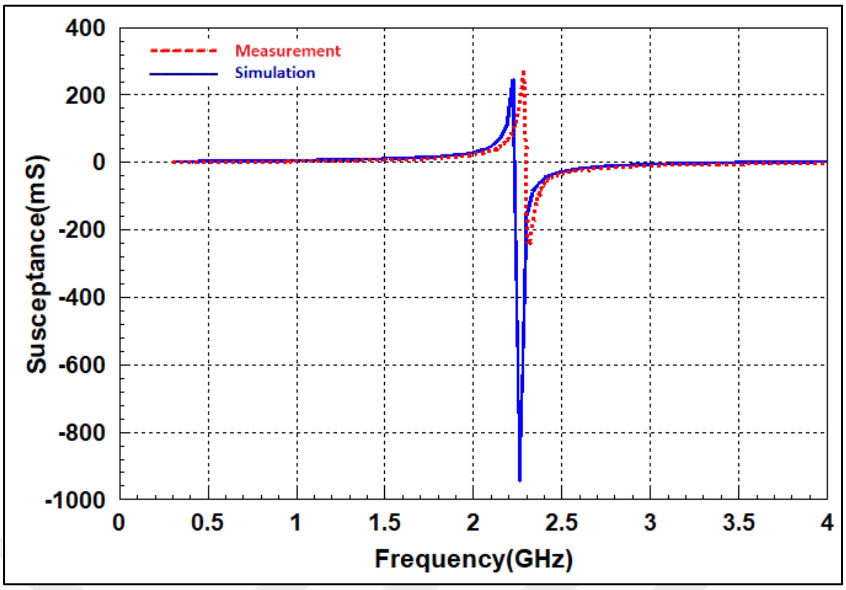

Figure 5.64. Susceptance value plot for 3 cm monopole in windowless bulkhead, 4 mm top aperture, 15 mm off-axis.

5.1.2.5. Top with no Aperture

Axisymmetric position (Position 1)

Figure 5.65 and Figure 5.66 show conductance and susceptance value plots for 3 cm monopole in windowless bulkhead, closed top aperture, axisymmetric position. Some agreement between susceptance values is observed.

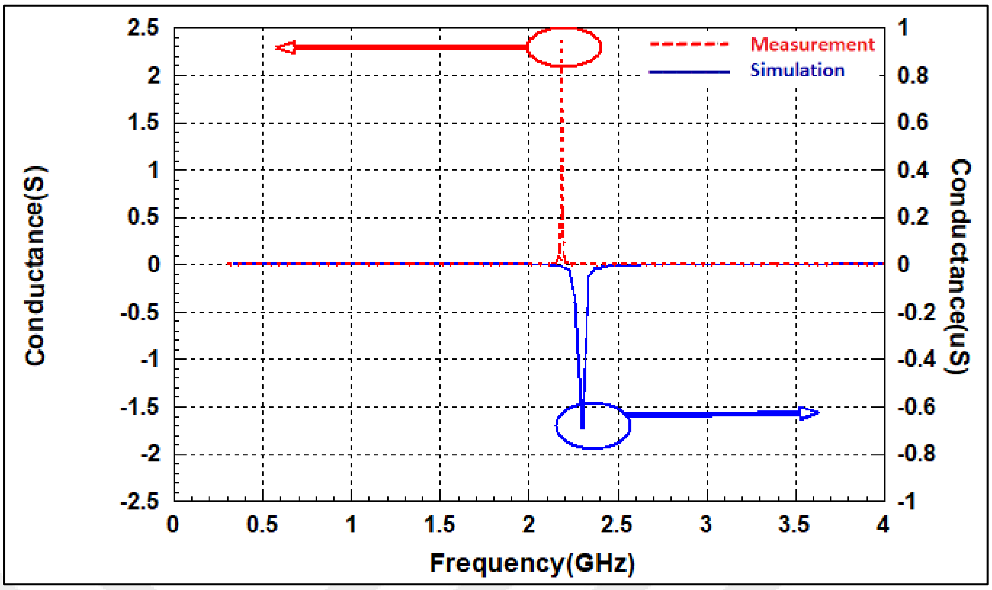

Figure 5.65. Conductance value plot for 3 cm monopole in windowless bulkhead, closed top aperture, axisymmetric position.

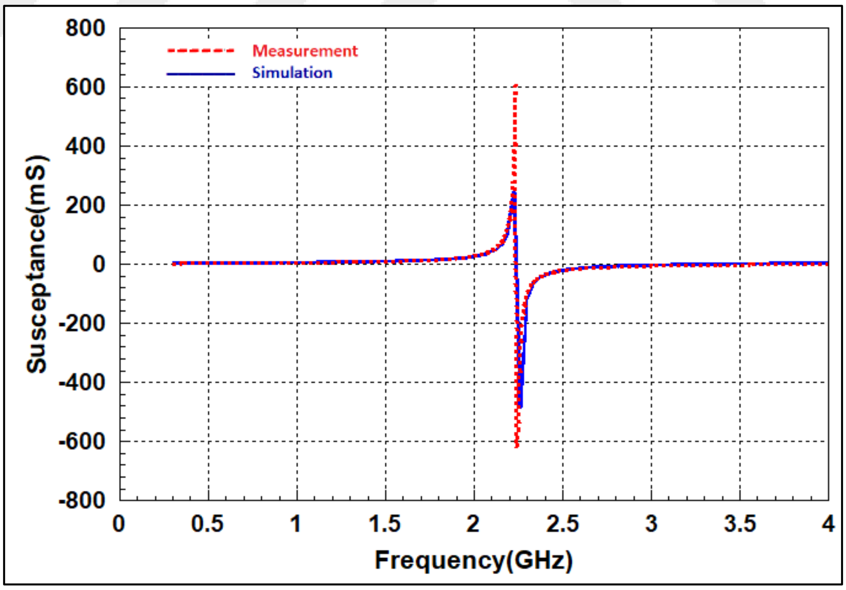

Figure 5.66. Susceptance value plot for 3 cm monopole in windowless bulkhead, closed top aperture, axisymmetric position.

10 mm off-axis (Position 2)

Figure 5.67 and Figure 5.68 show conductance and susceptance value plots for 3 cm monopole in windowless bulkhead, closed top aperture, 10 mm off-axis position. A small discrepancy between measurements and simulation values is observed.

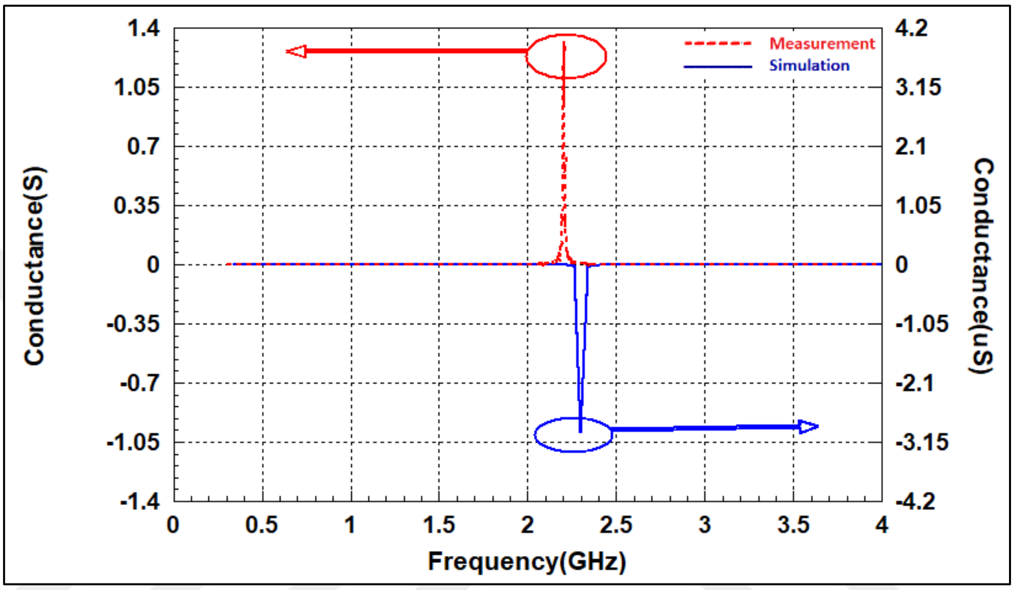

Figure 5.67. Conductance value plot for 3 cm monopole in windowless bulkhead, closed top aperture, 10 mm off-axis.

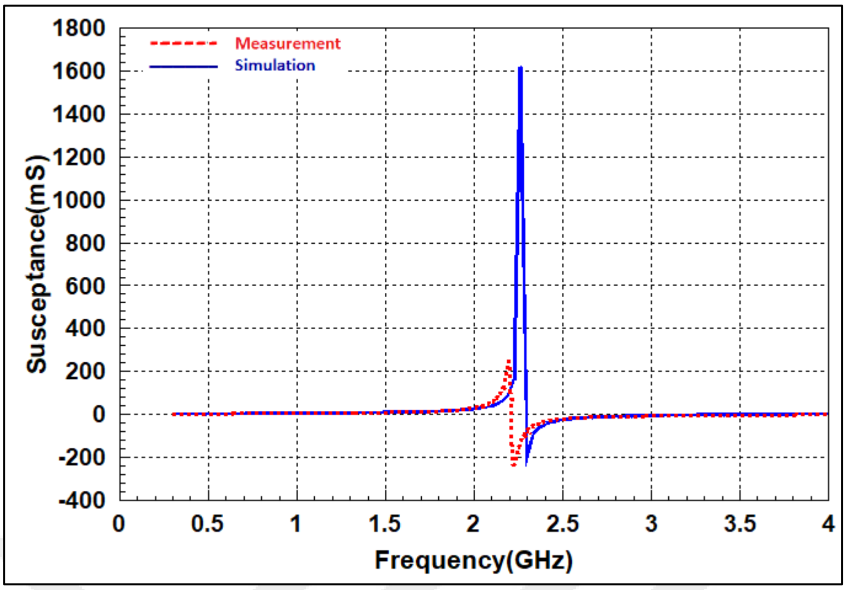

Figure 5.68. Susceptance value plot for 3 cm monopole in windowless bulkhead, closed top aperture, 10 mm off-axis.

15 mm off-axis (Position 3)

Figure 5.69 and Figure 5.70 show conductance and susceptance value plots for 3 cm monopole in windowless bulkhead, closed top aperture, 15 mm off-axis position. A small discrepancy between measurements and simulation values is observed.

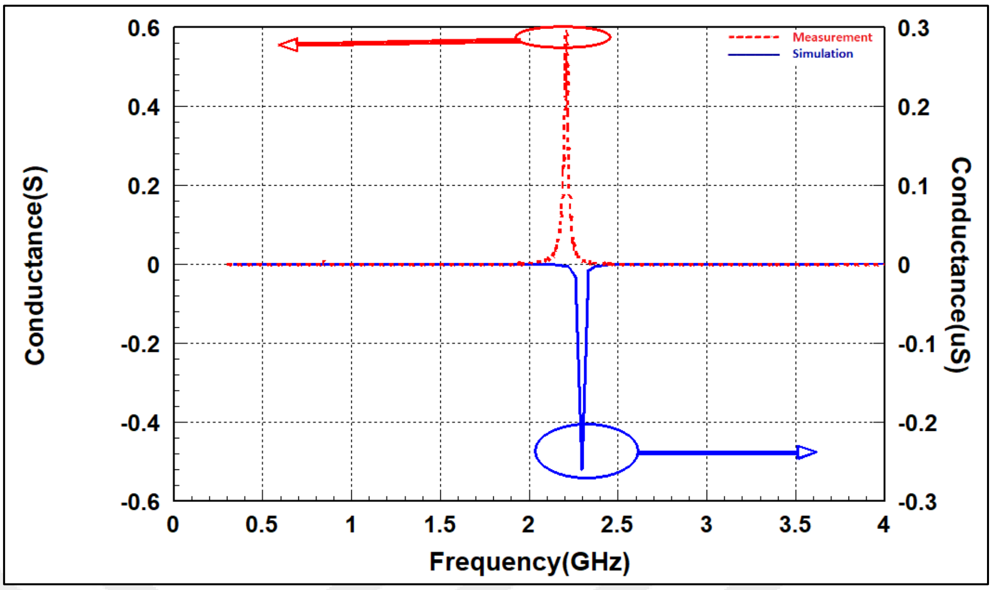

Figure 5.69. Conductance value plot for 3 cm monopole in windowless bulkhead, closed top aperture, 15 mm off-axis.

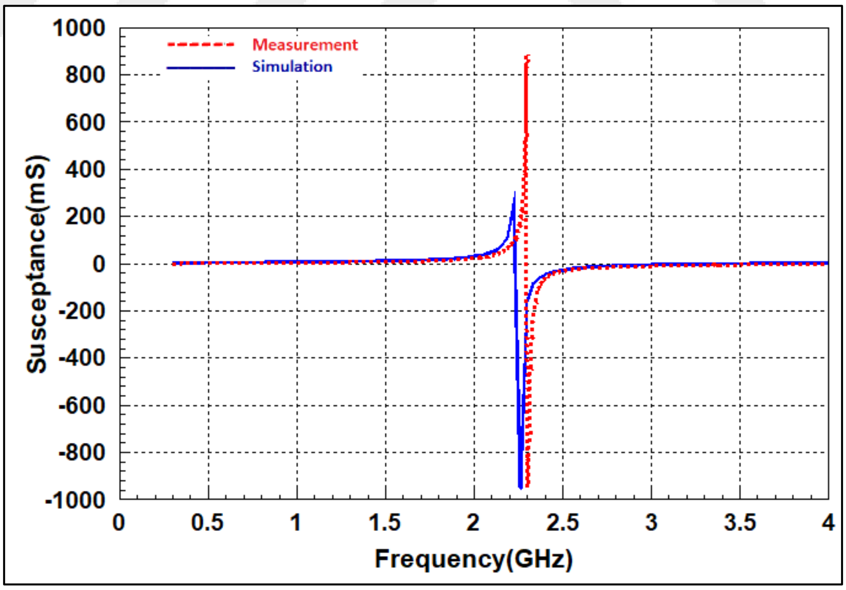

Figure 5.70. Susceptance value plot for 3 cm monopole in windowless bulkhead, closed top aperture, 15 mm off-axis.

5.1.3. Summary and Discussion of 3 cm Antenna Results

As can be seen in 5.1.1 and 5.1.2 there is a frequency shift between calculations from measurements and simulations. This frequency difference is seen in Table 5.1, Table 5.2, Table 5.3, Table 5.4, Table 5.5, Table 5.6, Table 5.7 and Table 5.8 below. Among all of the results best match is obtained at susceptance value comparisions for axisymmetric position as 5.2 MHz deviation from simulations while the rest of the measurements differ more than 10 MHz from simulations. Most of the measurement results are lower than the simulated results by -95.8 MHz to -63.4 MHz while measurements for 15 mm off-axis towards window scenario resulted in positive difference for both susceptance and conductance comparisons. The results agree with the previous works done on the subject [10,11].

Table 5.1. Conductance difference between measurements and simulations for 3 cm antenna at axisymmetric position (position 1)

Structure		**Measurement (MHz)**	**Simulated (MHz)**	**Difference (MHz)**
bulkhead with window	open top aperture	2149	2245	-96
	15 mm top aperture	2145	2244	-99
	10 mm top aperture	2130	2244	-114
	4 mm top aperture	2163	2244	-81
	closed top aperture	2155	2244	-89
	AVERAGE			-95.8
bulkhead without window	open top aperture	2184	2249	-65
	15 mm top aperture	2182	2249	-67
	10 mm top aperture	2182	2249	-67
	4 mm top aperture	2184	2249	-65
	closed top aperture	2184	2249	-65
	AVERAGE			-82.2

Table 5.2. Susceptance difference between measurements and simulations for 3 cm antenna at axisymmetric position (position 1)

Structure		Measurement (MHz)	Simulated (MHz)	Difference (MHz)
bulkhead with window	open top aperture	2230	2240	-10
	15 mm top aperture	2251	2234	17
	10 mm top aperture	2144	2241	-97
	4 mm top aperture	2149	2241	-92
	closed top aperture	2239	2241	-2
	Average difference			-36.8
bulkhead without window	open top aperture	2241	2236	5
	15 mm top aperture	2240	2237	3
	10 mm top aperture	2243	2237	6
	4 mm top aperture	2245	2237	8
	closed top aperture	2240	2236	4
	Average difference			5.2

Table 5.3. Conductance difference between measurements and simulations for 3 cm antenna at 10 mm off-axis position towards window (position 2)

Structure		Measurement (MHz)	Simulated (MHz)	Difference (MHz)
bulkhead with window	open top aperture	2157	2251	-94
	15 mm top aperture	2178	2251	-73
	10 mm top aperture	2165	2254	-89
	4 mm top aperture	2158	2251	-93
	closed top aperture	2168	2251	-83
	Average difference			-86.4
bulkhead without window	open top aperture	2202	2265	-63
	15 mm top aperture	2202	2265	-63
	10 mm top aperture	2198	2265	-67
	4 mm top aperture	2197	2265	-68
	closed top aperture	2200	2265	-65
	Average difference			-76.8

Table 5.4. Susceptance difference between measurements and simulations for 3 cm antenna at 10 mm off-axis position towards window (position 2)

Structure		**Measurement (MHz)**	**Simulated (MHz)**	**Difference (MHz)**
bulkhead with window	open top aperture	2193	2234	-41
	15 mm top aperture	2204	2231	-27
	10 mm top aperture	2203	2234	-31
	4 mm top aperture	2157	2234	-77
	closed top aperture	2206	2234	-28
	Average difference			-40.8
bulkhead without window	open top aperture	2218	2294	-76
	15 mm top aperture	2213	2294	-81
	10 mm top aperture	2217	2294	-77
	4 mm top aperture	2217	2294	-77
	closed top aperture	2215	2294	-79
	Average difference			-78

Table 5.5. Conductance difference between measurements and simulations for 3 cm antenna at 15 mm off-axis position towards window (position 3)

Structure		**Measurement (MHz)**	**Simulated (MHz)**	**Difference (MHz)**
bulkhead with window	open top aperture	2143	2240	-97
	15 mm top aperture	2143	2237	-94
	10 mm top aperture	2135	2240	-105
	4 mm top aperture	2187	2238	-51
	closed top aperture	2133	2239	-106
	Average difference			-90.6
bulkhead without window	open top aperture	2186	2253	-67
	15 mm top aperture	2199	2253	-54
	10 mm top aperture	2195	2253	-58
	4 mm top aperture	2199	2253	-54
	closed top aperture	2207	2253	-46
	Average difference			-74.8

Table 5.6. Susceptance difference between measurements and simulations for 3 cm antenna at 15 mm off-axis position towards window (position 3)

Structure		Measurement (MHz)	Simulated (MHz)	Difference (MHz)
bulkhead with window	open top aperture	2221	2246	-25
	15 mm top aperture	2287	2245	42
	10 mm top aperture	2270	2247	23
	4 mm top aperture	2283	2246	37
	closed top aperture	2286	2247	39
	Average difference			23.2
bulkhead without window	open top aperture	2277	2232	45
	15 mm top aperture	2303	2232	71
	10 mm top aperture	2306	2232	74
	4 mm top aperture	2299	2232	67
	closed top aperture	2303	2232	71
	Average difference			65.6

Table 5.7. Conductance difference between measurements and simulations for 3 cm antenna at 10 mm off-axis position away from window (position 4)

Structure		Measurement (MHz)	Simulated (MHz)	Difference (MHz)
bulkhead with window	open top aperture	2168	2260	-92
	15 mm top aperture	2189	2260	-71
	10 mm top aperture	2167	2263	-96
	4 mm top aperture	2187	2248	-61
	closed top aperture	2177	2261	-84
	Average difference			-80.8

Table 5.8. Susceptance difference between measurements and simulations for 3 cm antenna at 10 mm off-axis position away from window (position 4)

Structure		Measurement (MHz)	Simulated (MHz)	Difference (MHz)
bulkhead with window	open top aperture	2188	2238	-50
	15 mm top aperture	2168	2296	-128
	10 mm top aperture	2190	2225	-35
	4 mm top aperture	2169	2225	-56
	closed top aperture	2177	2225	-48
	AVERAGE			-63.4

5.2. 5 CM ANTENNA

5.2.1. Bulkhead with Window

For this comparision scenario from Figure 4.3(b) is used as bulkhead. All of the simulations and measurments made accordingly.

5.2.1.1. Open Top Aperture

Axisymmetric position (Position 1)

Figure 5.71 and Figure 5.72 show conductance and susceptance value plots for 5 cm monopole in windowed bulkhead, open top aperture, axisymmetric position. Some agreement can be seen in the measurements of susceptance plot.

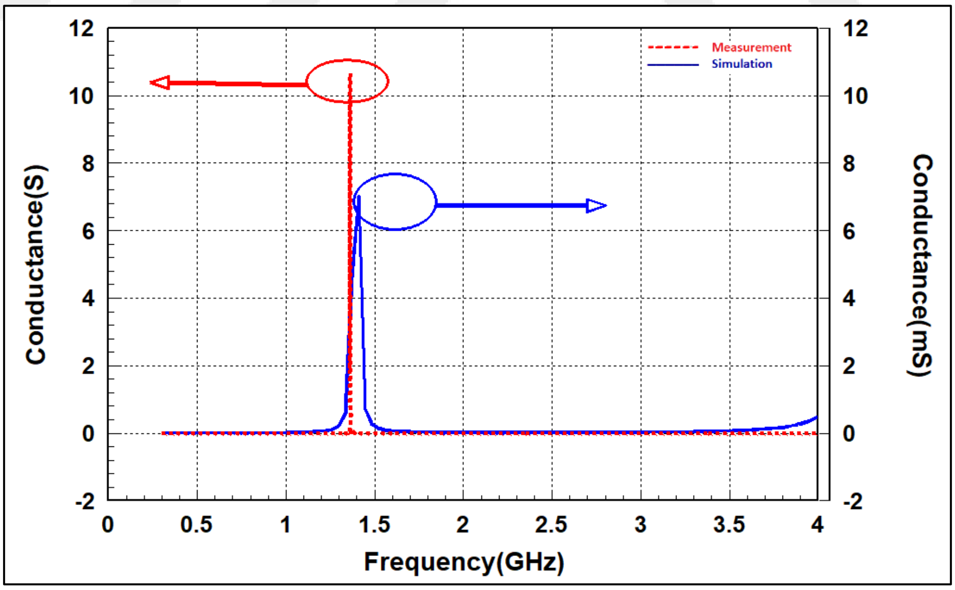

Figure 5.71. Conductance value plot for 5 cm monopole in windowed bulkhead, open top aperture, axisymmetric position.

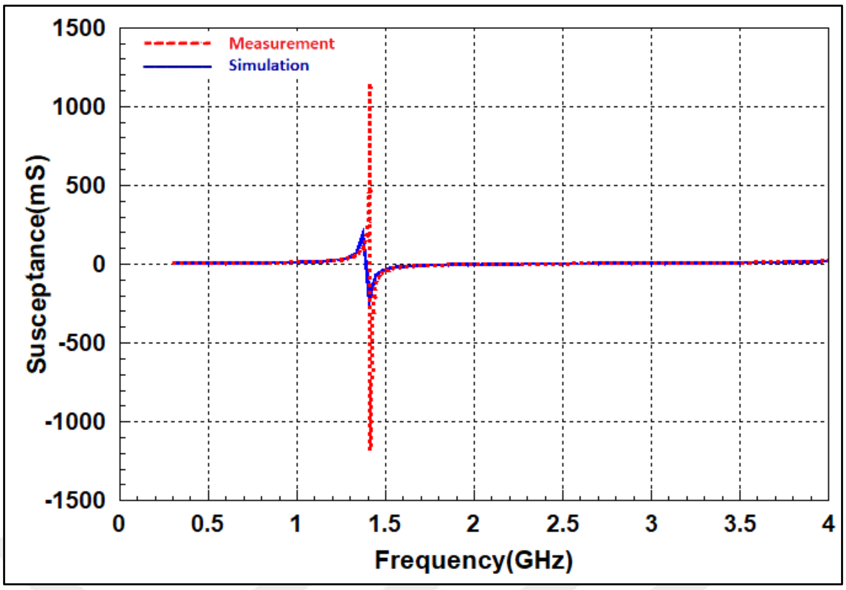

Figure 5.72. Susceptance value plot for 5 cm monopole in windowed bulkhead, open top aperture, axisymmetric position.

10 mm off-axis towards bulkhead window (Position 2)

Figure 5.73 and Figure 5.74 show conductance and susceptance value plots for 5 cm monopole in windowed bulkhead, open top aperture, 10 mm off-axis towards window. Some agreement can be seen in the measurements of susceptance plot.

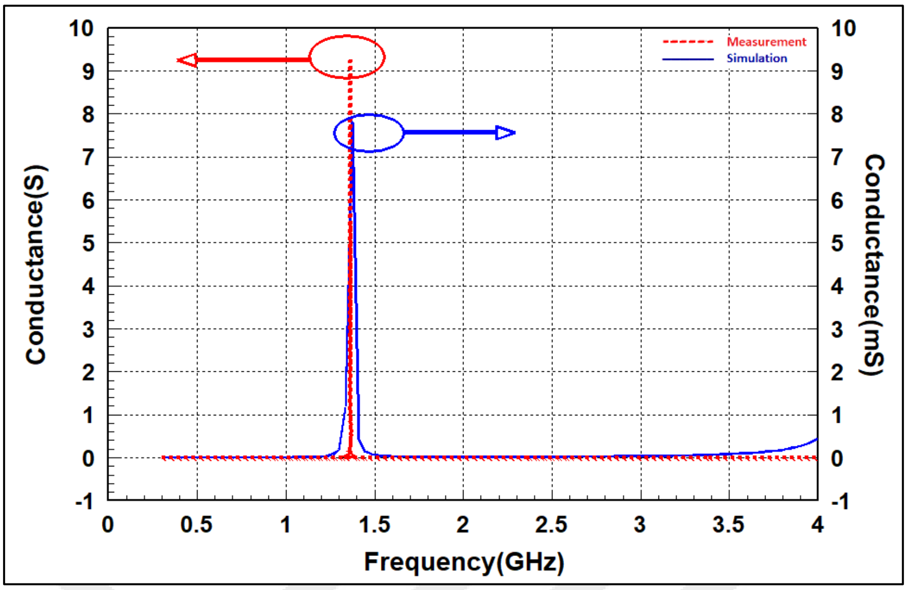

Figure 5.73. Conductance value plot for 5 cm monopole in windowed bulkhead, open top aperture, 10 mm off-axis towards window.

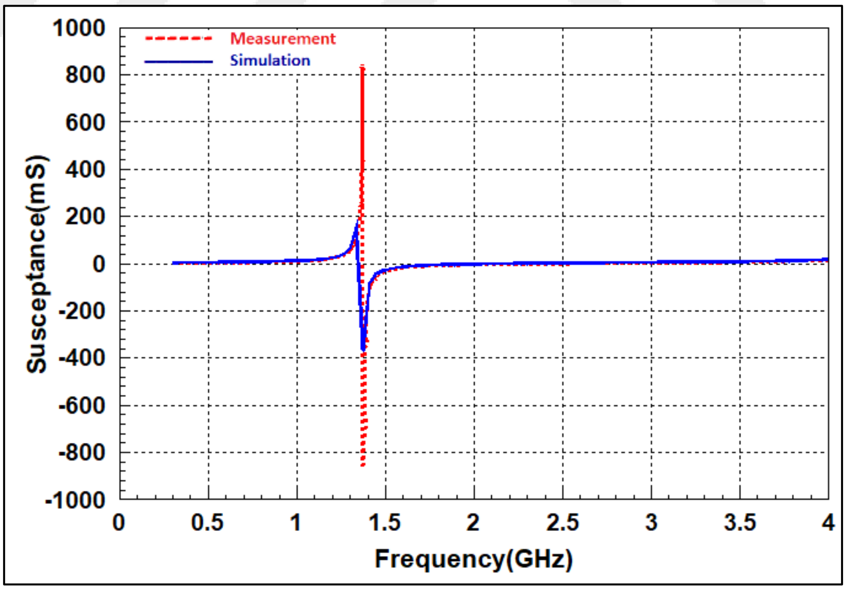

Figure 5.74. Susceptance value plot for 5 cm monopole in windowed bulkhead, open top aperture, 10 mm off-axis towards window.

15 mm off-axis towards bulkhead window (Position 3)

Figure 5.75 and Figure 5.76 show conductance and susceptance value plots for 5 cm monopole in windowed bulkhead, open top aperture, 15 mm off-axis towards window. 164 MHz frequency difference is observed between simulations and measurements for conductance values.

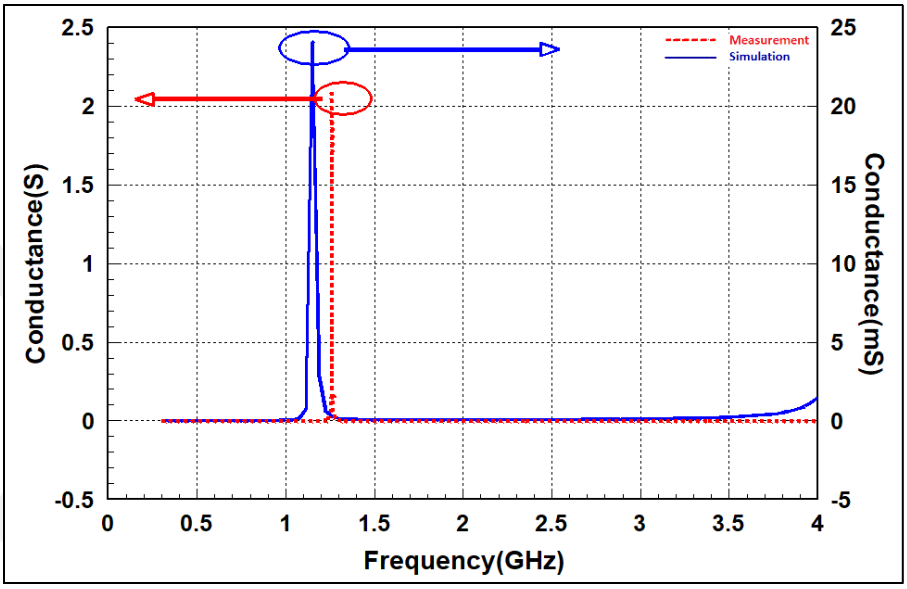

Figure 5.75. Conductance value plot for 5 cm monopole in windowed bulkhead, open top aperture, 15 mm off-axis towards window.

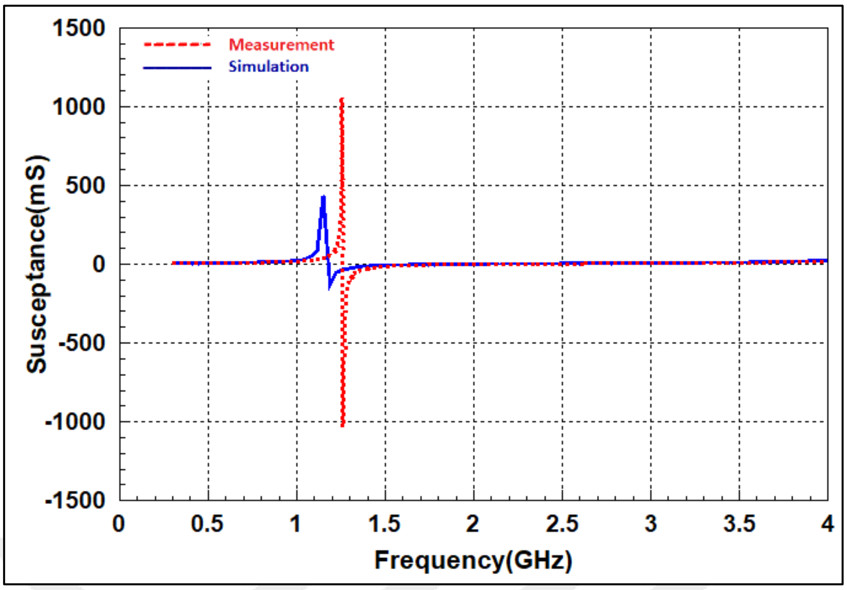

Figure 5.76. Susceptance value plot for 5 cm monopole in windowed bulkhead, open top aperture, 15 mm off-axis towards window.

10 mm off-axis away from bulkhead window (Position 4)

Figure 5.77 and Figure 5.78 show conductance and susceptance value plots for 5 cm monopole in windowed bulkhead, open top aperture, 10 mm off-axis away from window.Some agreement can be observed between simulations and measurements for both conductance and susceptance values.

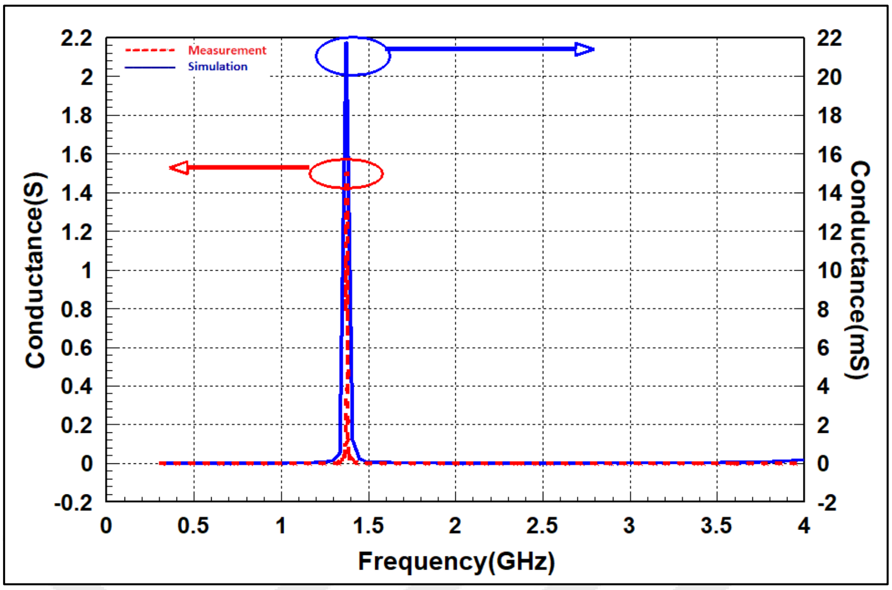

Figure 5.77. Conductance value plot for 5 cm monopole in windowed bulkhead, open top aperture, 10 mm off-axis away from window.

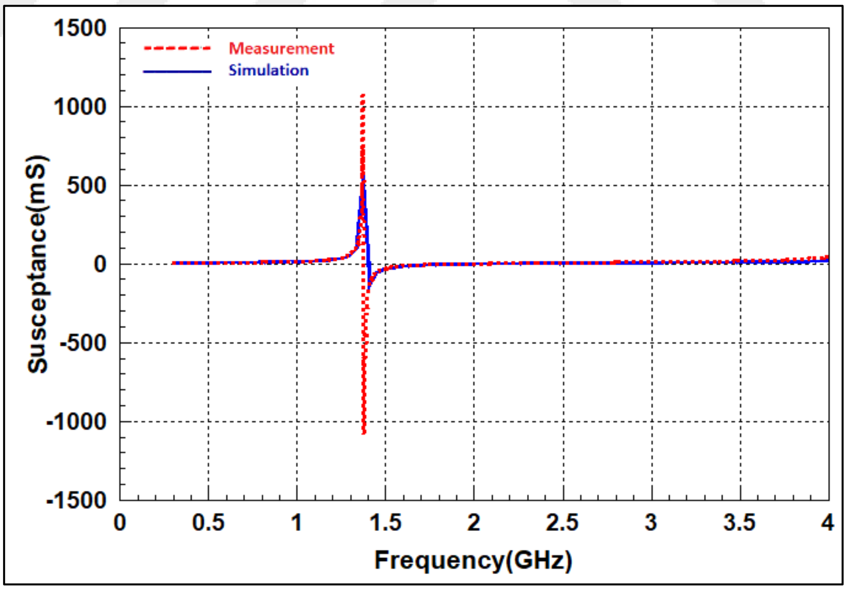

Figure 5.78. Susceptance value plot for 5 cm monopole in windowed bulkhead, open top aperture, 10 mm off-axis away from window.

5.2.1.2. Top with 15 mm Aperture

Axisymmetric position (Position 1)

Figure 5.79 and Figure 5.80 below show conductance and susceptance plots for 5 cm monopole in windowed bulkhead, 15 mm top aperture, axisymmetric position.Some agreement between the measurements and the simulations can be observed.

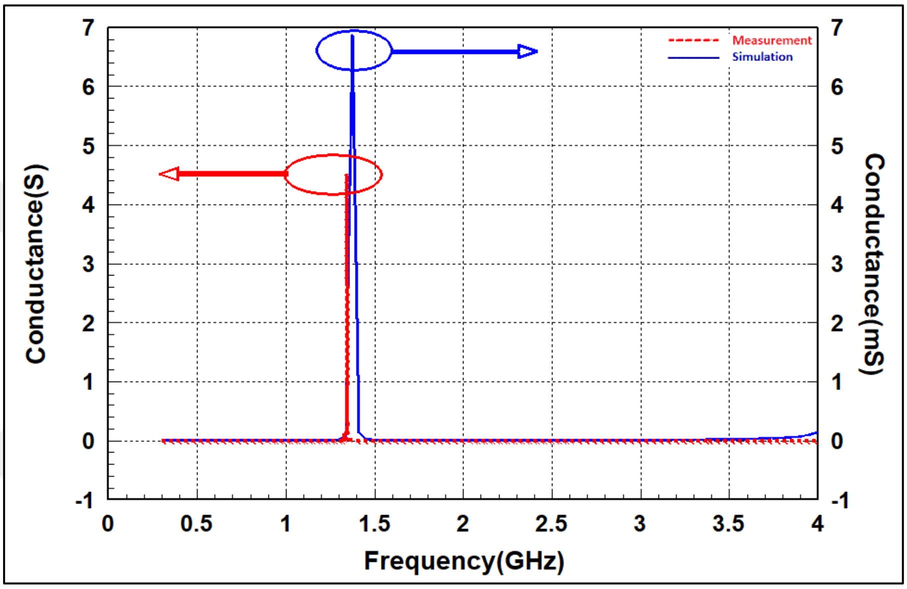

Figure 5.79. Conductance value plot for 5 cm monopole in windowed bulkhead, 15 mm top aperture, axisymmetric position.

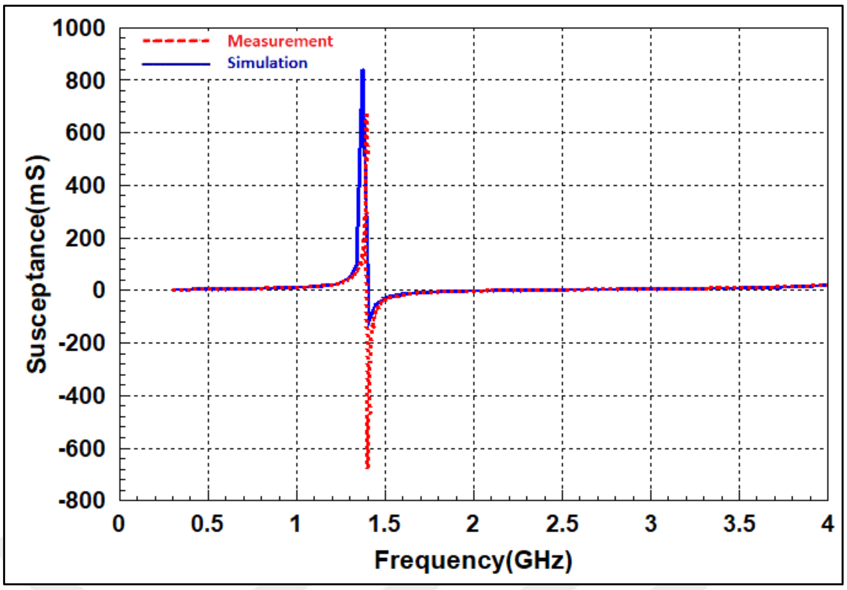

Figure 5.80. Susceptance value plot for 5 cm monopole in windowed bulkhead, 15 mm top aperture, axisymmetric position.

10 mm off-axis towards bulkhead window (Position 2)

Figure 5.81 and Figure 5.82 show conductance and susceptance value plots for 5 cm monopole in windowed bulkhead, 15 mm top aperture, 10 mm off-axis towards window. Some agreement between the measurements and the simulations can be observed.

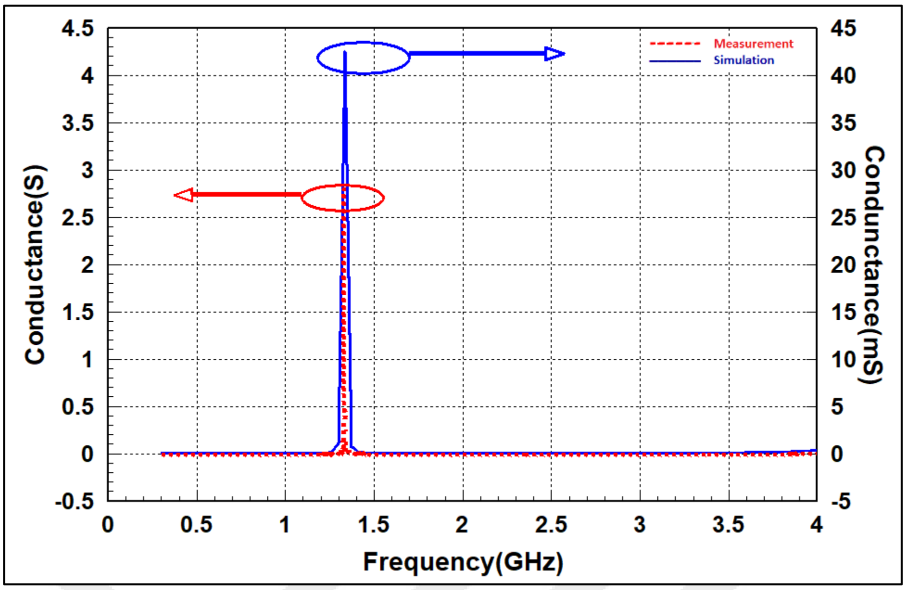

Figure 5.81. Conductance value plot for 5 cm monopole in windowed bulkhead, 15 mm top aperture, 10 mm off-axis towards window.

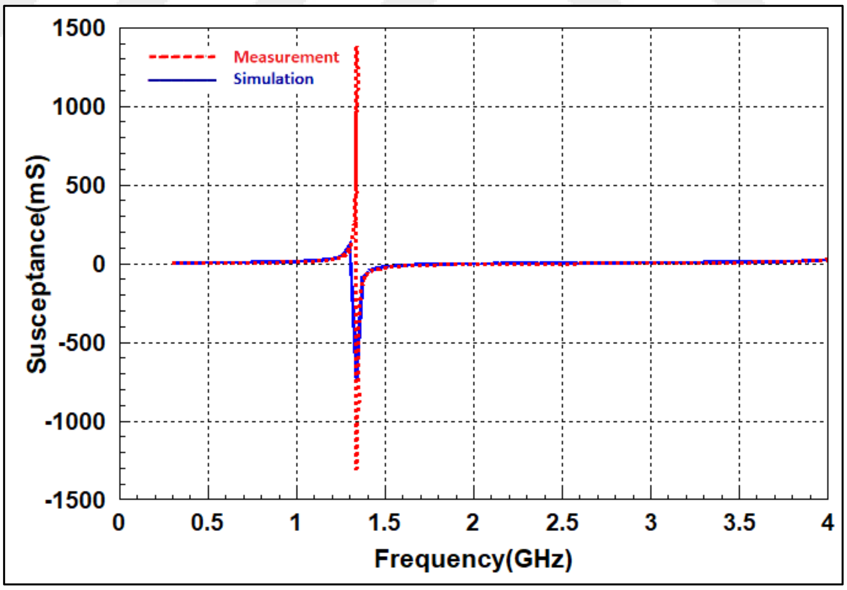

Figure 5.82. Susceptance value plot for 5 cm monopole in windowed bulkhead, 15 mm top aperture, 10 mm off-axis towards window.

15 mm off-axis towards bulkhead window (Position 3)

Figure 5.83 and Figure 5.84 show conductance and susceptance value plots for 5 cm monopole in windowed bulkhead, 15 mm top aperture, 15 mm off-axis towards window. 173 MHz frequency difference is observed between simulations and measurements for susceptance values.

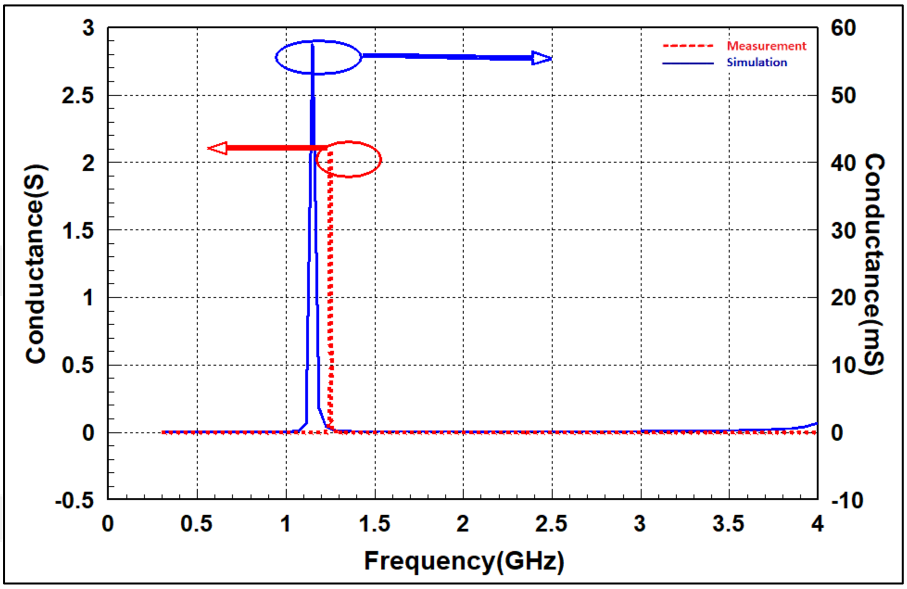

Figure 5.83. Conductance value plot for 5 cm monopole in windowed bulkhead, 15 mm top aperture, 15 mm off-axis towards window.

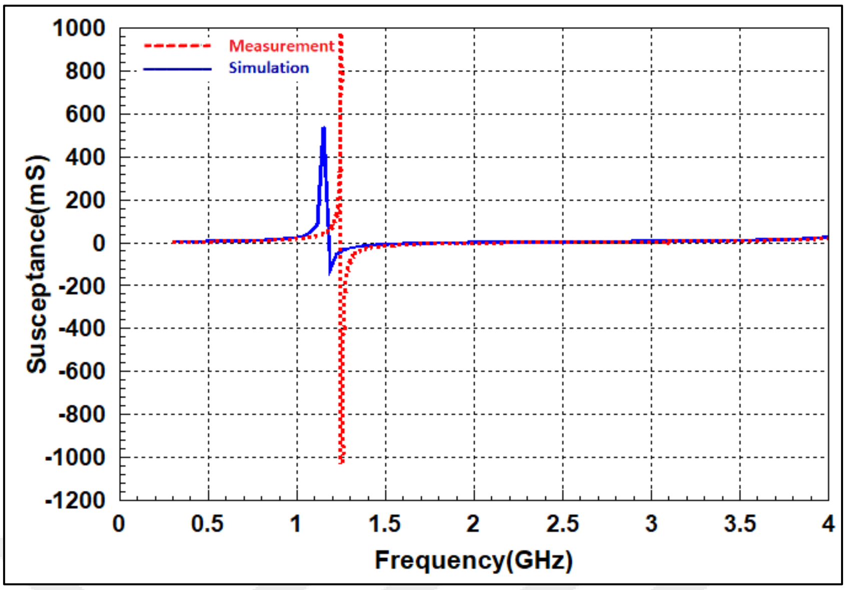

Figure 5.84. Susceptance value plot for 5 cm monopole in windowed bulkhead, 15 mm top aperture, 15 mm off-axis towards window.

10 mm off-axis away from bulkhead window (Position 4)

Figure 5.85 and Figure 5.86 show conductance and susceptance value plots for 5 cm monopole in windowed bulkhead, 15 mm top aperture, 10 mm off-axis away from window. Some agreement between the susceptance measurements and the simulations for both conductance and susceptance values is observed.

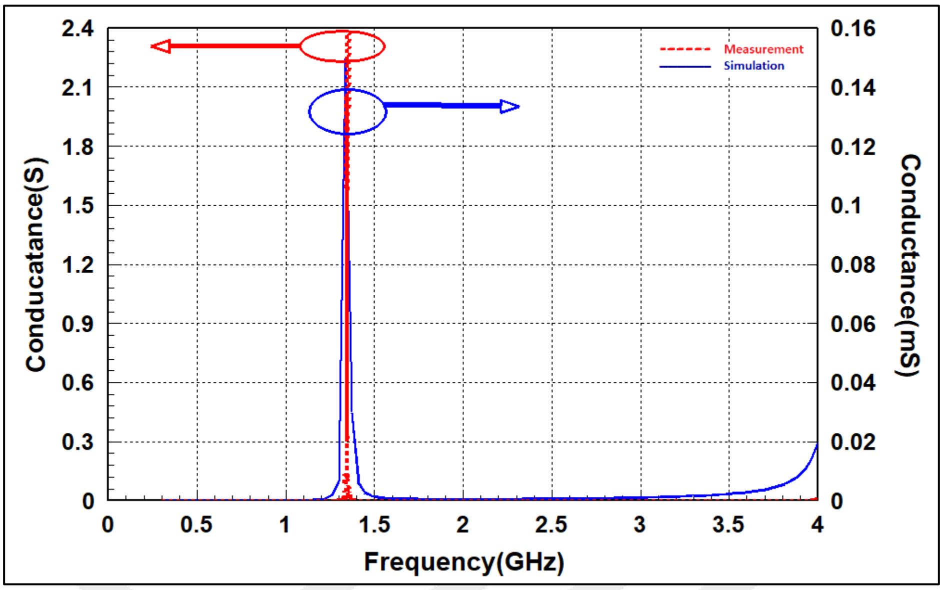

Figure 5.85. Conductance value plot for 5 cm monopole in windowed bulkhead, 15 mm top aperture, 10 mm off-axis away from window.

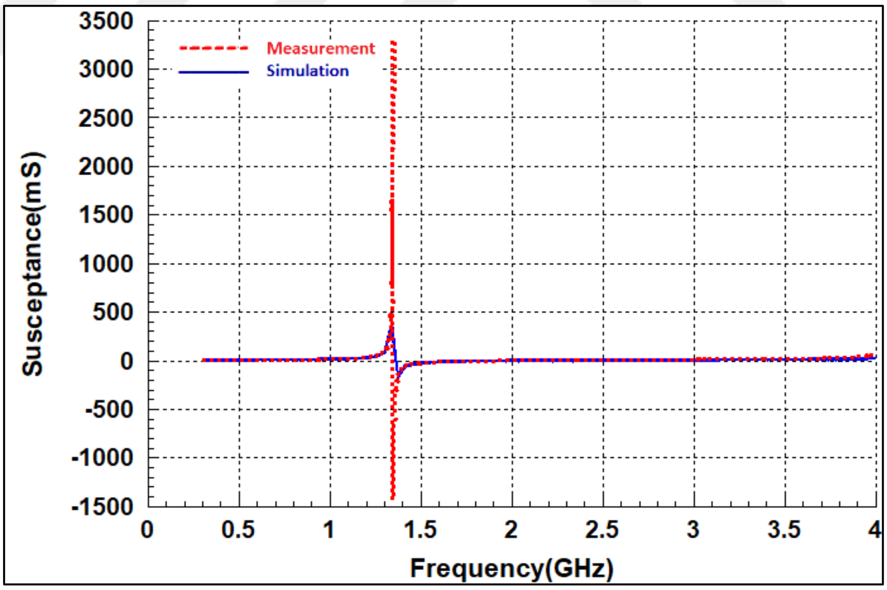

Figure 5.86. Susceptance value plot plot for 5 cm monopole in windowed bulkhead, 15 mm top aperture, 10 mm off-axis away from window.

5.2.1.3. Top with 10 mm Aperture

Axisymmetric position (Position 1)

Figure 5.87 and Figure 5.88 show conductance and susceptance value plots for 5 cm monopole in windowed bulkhead, 10 mm top aperture, axisymmetric position. A small discrepancy between measurements and simulation values is observed.

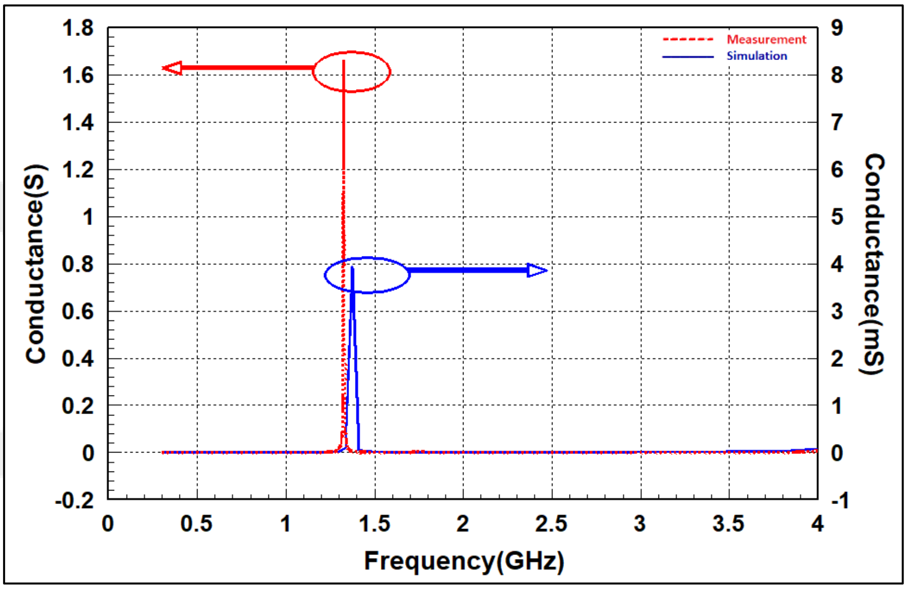

Figure 5.87. Conductance value plot for 5 cm monopole in windowed bulkhead, 10 mm top aperture, axisymmetric position.

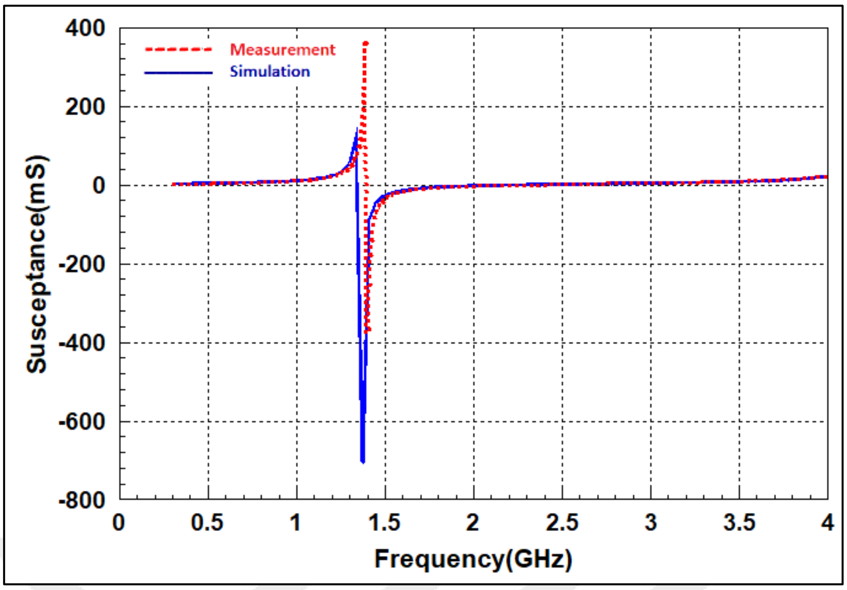

Figure 5.88. Susceptance value plot for 5 cm monopole in windowed bulkhead, 10 mm top aperture, axisymmetric position.

10 mm off-axis towards bulkhead window (Position 2)

Figure 5.89 and Figure 5.90 show conductance and susceptance value plots for 5 cm monopole in windowed bulkhead, 10 mm top aperture, 10 mm off-axis towards window. Some agreement between the susceptance measurements and the simulations for both conductance and susceptance values is observed.

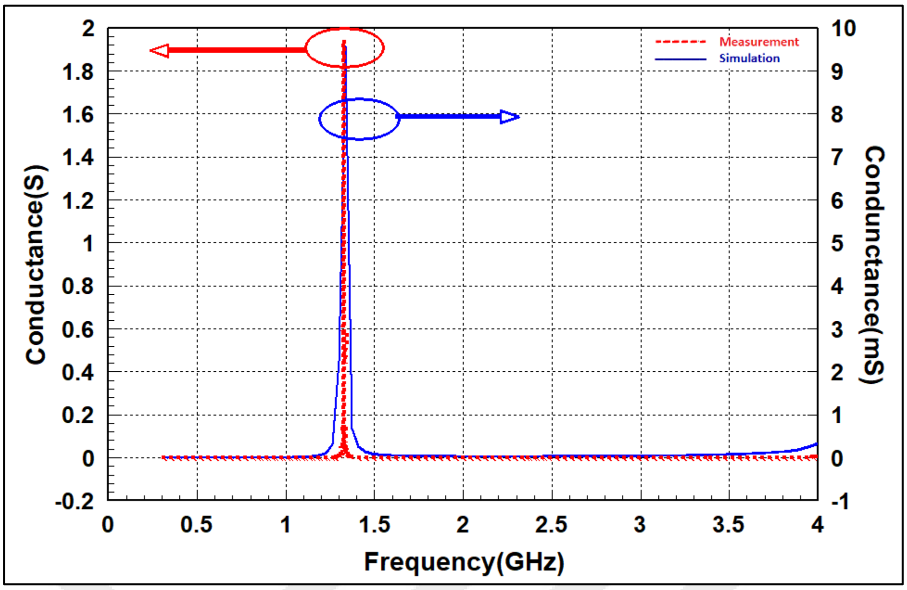

Figure 5.89. Conductance value plot for 5 cm monopole in windowed bulkhead, 10 mm top aperture, 10 mm off-axis towards window.

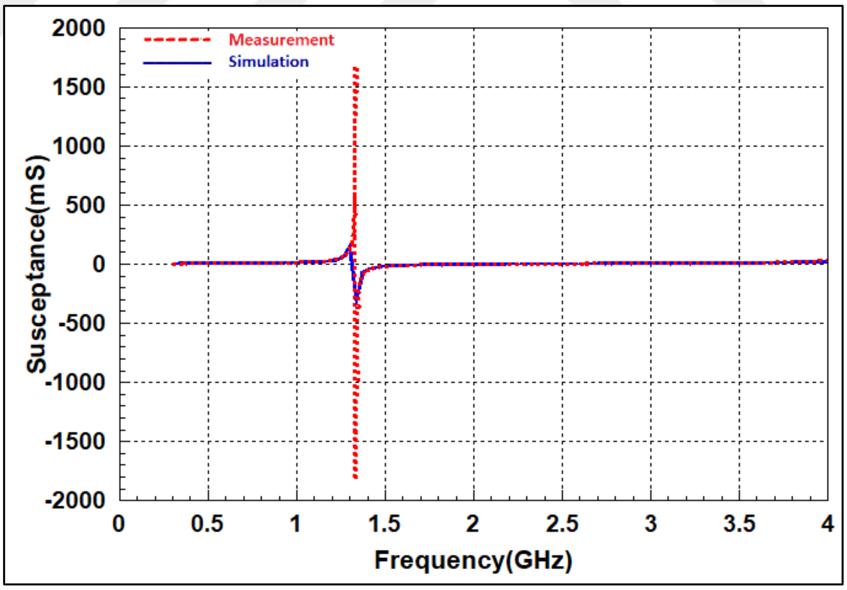

Figure 5.90. Susceptance value plot for 5 cm monopole in windowed bulkhead, 10 mm top aperture, 10 mm off-axis towards window.

15 mm off-axis towards bulkhead window (Position 3)

Figure 5.91 and Figure 5.92 show conductance and susceptance value plots for 5 cm monopole in windowed bulkhead, 10 mm top aperture, 15 mm off-axis towards window. A huge difference between the measurements and the simulations can be observed.

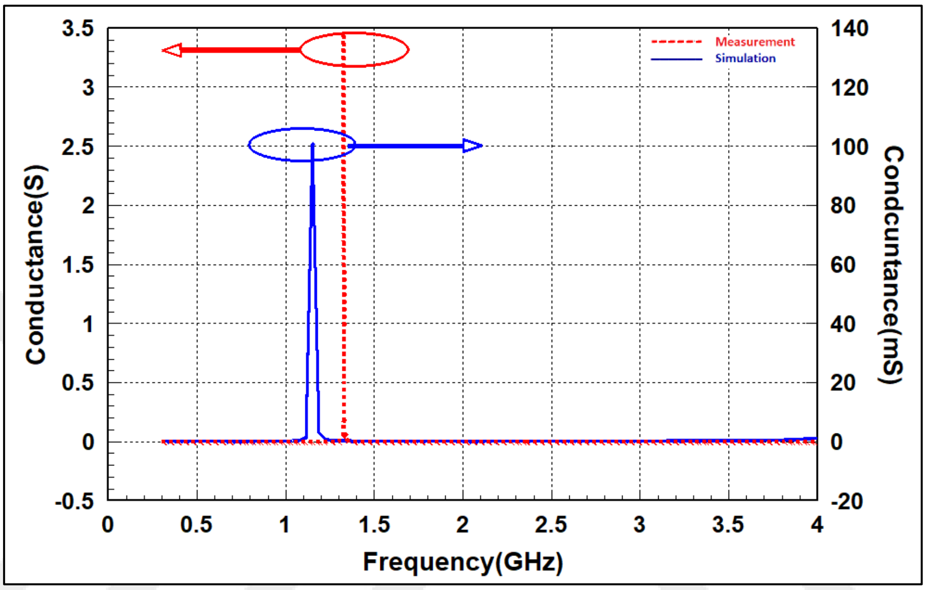

Figure 5.91. Conductance value plot for 5 cm monopole in windowed bulkhead, 10 mm top aperture, 15 mm off-axis towards window.

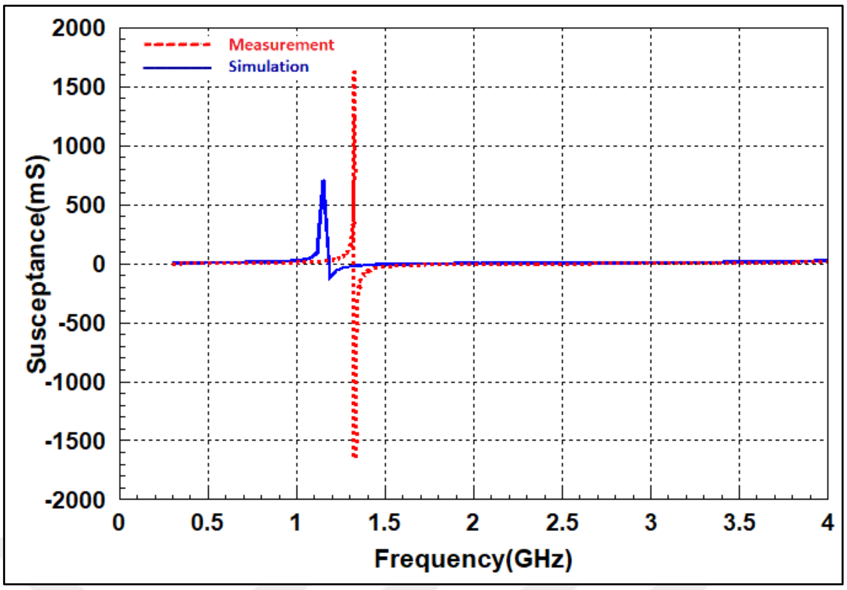

Figure 5.92. Susceptance value plot for 5 cm monopole in windowed bulkhead, 10 mm top aperture, 15 mm off-axis towards window.

10 mm off-axis away from bulkhead window (Position 4)

Figure 5.93 and Figure 5.94 show conductance and susceptance value plots for 5 cm monopole in windowed bulkhead, 10 mm top aperture, 10 mm off-axis away from window. Some agreement between the susceptance measurements and the simulations can be observed.

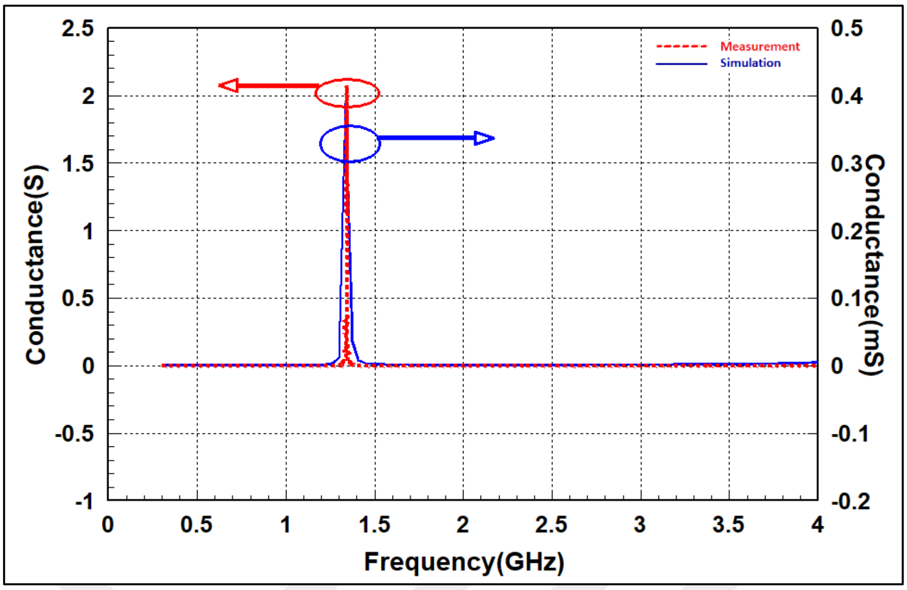

Figure 5.93. Conductance value plot for 5 cm monopole in windowed bulkhead, 10 mm top aperture, 10 mm off-axis away from window.

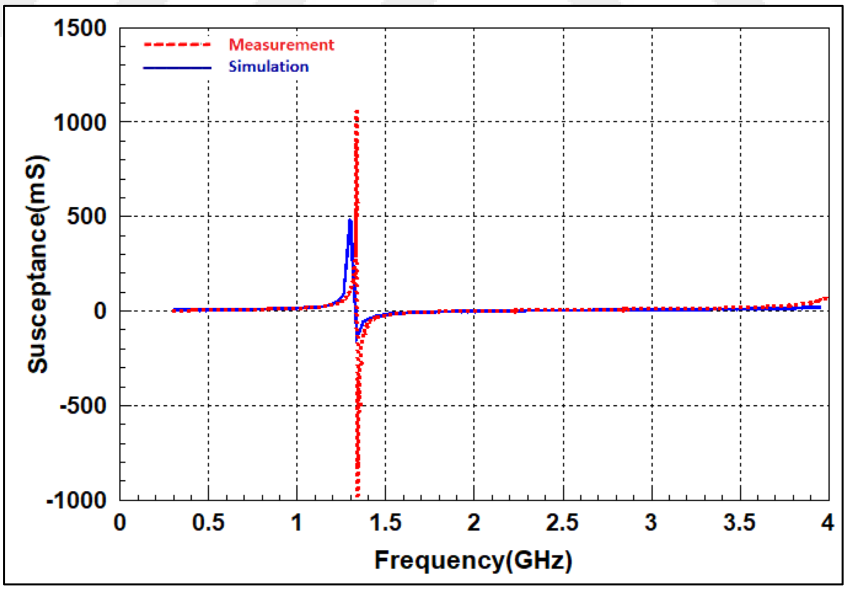

Figure 5.94. Susceptance value plot for 5 cm monopole in windowed bulkhead, 10 mm top aperture, 10 mm off-axis away from window.

5.2.1.4. Top with 4 mm Aperture

Axisymmetric position (Position 1)

Figure 5.95 and Figure 5.96 show conductance and susceptance value plots for 5 cm monopole in windowed bulkhead, 4 mm top aperture, axisymmetric position. Some agreement between measurements and the simulations can be observed.

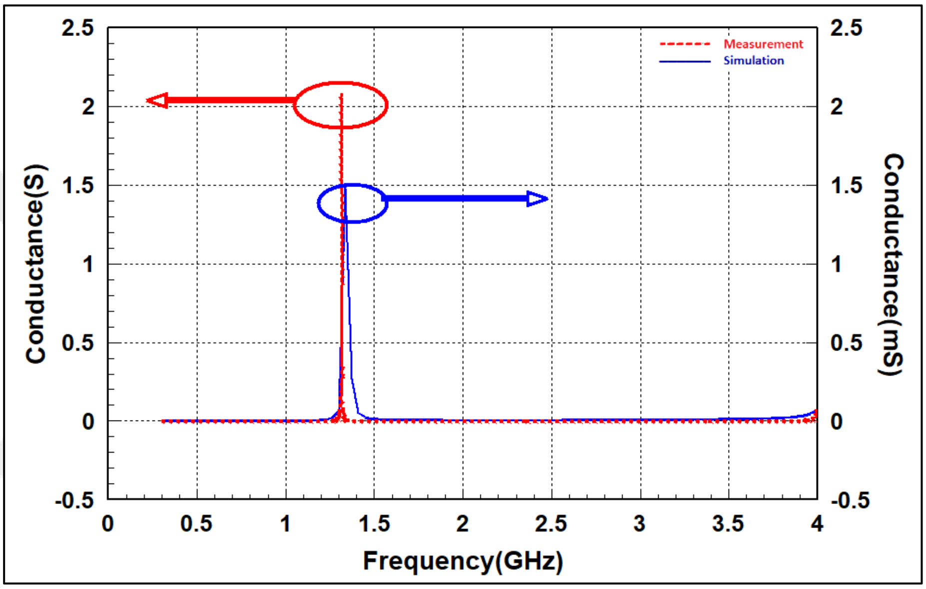

Figure 5.95. Conductance value plot for 5 cm monopole in windowed bulkhead, 4 mm top aperture, axisymmetric position.

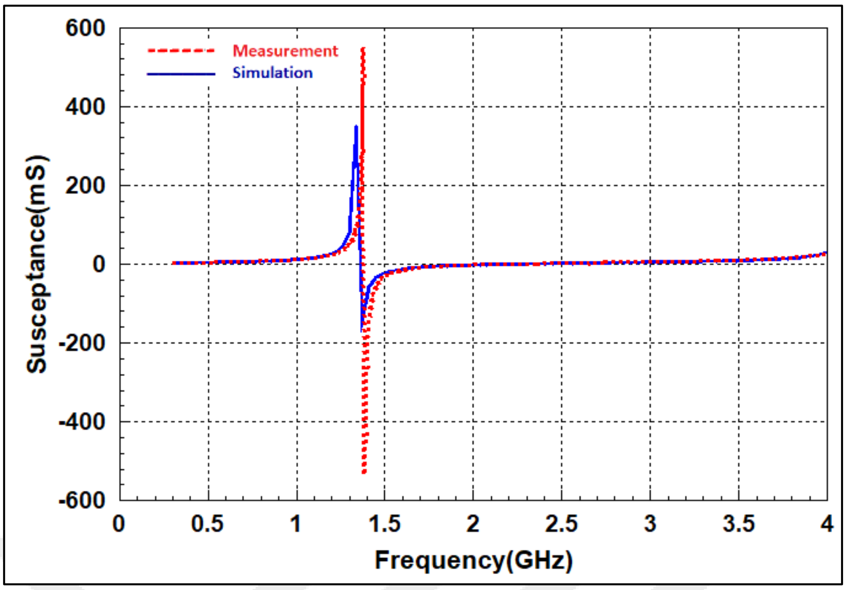

Figure 5.96. Susceptance value plot for 5 cm monopole in windowed bulkhead, 4 mm top aperture, axisymmetric position.

10 mm off-axis towards bulkhead window (Position 2)

Figure 5.97 and Figure 5.98 show conductance and susceptance value plots for 5 cm monopole in windowed bulkhead, 4 mm top aperture, 10 mm off-axis towards window.Some agreement between the susceptance measurements and the simulations can be observed.

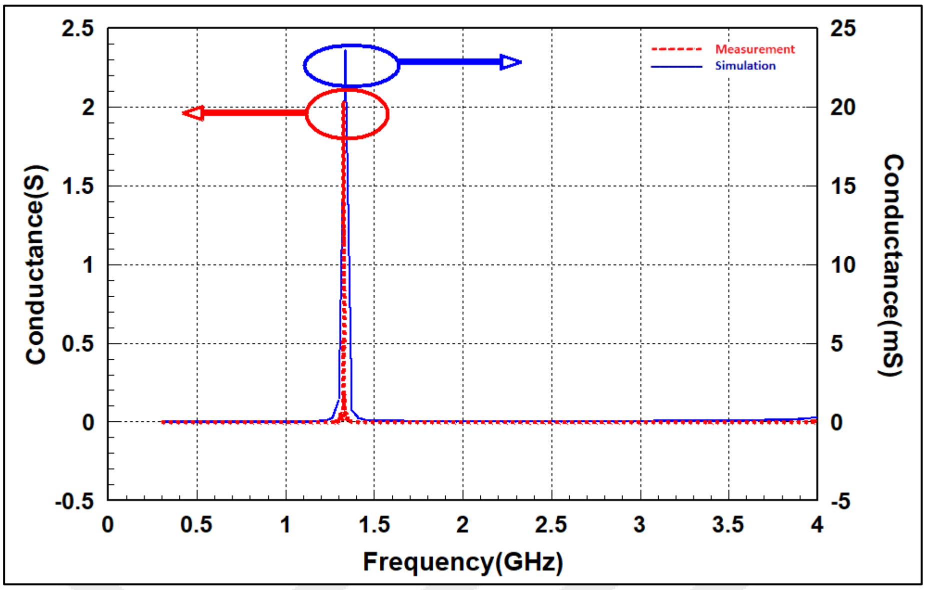

Figure 5.97. Conductance value plot for 5 cm monopole in windowed bulkhead, 4 mm top aperture, 10 mm off-axis towards window.

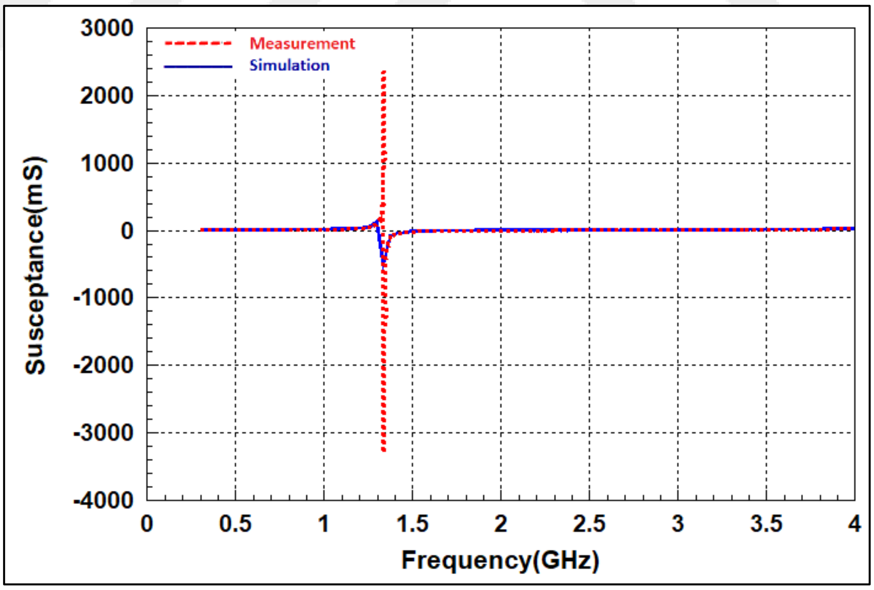

Figure 5.98. Susceptance value plot for 5 cm monopole in windowed bulkhead, 4 mm top aperture, 10 mm off-axis towards window.

15 mm off-axis towards bulkhead window (Position 3)

Figure 5.99 and Figure 5.100 show conductance and susceptance value plots for 5 cm monopole in windowed bulkhead, 4 mm top aperture, 10 mm off-axis towards window.A big discrepancy between measurements and simulation values is observed.

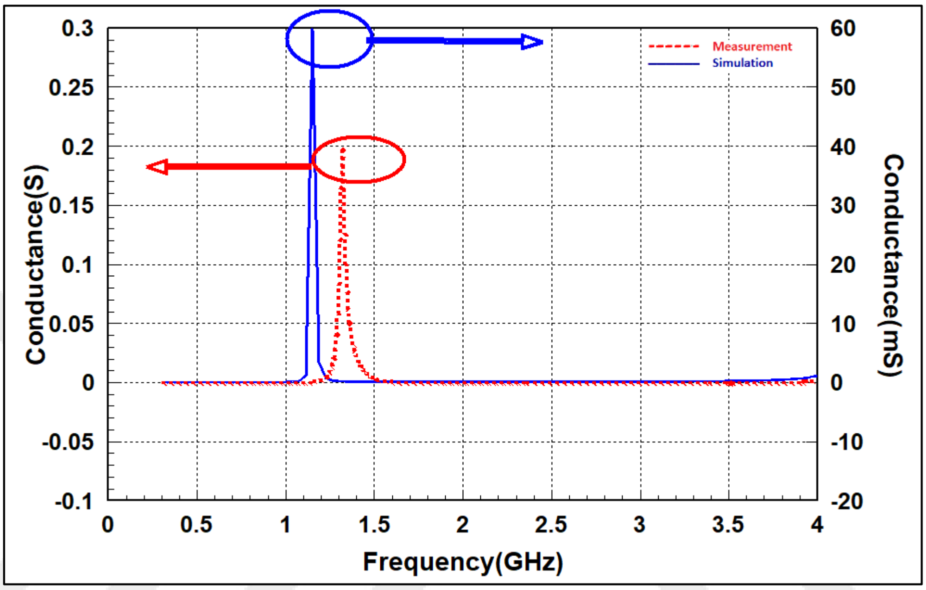

Figure 5.99. Conductance value plot for 5 cm monopole in windowed bulkhead, 4 mm top aperture, 15 mm off-axis towards window.

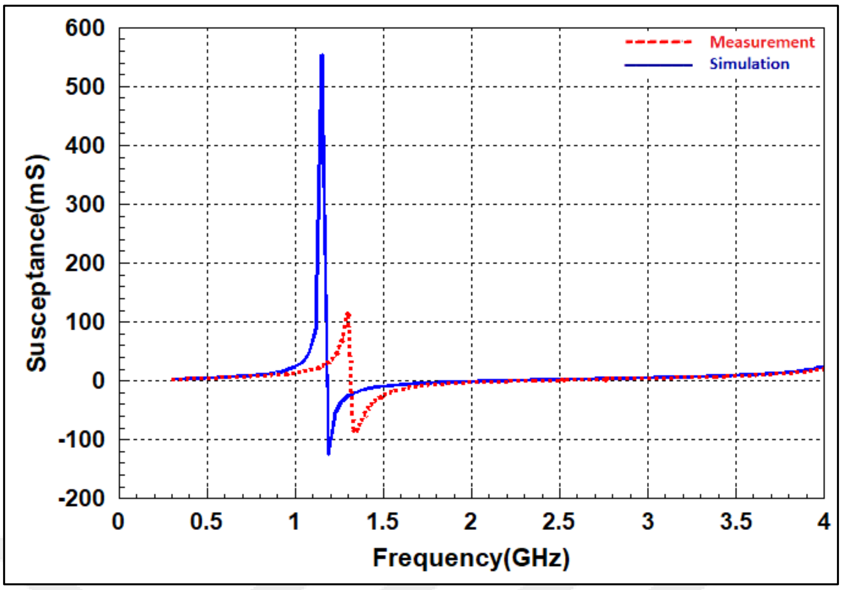

Figure 5.100. Susceptance value plot for 5 cm monopole in windowed bulkhead, 4 mm top aperture, 15 mm off-axis towards window.

10 mm off-axis away from bulkhead window (Position 4)

Figure 5.101 and Figure 5.102 show conductance and susceptance value plots for 5 cm monopole in windowed bulkhead, 4 mm top aperture, 10 mm off-axis away from window. Some agreement between measurements and simulations is observed.

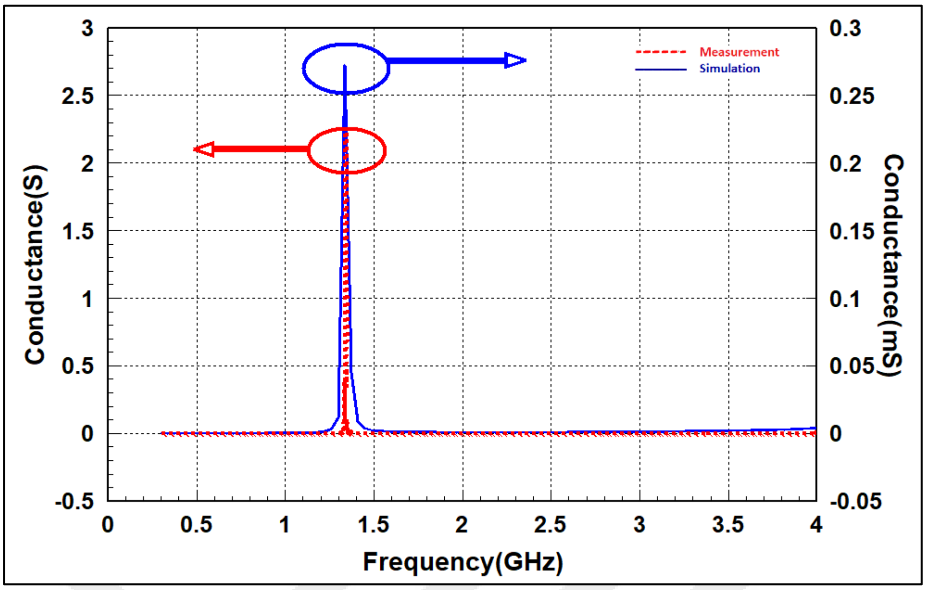

Figure 5.101. Conductance value plot for 5 cm monopole in windowed bulkhead, 4 mm top aperture, 10 mm off-axis away from window.

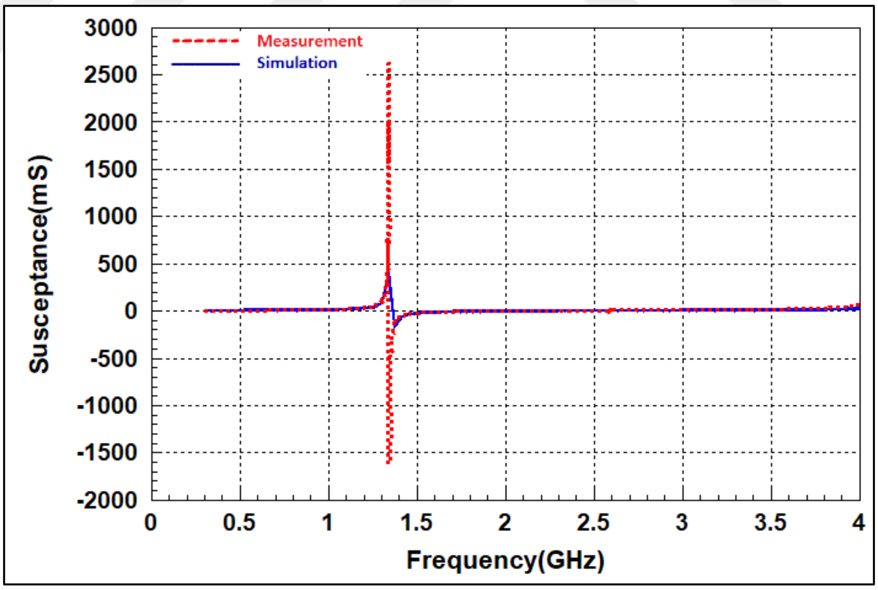

Figure 5.102. Susceptance value plot for 5 cm monopole in windowed bulkhead, 4 mm top aperture, 10 mm off-axis away from window.

5.2.1.5. Top with no Aperture

Axisymmetric position (Position 1)

Figure 5.103 and Figure 5.104 show conductance and susceptance value plots for 5 cm monopole in windowed bulkhead with no top aperture, at an axisymmetric position. Some agreement between measurements and simulations is observed.

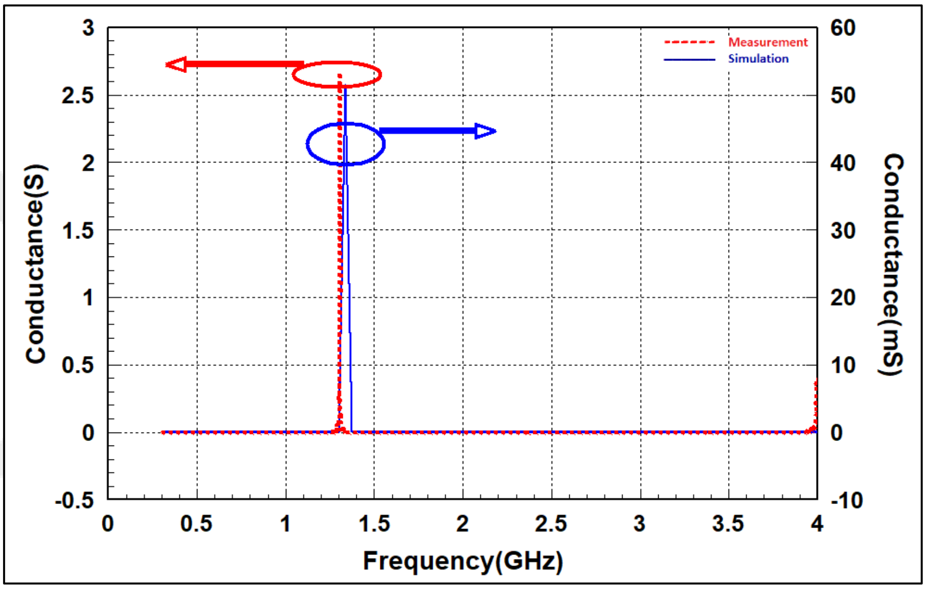

Figure 5.103. Conductance value plot for 5 cm monopole in windowed bulkhead, closed top aperture, axisymmetric position.

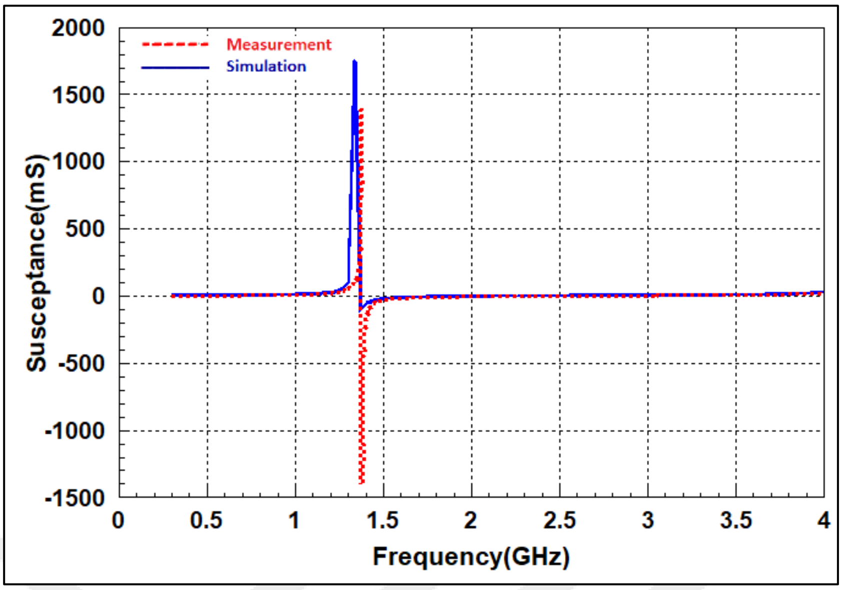

Figure 5.104. Susceptance value plot for 5 cm monopole in windowed bulkhead, closed top aperture, axisymmetric position.

10 mm off-axis towards bulkhead window (Position 2)

Figure 5.105 and Figure 5.106 show conductance and susceptance value plots for 5 cm monopole in windowed bulkhead with no top aperture, 10 mm off-axis towards window. Some agreement between measurements and simulations is observed.

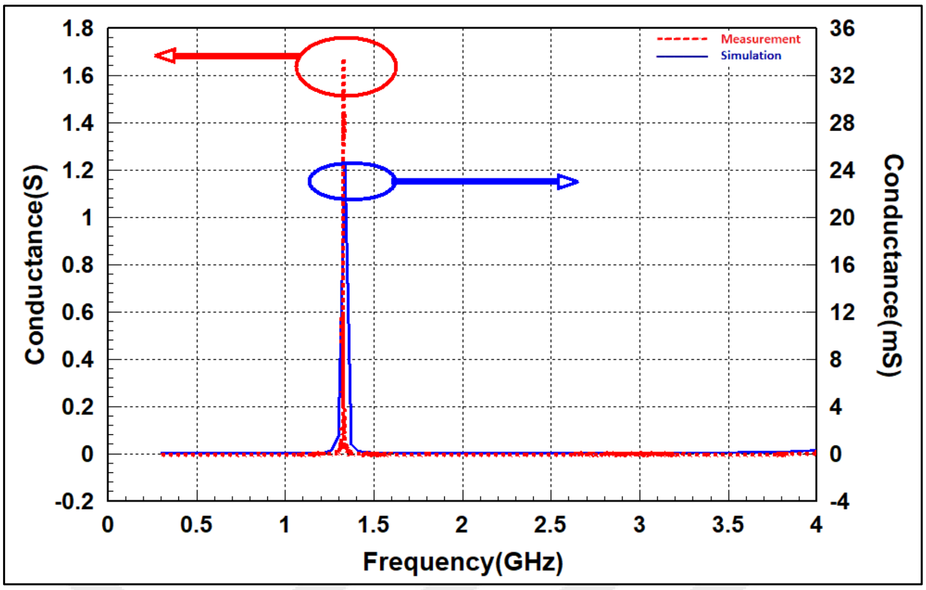

Figure 5.105. Conductance value plot for 5 cm monopole in windowed bulkhead, closed top aperture, 10 mm off-axis towards window.

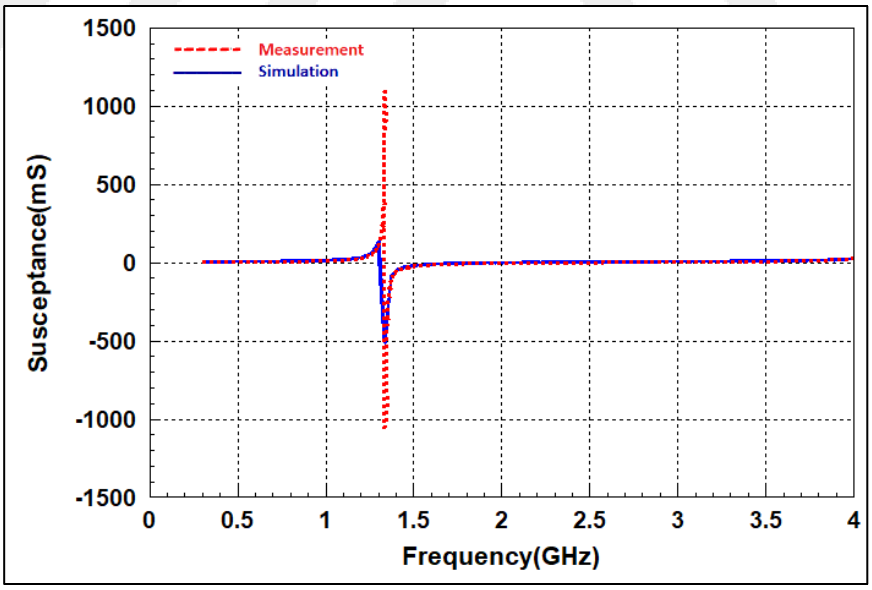

Figure 5.106. Susceptance value plot for 5 cm monopole in windowed bulkhead, closed top aperture, 10 mm off-axis towards window.

15 mm off-axis towards bulkhead window (Position 3)

Figure 5.107 and Figure 5.108 show conductance and susceptance value plots for 5 cm monopole in windowed bulkhead, 4 mm top aperture, 15 mm off-axis towards window.A discrepancy between measurements and simulation values is observed.

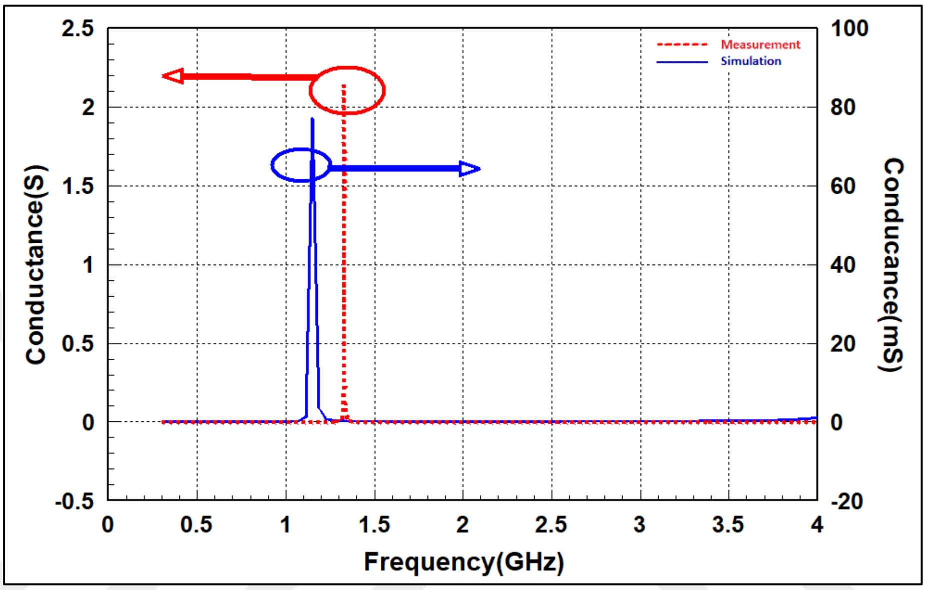

Figure 5.107. Conductance value plot for 5 cm monopole in windowed bulkhead, closed top aperture, 15 mm off-axis towards window.

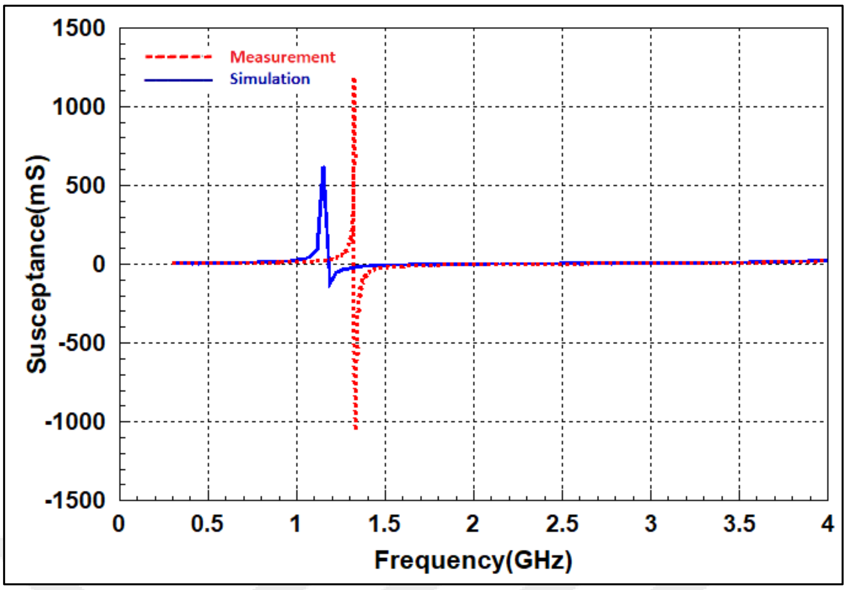

Figure 5.108. Susceptance value plot for 5 cm monopole in windowed bulkhead, closed top aperture, 15 mm off-axis towards window.

10 mm off-axis away from bulkhead window (Position 4)

Figure 5.109 and Figure 5.110 show conductance and susceptance value plots for 5 cm monopole in windowed bulkhead, 4 mm top aperture, 10 mm off-axis away from window. Some agreement between measurements and simulations is observed.

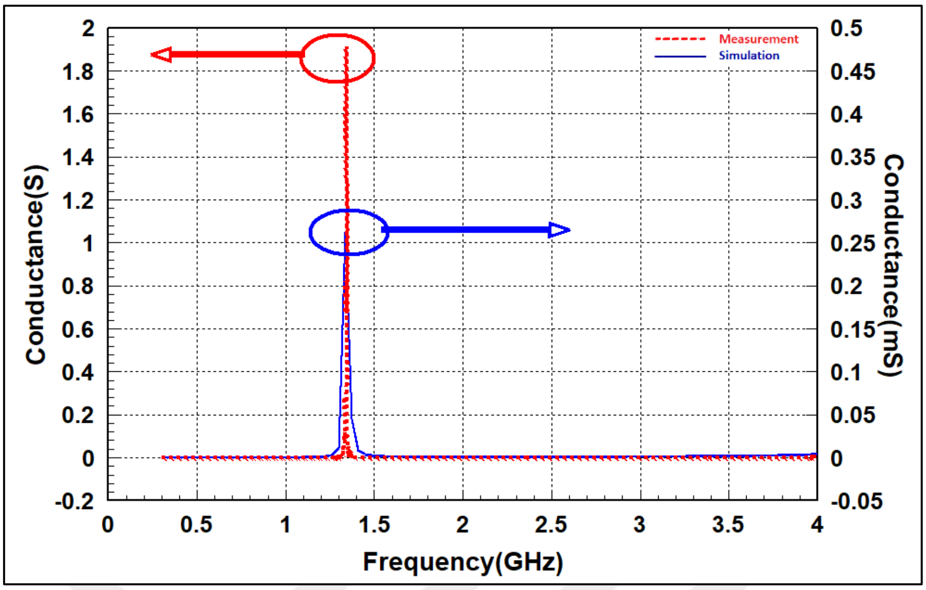

Figure 5.109. Conductance value plot for 5 cm monopole in windowed bulkhead, closed top aperture, 10 mm off-axis away from window.

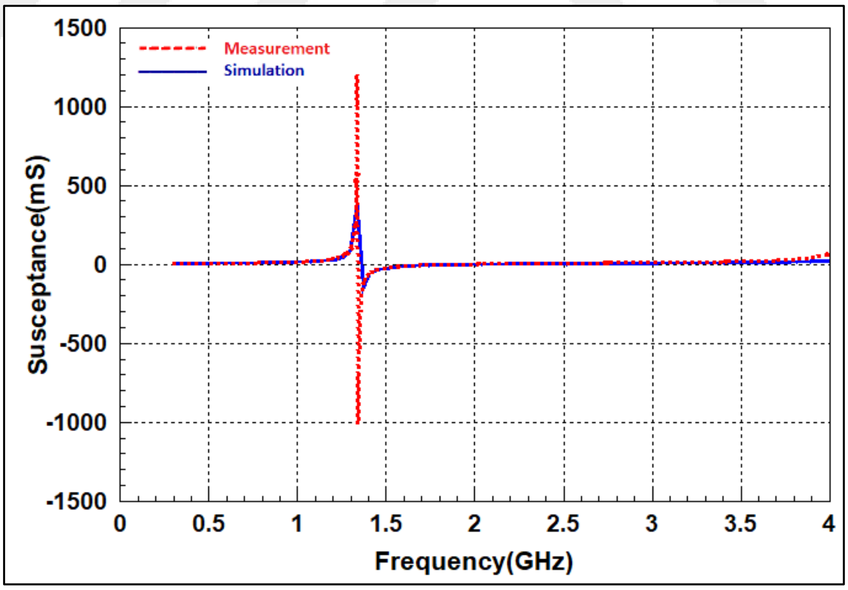

Figure 5.110. Susceptance value plot for 5 cm monopole in windowed bulkhead, closed top aperture, 10 mm off-axis away from window.

5.2.2. Bulkhead without Window

For this comparision scenario from Figure 4.3(a) is used as bulkhead. All of the simulations and measurments made accordingly.

5.2.2.1. Open Top Aperture

Axisymmetric position (Position 1)

Figure 5.111 and Figure 5.112 show conductance and susceptance value plots for 5 cm monopole in windowless bulkhead, open top aperture, axisymmetric position. Some agreement between measurements and simulations is observed.

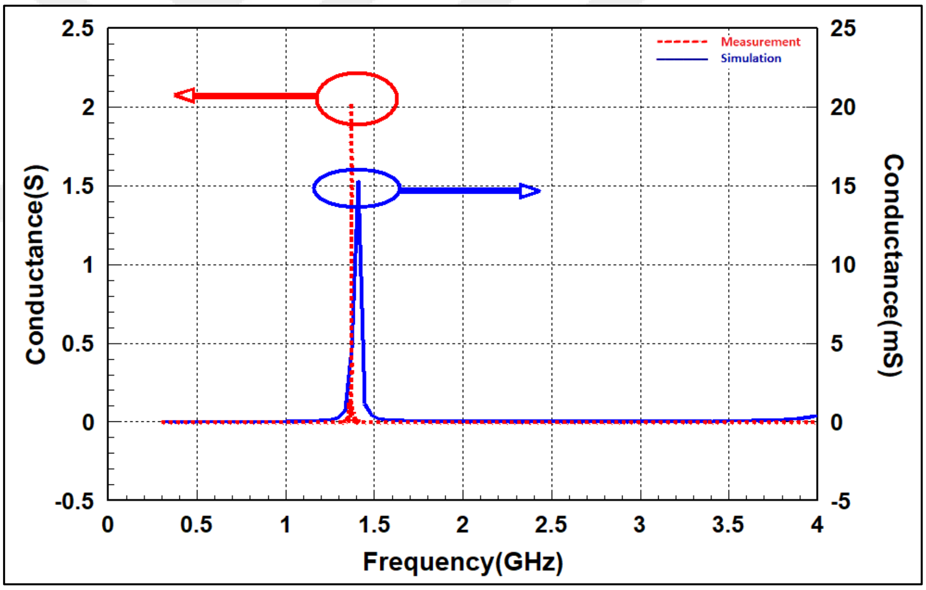

Figure 5.111. Conductance value plot for 5 cm monopole in windowless bulkhead, open top aperture, axisymmetric position.

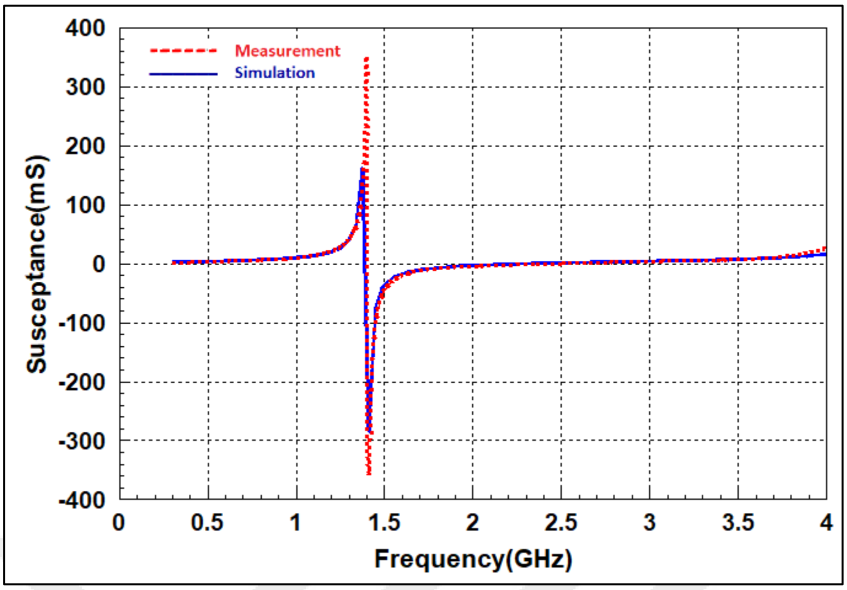

Figure 5.112. Susceptance value plot for 5 cm monopole in windowless bulkhead, open top aperture, axisymmetric position.

10 mm off-axis (Position 2)

Figure 5.113 and Figure 5.114 show conductance and susceptance value plots for 5 cm monopole in windowless bulkhead, open top aperture and 10 mm off-axis position. Some agreement between the susceptance measurements and the simulations for both conductance and susceptance values is observed.

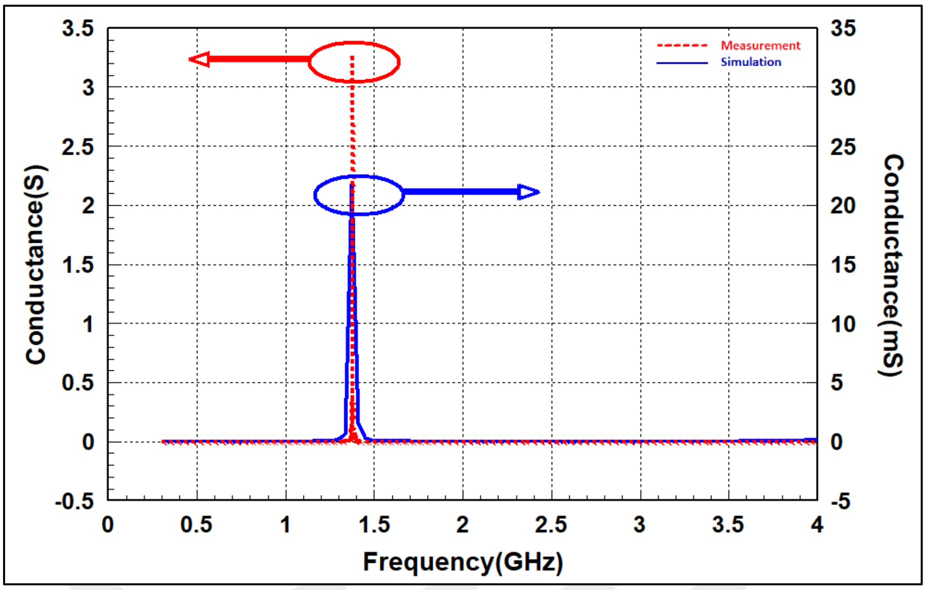

Figure 5.113. Conductance value plot for 5 cm monopole in windowless bulkhead, open top aperture, 10 mm off-axis.

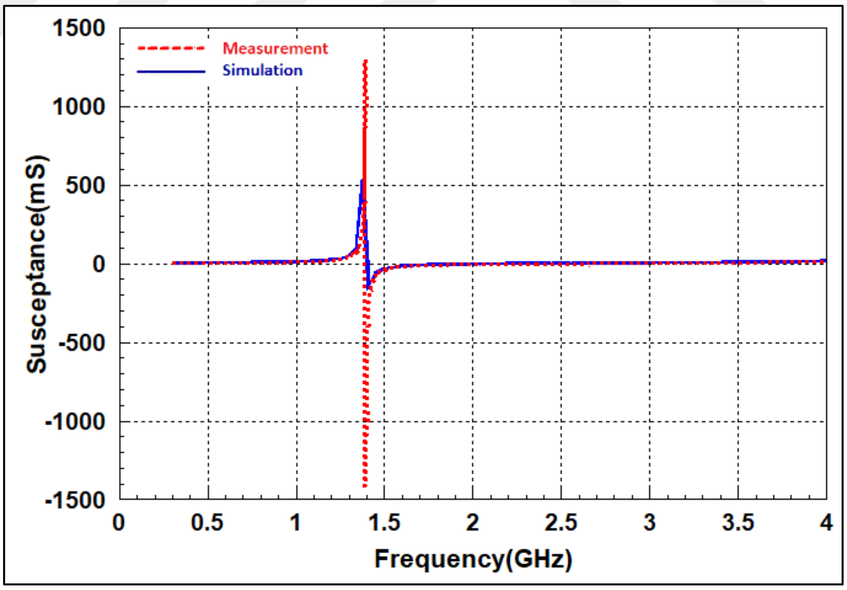

Figure 5.114. Susceptance value plot for 5 cm monopole in windowless bulkhead, open top aperture, 10 mm off-axis.

15 mm off-axis (Position 3)

Figure 5.115 and Figure 5.116 show conductance and susceptance value plots for 5 cm monopole in windowless bulkhead, open top aperture and 15 mm off-axis position. Some agreement between the susceptance measurements and the simulations for both conductance and susceptance values is observed.

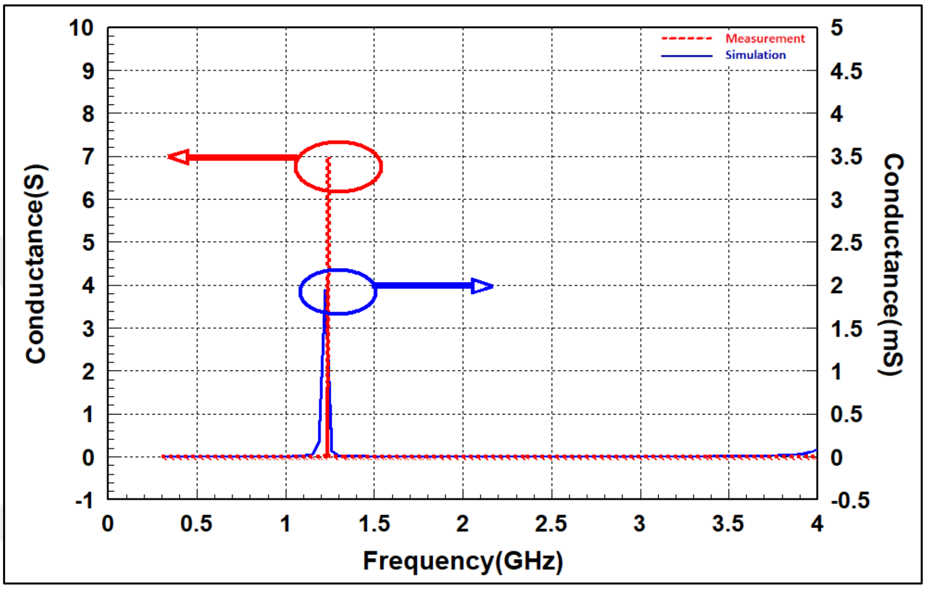

Figure 5.115. Conductance value plot for 5 cm monopole in windowless bulkhead, open top aperture, 15 mm off-axis.

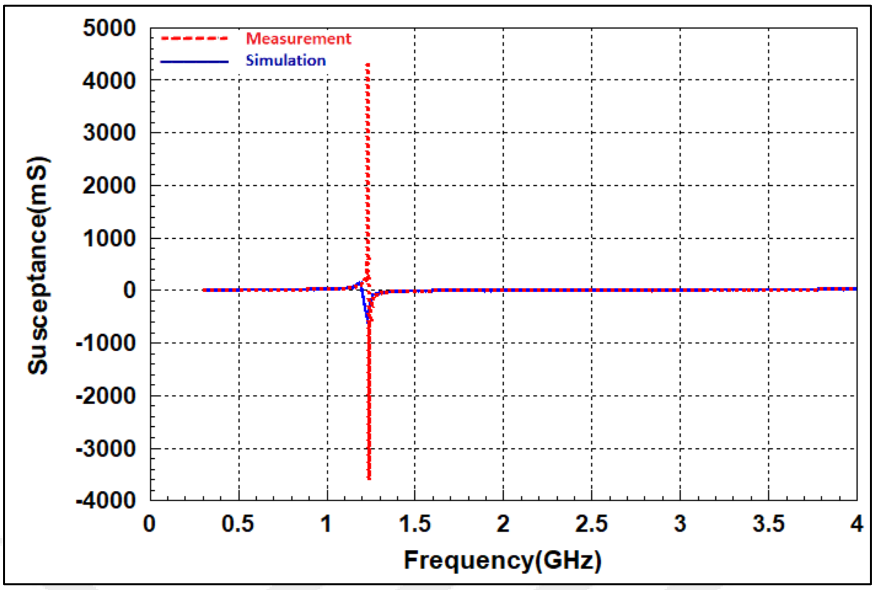

Figure 5.116. Susceptance value plot for 5 cm monopole in win4dowless bulkhead, open top aperture, 15 mm off-axis.

5.2.2.2. Top with 15 mm Aperture

Axisymmetric position (Position 1)

Figure 5.117 and Figure 5.118 show conductance and susceptance value plots for 5 cm monopole in windowless bulkhead, 15 mm top aperture, axisymmetric position. Some agreement between the susceptance measurements and the simulations for both conductance and susceptance values is observed.

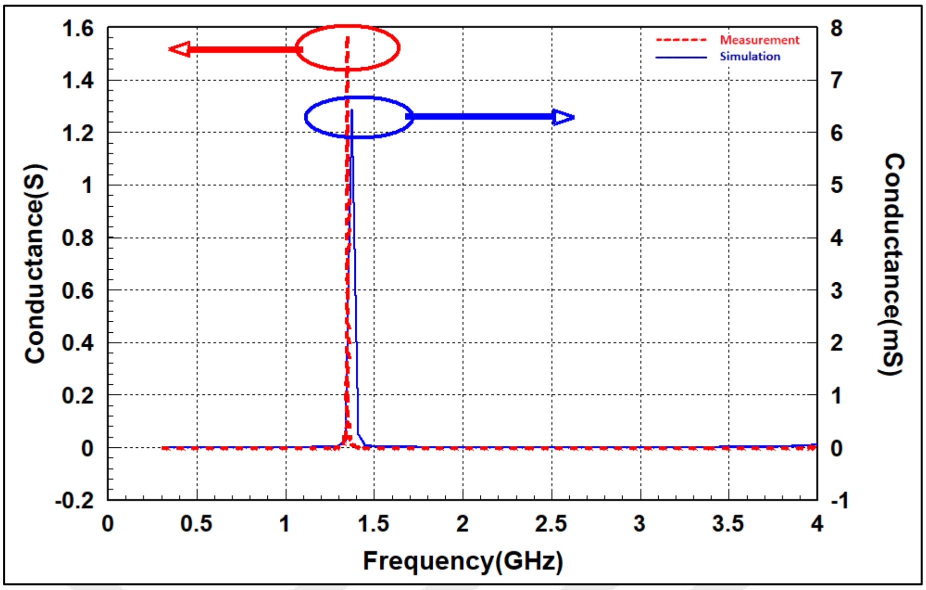

Figure 5.117. Conductance value plot for 5 cm monopole in windowless bulkhead, 15 mm top aperture, axisymmetric position.

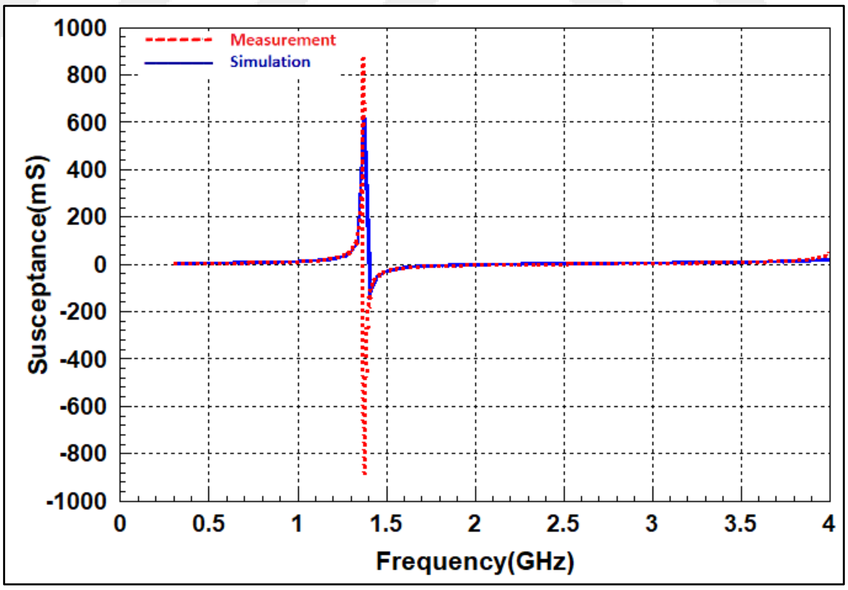

Figure 5.118. Susceptance value plot for 5 cm monopole in windowless bulkhead, 15 mm top aperture, axisymmetric position

10 mm off-axis (Position 2)

Figure 5.119 and Figure 5.120 show conductance and susceptance value plots for 5 cm monopole in windowless bulkhead, 15 mm top aperture, 10 mm off-axis position. Small discrepancy between the simulation and measurements can be observed.

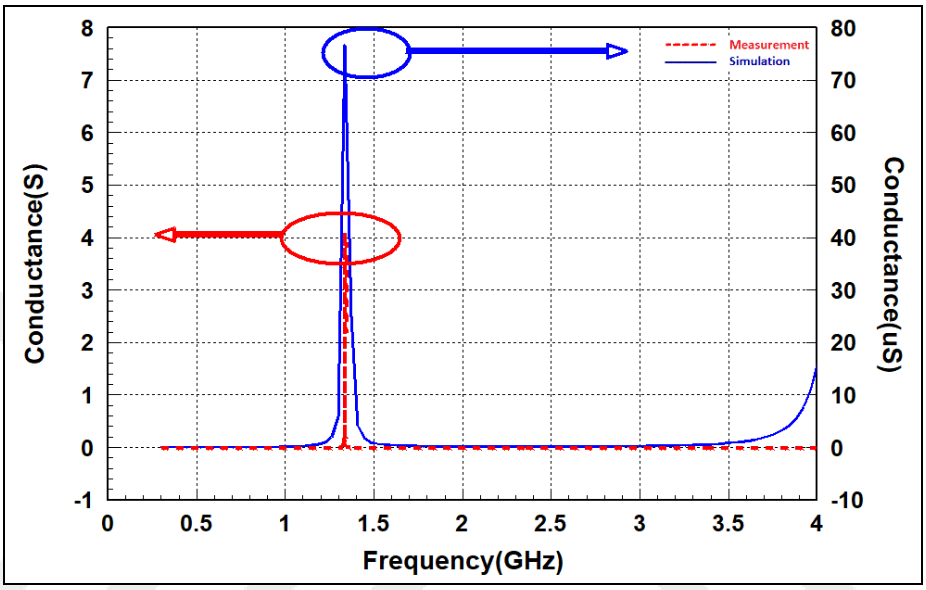

Figure 5.119. Conductance value plot for 5 cm monopole in windowless bulkhead, 15 mm top aperture, 10 mm off-axis.

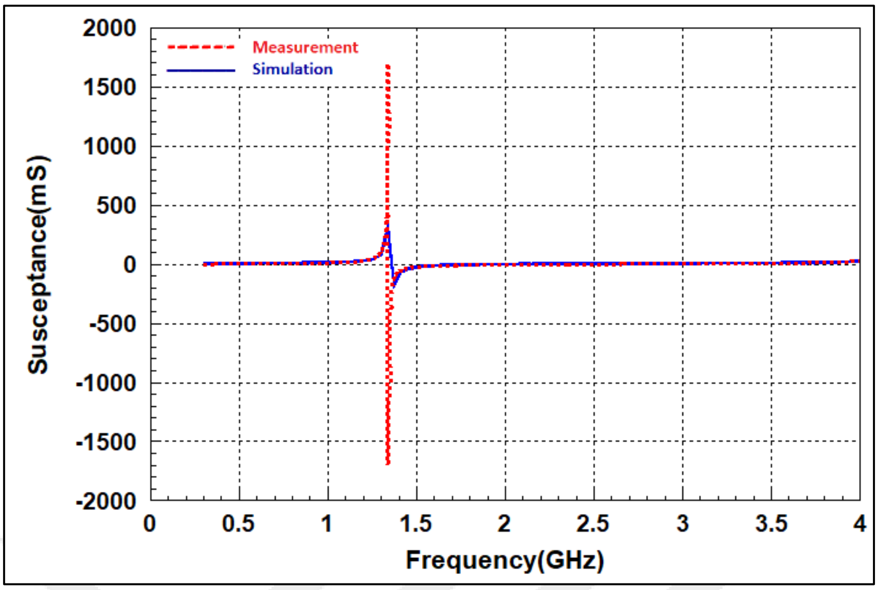

Figure 5.120. Susceptance value plot for 5 cm monopole in windowless bulkhead, 15 mm top aperture,10 mm off-axis.

15 mm off-axis (Position 3)

Figure 5.121 and Figure 5.122 show conductance and susceptance value plots for 5 cm monopole in windowless bulkhead, 15 mm top aperture, 15 mm off-axis position. Very small discrepancy between the simulation and measurements can be observed.

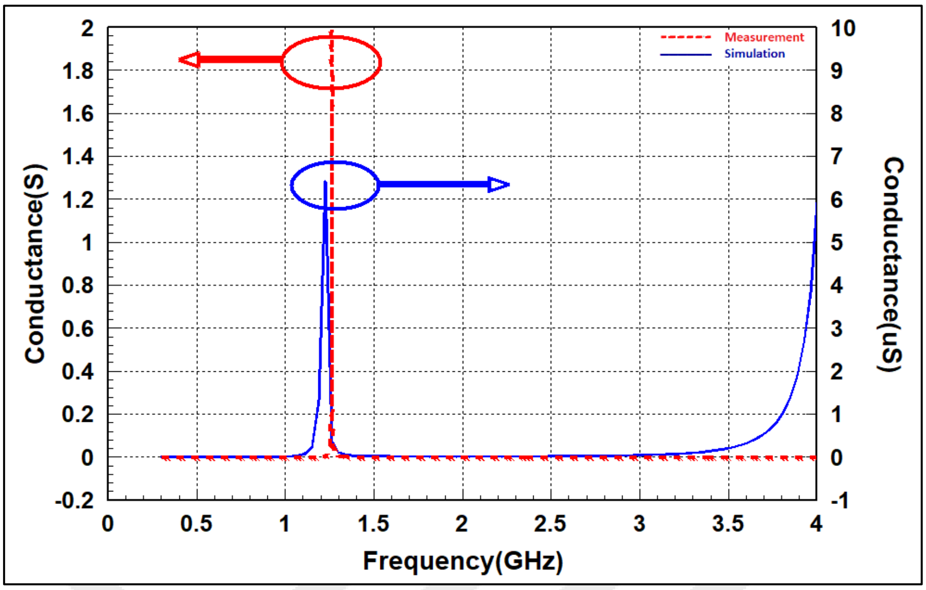

Figure 5.121. Conductance value plot for 5 cm monopole in windowless bulkhead, 15 mm top aperture, 15 mm off-axis.

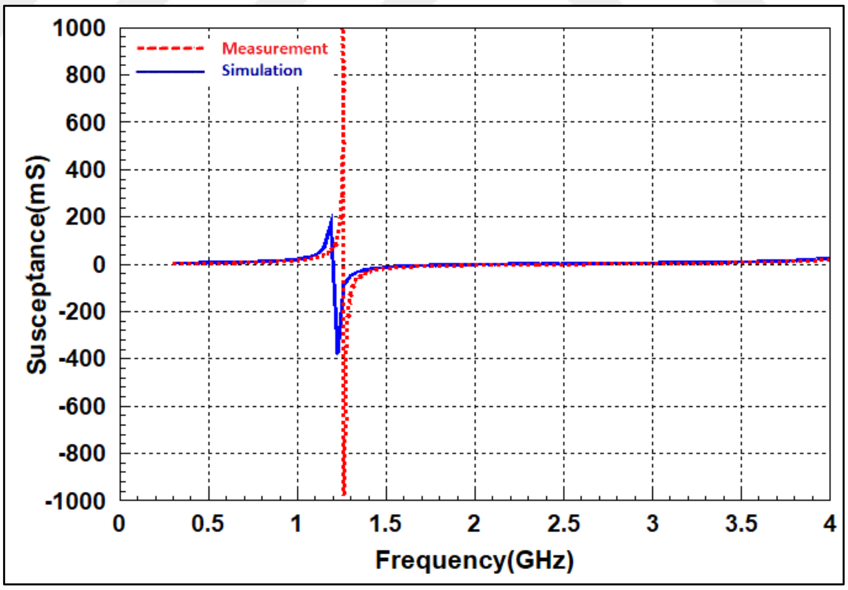

Figure 5.122. Susceptance value plot for 5 cm monopole in windowless bulkhead, 15 mm top aperture,15 mm off-axis.

5.2.2.3. Top with 10 mm Aperture

Axisymmetric position (Position 1)

Figure 5.123 and Figure 5.124 show conductance and susceptance value plots for 5 cm monopole in windowless bulkhead, 10 mm top aperture, axisymmetric position. Some agreement between the susceptance measurements and the simulations for both conductance and susceptance values is observed.

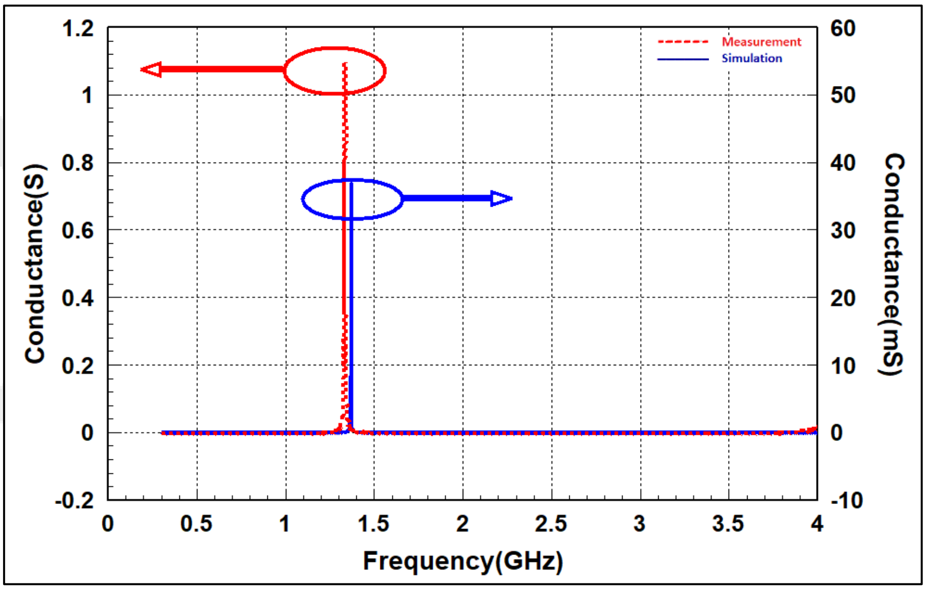

Figure 5.123. Conductance value plot for 5 cm monopole in windowless bulkhead, 10 mm top aperture, axisymmetric position.

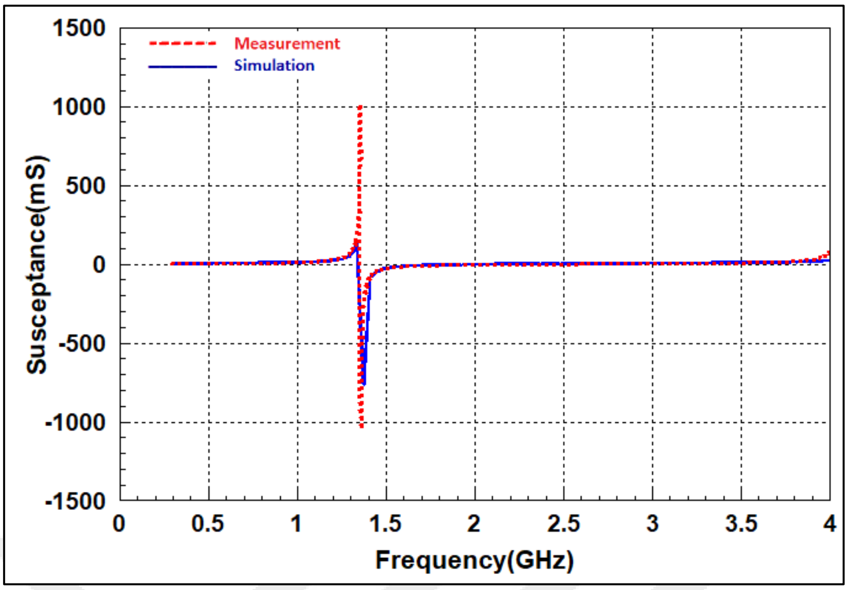

Figure 5.124. Susceptance value plot for 5 cm monopole in windowless bulkhead, 10 mm top aperture, axisymmetric position.

10 mm off-axis (Position 2)

Figure 5.125 and Figure 5.126 show conductance and susceptance value plots for 3 cm monopole in windowless bulkhead, 10 mm top aperture, 10 mm off-axis position. Very good agreement between the susceptance measurements and the simulations for both conductance and susceptance values is observed.

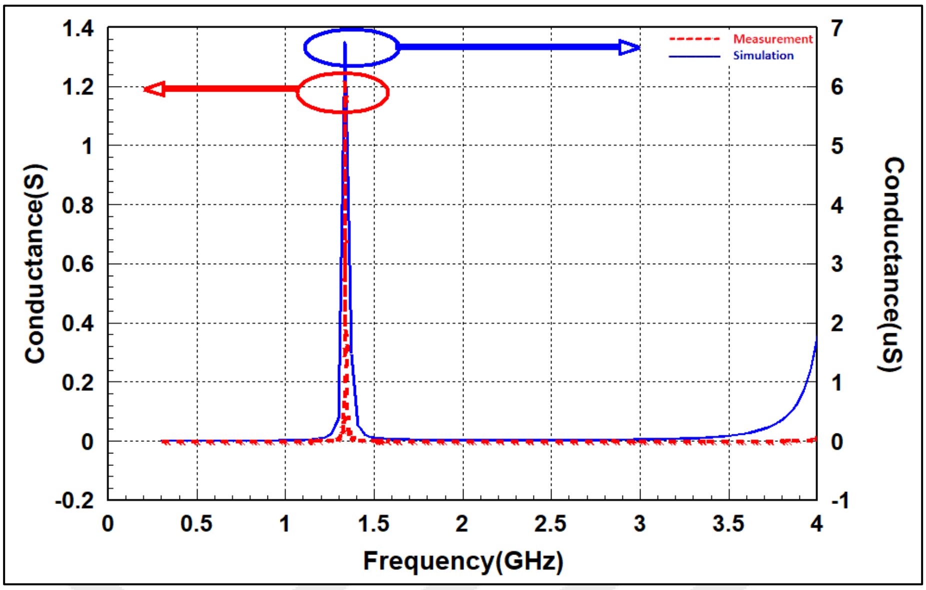

Figure 5.125. Conductance value plot for 5 cm monopole in windowless bulkhead, 10 mm top aperture, 10 mm off-axis.

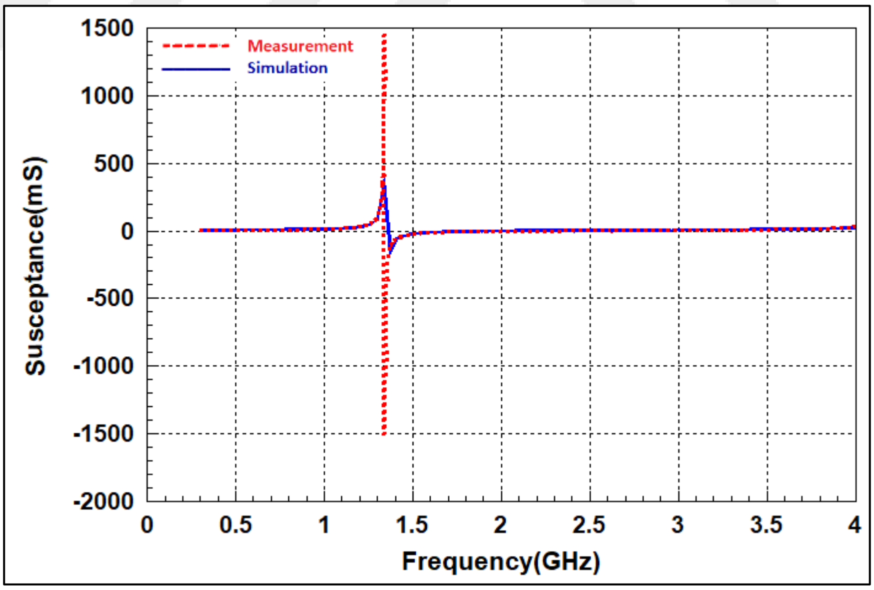

Figure 5.126. Susceptance value plot for 5 cm monopole in windowless bulkhead, 10 mm top aperture, 10 mm off-axis.

15 mm off-axis (Position 3)

Figure 5.127 and Figure 5.128 show conductance and susceptance value plots for 5 cm monopole in windowless bulkhead, 10 mm top aperture, 15 mm off-axis position. Some agreement between measurements and simulation values is observed.

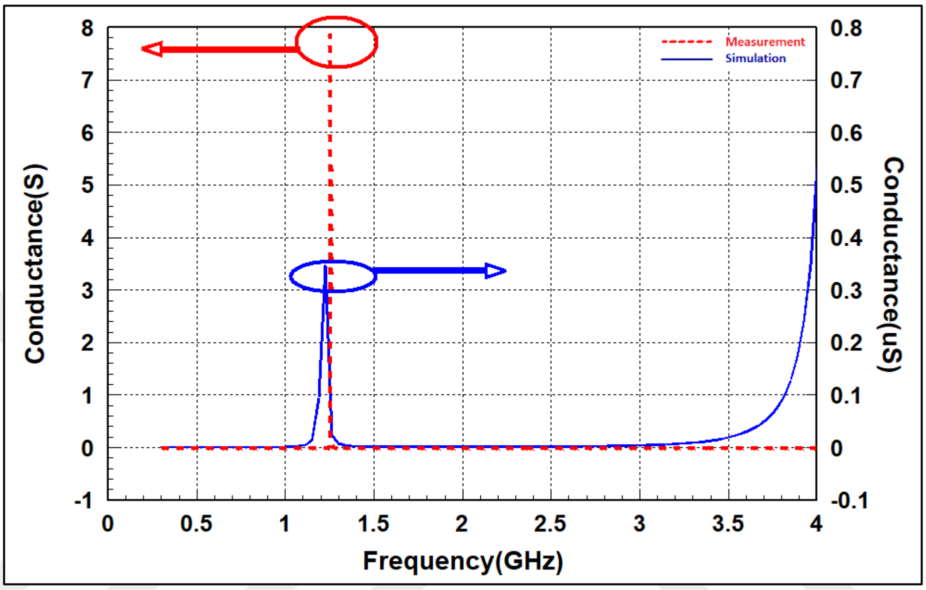

Figure 5.127. Conductance value plot for 5 cm monopole in windowless bulkhead, 10 mm top aperture, 15 mm off-axis.

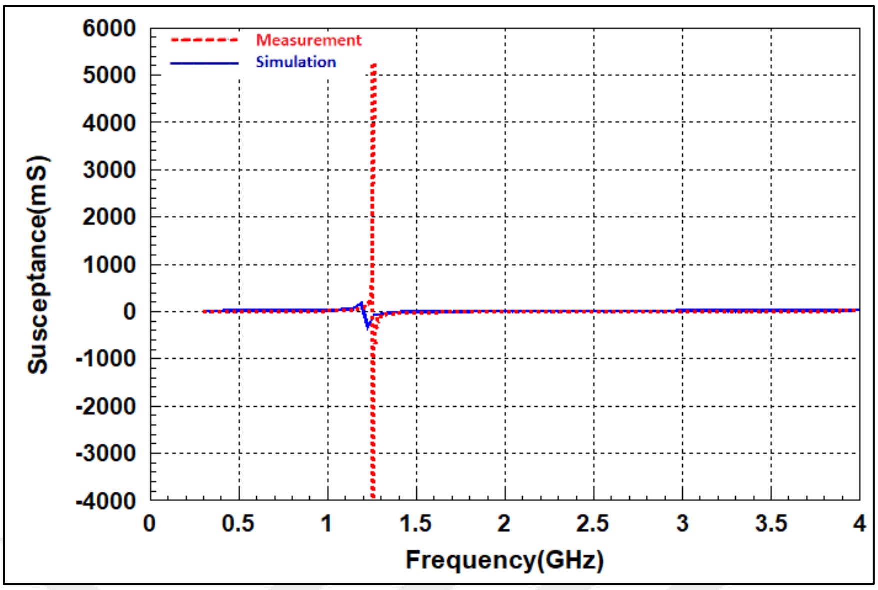

Figure 5.128. Susceptance value plot for 5 cm monopole in windowless bulkhead, 10 mm top aperture, 15 mm off-axis.

5.2.2.4. Top with 4 mm Aperture

Axisymmetric position (Position 1)

Figure 5.129 and Figure 5.130 show conductance and susceptance value plots for 5 cm monopole in windowless bulkhead, 4 mm top aperture, axisymmetric position. Some agreement between susceptance values is observed.

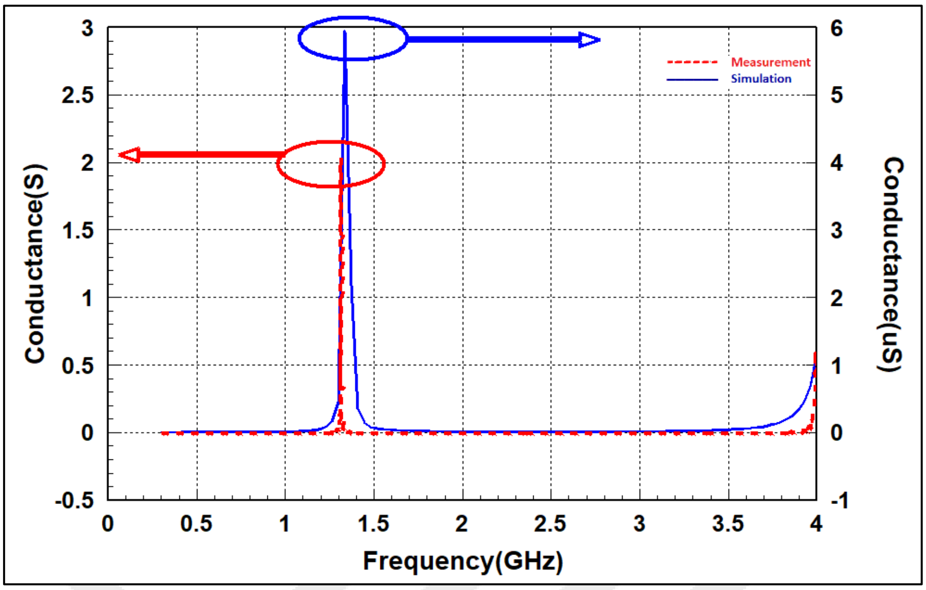

Figure 5.129. Conductance value plot for 5 cm monopole in windowless bulkhead, 4 mm top aperture, axisymmetric position.

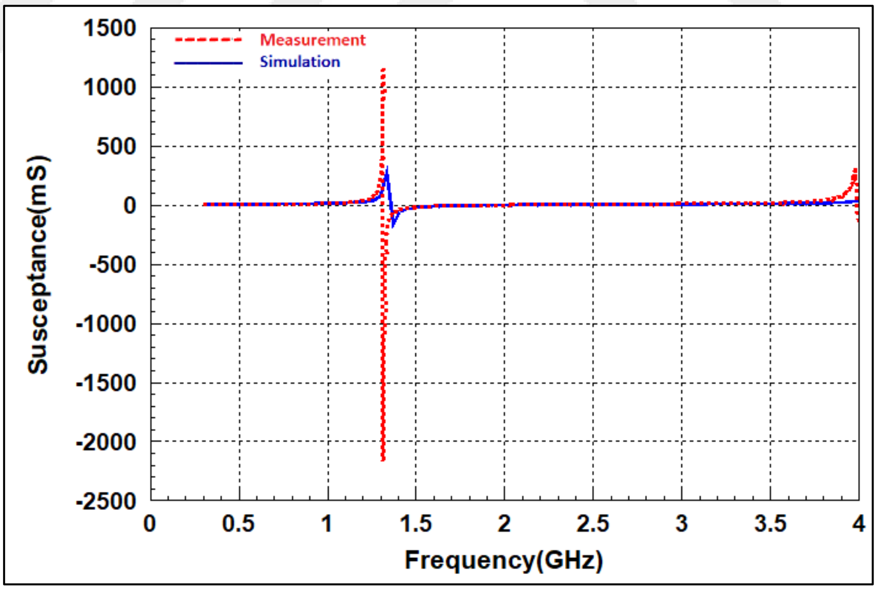

Figure 5.130. Susceptance value plot for 5 cm monopole in windowless bulkhead, 4 mm top aperture, axisymmetric position.

10 mm off-axis (Position 2)

Figure 5.131 and Figure 5.132 show conductance and susceptance value plots for 5 cm monopole in windowless bulkhead, 4 mm top aperture, 10 mm off-axis position. Very good agreement between measurements and simulations for both conductance and susceptance values is observed.

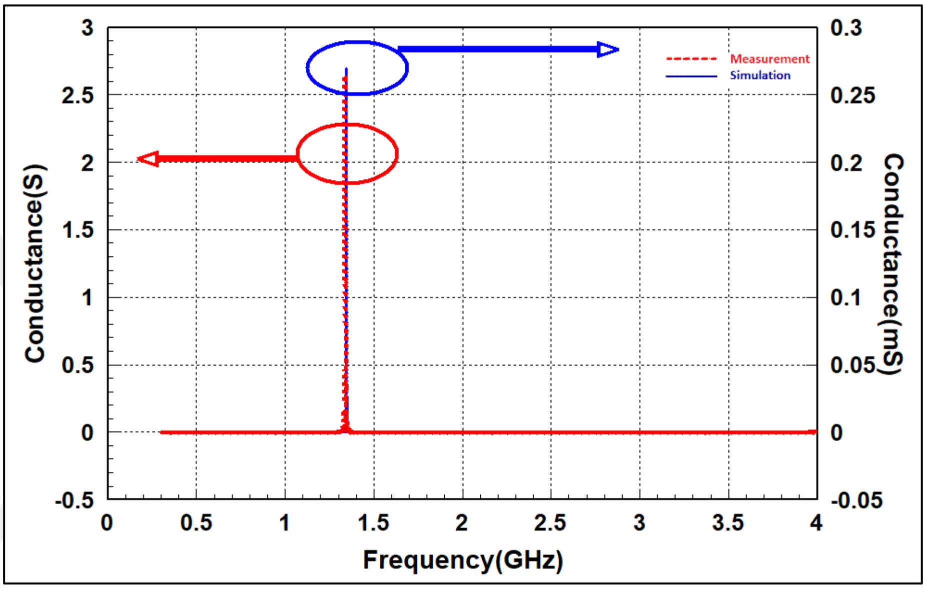

Figure 5.131. Conductance value plot for 5 cm monopole in windowless bulkhead, 4 mm top aperture,10 mm off-axis.

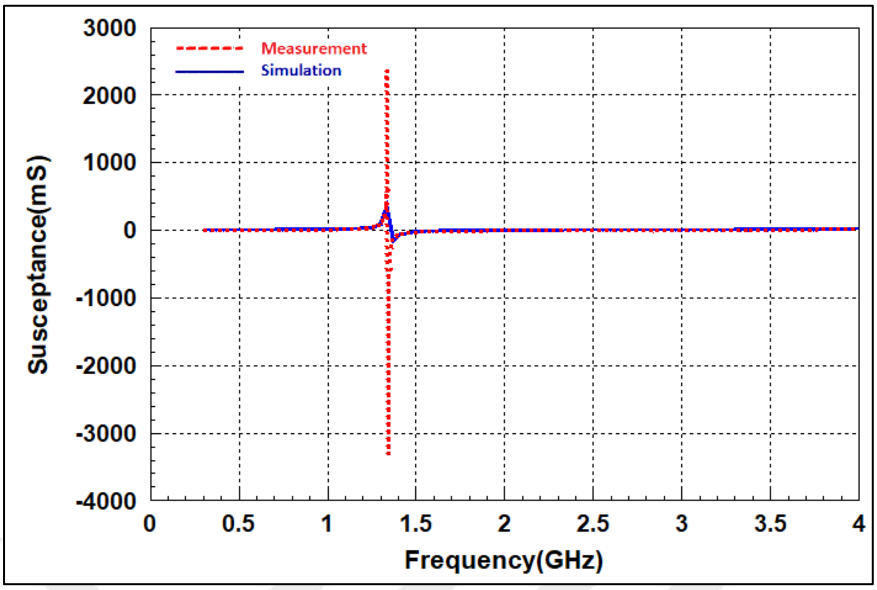

Figure 5.132. Susceptance value plot for 5 cm monopole in windowless bulkhead, 4 mm top aperture, 10 mm off-axis.

15 mm off-axis (Position 3)

Figure 5.133 and Figure 5.134 show conductance and susceptance value plots for 5 cm monopole in windowless bulkhead, 4 mm top aperture, 15 mm off-axis position. A small discrepancy between measurements and simulation values is observed.

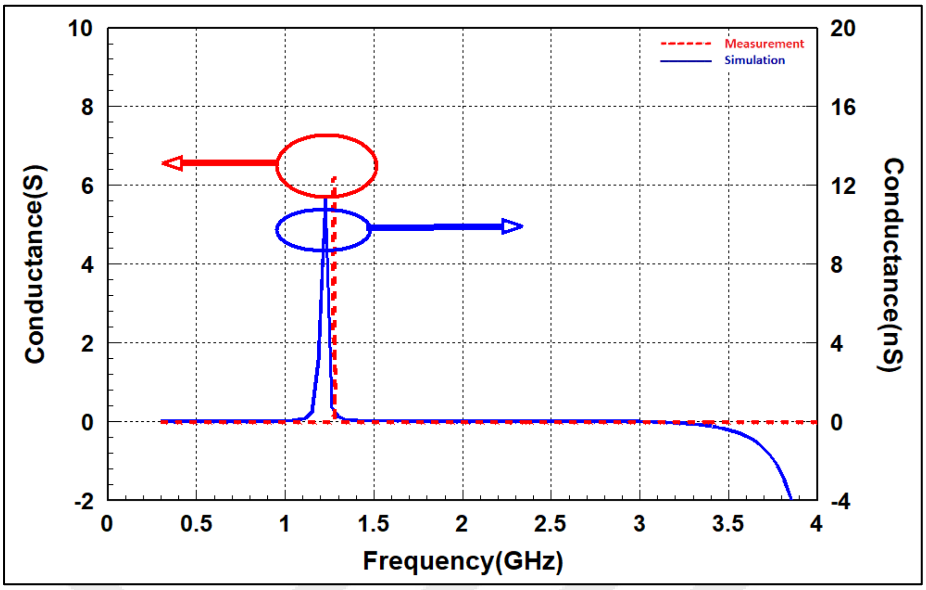

Figure 5.133. Conductance value plot for 5 cm monopole in windowless bulkhead, 4 mm top aperture,15 mm off-axis.

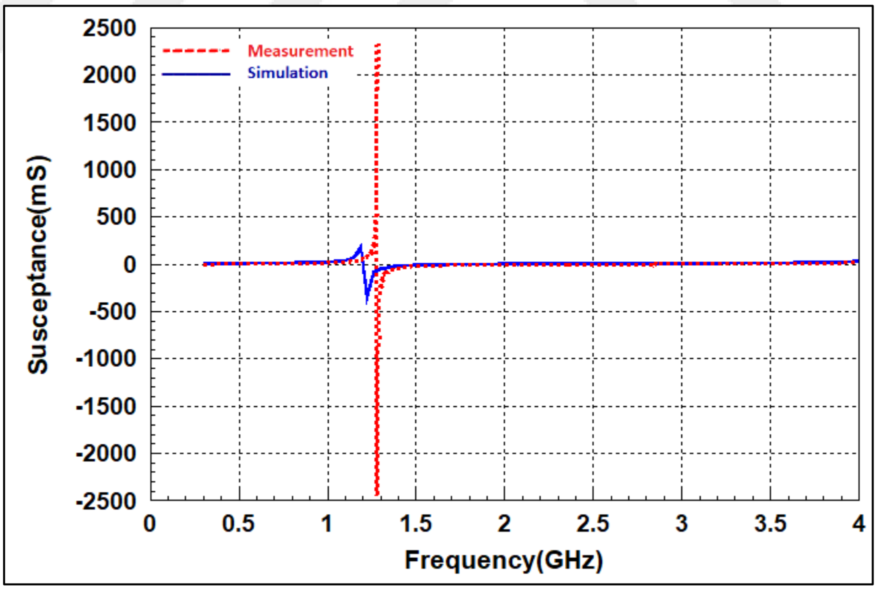

Figure 5.134. Susceptance value plot for 5 cm monopole in windowless bulkhead, 4 mm top aperture, 15 mm off-axis.

5.2.2.5. Top with no Aperture

Axisymmetric position (Position 1)

Figure 5.135 and Figure 5.136 show conductance and susceptance value plots for 5 cm monopole in windowless bulkhead, closed top aperture, axisymmetric position. Some agreement between susceptance values is observed.

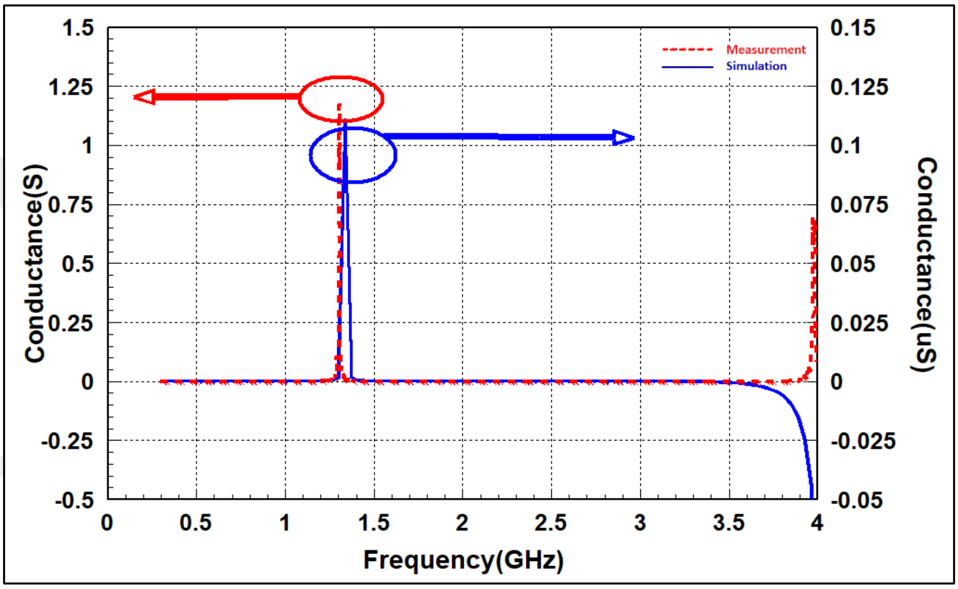

Figure 5.135. Conductance value plot for 5 cm monopole in windowless bulkhead, closed top aperture, axisymmetric position.

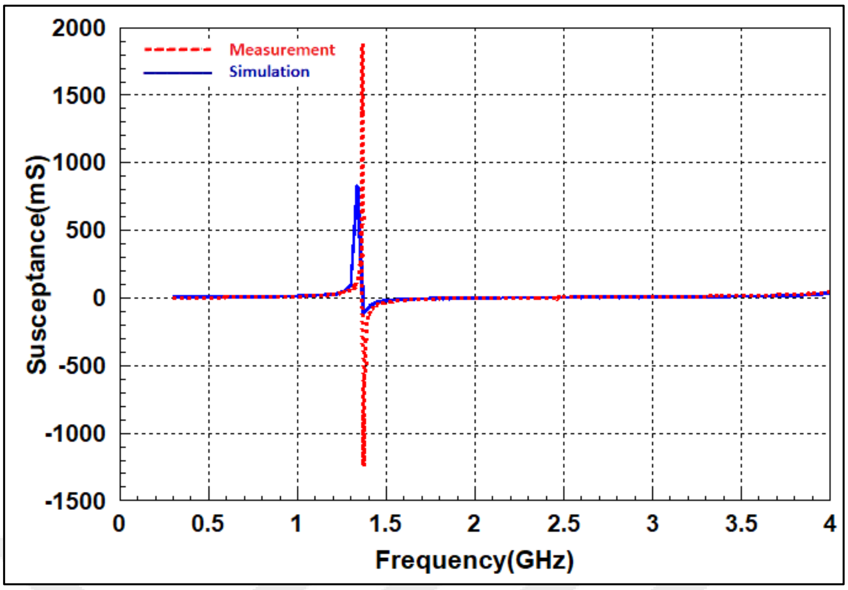

Figure 5.136. Susceptance value plot for 5 cm monopole in windowless bulkhead, closed top aperture, axisymmetric position.

10 mm off-axis (Position 2)

Figure 5.137 and Figure 5.138 show conductance and susceptance value plots for 5 cm monopole in windowless bulkhead, closed top aperture, 10 mm off-axis position. Some agreement between measurements and simulations for conductance values is observed.

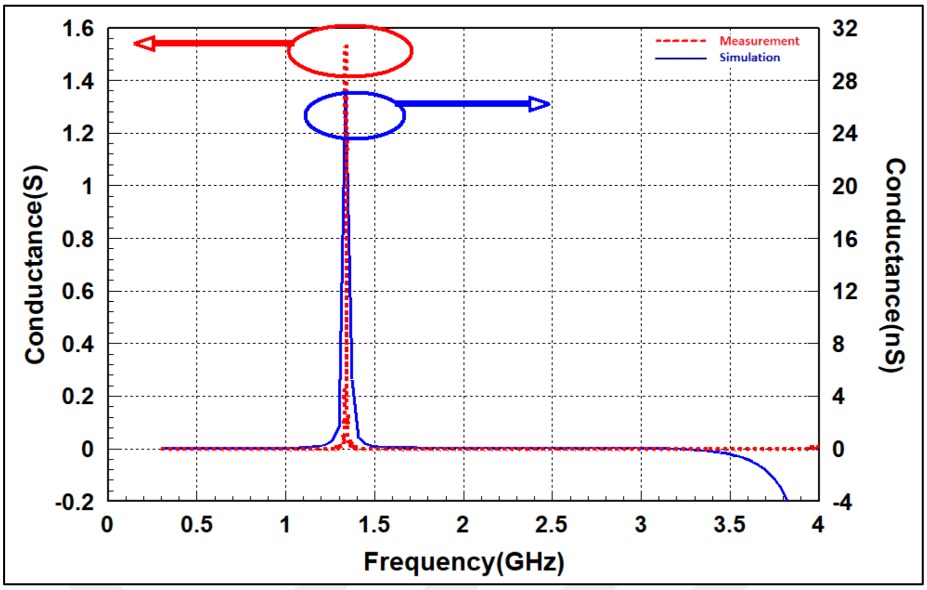

Figure 5.137. Conductance value plot for 5 cm monopole in windowless bulkhead, closed top aperture, 10 mm off-axis.

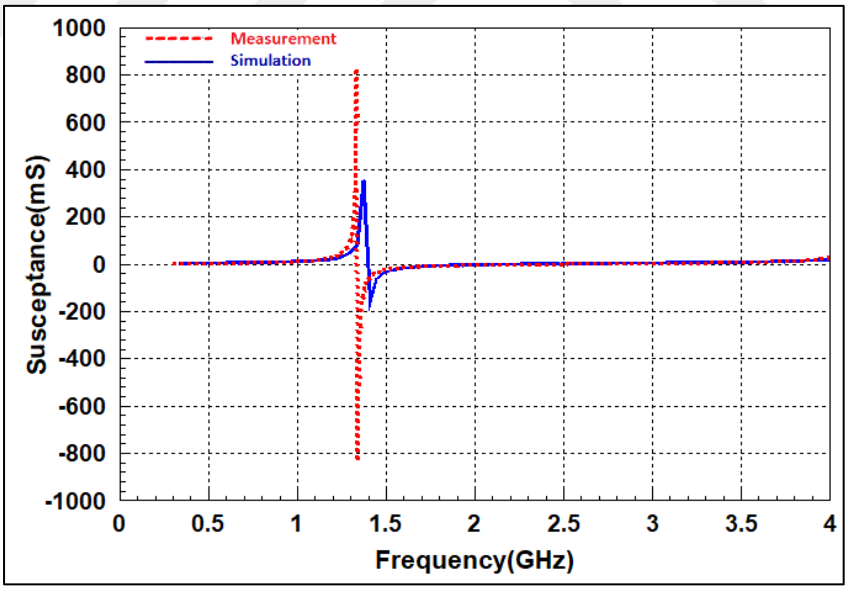

Figure 5.138. Susceptance value plot for 5 cm monopole in windowless bulkhead, closed top aperture, 10 mm off-axis.

15 mm off-axis (Position 3)

Figure 5.139 and Figure 5.140 show conductance and susceptance value plots for 5 cm monopole in windowless bulkhead, closed top aperture, 15 mm off-axis position. A discrepancy between measurements and simulation values is observed.

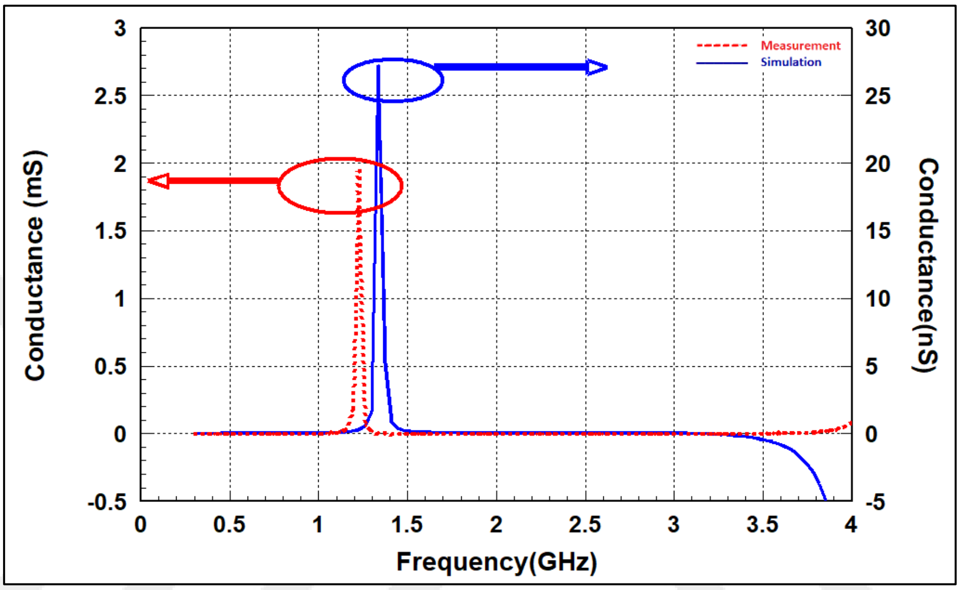

Figure 5.139. Conductance value plot for 5 cm monopole in windowless bulkhead, closed top aperture, 15 mm off-axis.

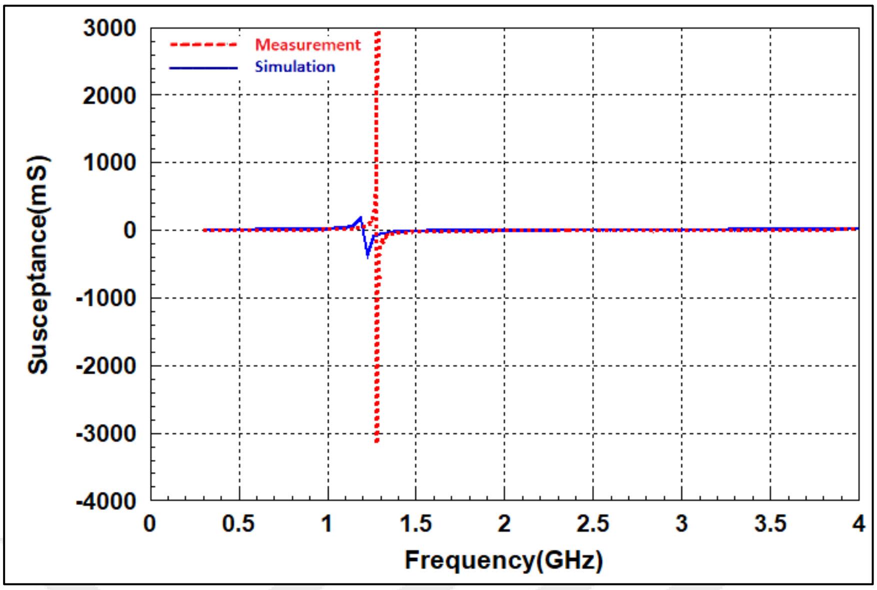

Figure 5.140. Susceptance value plot for 5 cm monopole in windowless bulkhead, closed top aperture, 15 mm off-axis.

5.2.3. Summary and Discussion of 5 cm Antenna Results

As seen in 5.2.1 and 5.2.2 there is a frequency shift between calculations from measurements and simulations. This frequency difference is seen in Table 5.9, Table 5.10, Table 5.11, Table 5.12, Table 5.13, Table 5.14, Table 5.15 and Table 5.16 below. Among all of the results best match is obtained at conductance value comparisions for axisymmetric position as 0 and 2.5 MHz deviation from simulations on average, while the rest of the measurements are mostly better than 3 cm antenna counterparts with the exception of conductance results for position 3. A high difference pattern is observed for both conductance and susceptance comparison for 15 mm off-axis position results, where the frequencies calculated from measurements are higher between 62.2 MHz minimum and 140.8 MHz maximum on average. The reason for this difference might be the probe length is too long for the bulkhead itself since probe length is 50 mm while the bulkhead length is 51.8 mm. This kind of result was predicted based on previous works [10,11].

Table 5.9. Conductance difference between measurements and simulations for 5 cm antenna at axisymmetric position (position 1)

Structure		Measurement (MHz)	Simulated (MHz)	Difference (MHz)
bulkhead with window	open top aperture	1315	1347	-32
	15 mm top aperture	1327	1368	-41
	10 mm top aperture	1344	1377	-33
	4 mm top aperture	1364	1394	-30
	closed top aperture	1305	1338	-33
	Average difference			-33.8
bulkhead without window	open top aperture	1370	1397	-27
	15 mm top aperture	1348	1379	-31
	10 mm top aperture	1333	1368	-35
	4 mm top aperture	1315	1350	-35
	closed top aperture	1304	1340	-36
	Average difference			-33.3

Table 5.10. Susceptance difference between measurements and simulations for 5 cm antenna at axisymmetric position (position 1)

Structure		Measurement (MHz)	Simulated (MHz)	Difference (MHz)
bulkhead with window	open top aperture	1416	1390	26
	15 mm top aperture	1400	1406	-6
	10 mm top aperture	1394	1342	52
	4 mm top aperture	1379	1363	16
	closed top aperture	1377	1371	6
	Average difference			18.8
bulkhead without window	open top aperture	1403	1386	17
	15 mm top aperture	1374	1404	-30
	10 mm top aperture	1357	1341	16
	4 mm top aperture	1315	1359	-44
	closed top aperture	1372	1369	3
	Average difference			-7.6

Table 5.11. Conductance difference between measurements and simulations for 5 cm antenna at 10 mm off-axis position towards window (position 2)

Structure		**Measurement (MHz)**	**Simulated (MHz)**	**Difference (MHz)**
bulkhead with window	open top aperture	1329	1329	0
	15 mm top aperture	1328	1324	4
	10 mm top aperture	1330	1331	-1
	4 mm top aperture	1361	1363	-2
	closed top aperture	1328	1329	-1
	Average difference			0.0
bulkhead without window	open top aperture	1380	1381	-1
	15 mm top aperture	1340	1349	-9
	10 mm top aperture	1341	1348	-7
	4 mm top aperture	1341	1347	-6
	closed top aperture	1342	1347	-5
	Average difference			-2.5

Table 5.12. Susceptance difference between measurements and simulations for 5 cm antenna at 10 mm off-axis position towards window (position 2)

Structure		**Measurement (MHz)**	**Simulated (MHz)**	**Difference (MHz)**
bulkhead with window	open top aperture	1375	1347	28
	15 mm top aperture	1341	1304	37
	10 mm top aperture	1334	1312	22
	4 mm top aperture	1331	1307	24
	closed top aperture	1335	1307	28
	Average difference			27.8
bulkhead without window	open top aperture	1390	1402	-12
	15 mm top aperture	1342	1360	-18
	10 mm top aperture	1339	1361	-22
	4 mm top aperture	1338	1362	-24
	closed top aperture	1337	1362	-25
	Average difference			-20.2

Table 5.13. Conductance difference between measurements and simulations for 5 cm antenna at 15 mm off-axis position towards window (position 3)

Structure		**Measurement (MHz)**	**Simulated (MHz)**	**Difference (MHz)**
bulkhead with window	open top aperture	1322	1158	164
	15 mm top aperture	1330	1157	173
	10 mm top aperture	1252	1159	93
	4 mm top aperture	1262	1160	102
	closed top aperture	1330	1158	172
	Average difference			140.8
bulkhead without window	open top aperture	1234	1217	17
	15 mm top aperture	1263	1213	50
	10 mm top aperture	1256	1212	44
	4 mm top aperture	1279	1212	67
	closed top aperture	1277	1213	64
	Average difference			98.8

Table 5.14. Susceptance difference between measurements and simulations for 5 cm antenna at 15 mm off-axis position towards window (position 3)

Structure		**Measurement (MHz)**	**Simulated (MHz)**	**Difference (MHz)**
bulkhead with window	open top aperture	1262	1179	83
	15 mm top aperture	1252	1181	71
	10 mm top aperture	1330	1183	147
	4 mm top aperture	1322	1181	141
	closed top aperture	1331	1182	149
	Average difference			118.2
bulkhead without window	open top aperture	1235	1197	38
	15 mm top aperture	1263	1200	63
	10 mm top aperture	1257	1201	56
	4 mm top aperture	1278	1201	77
	closed top aperture	1277	1200	77
	Average difference			62.2

Table 5.15. Conductance difference between measurements and simulations for 5 cm antenna at 10 mm off-axis position away from window (position 4)

Structure		**Measurement (MHz)**	**Simulated (MHz)**	**Difference (MHz)**
bulkhead with window	open top aperture	1342	1346	-4
	15 mm top aperture	1342	1344	-2
	10 mm top aperture	1346	1347	-1
	4 mm top aperture	1378	1380	-2
	closed top aperture	1342	1346	-4
	Average difference			-2.6

Table 5.16. Susceptance difference between measurements and simulations for 5 cm antenna at 10 mm off-axis position away from window (position 4)

Structure		**Measurement (MHz)**	**Simulated (MHz)**	**Difference (MHz)**
bulkhead with window	open top aperture	1378	1403	-25
	15 mm top aperture	1346	1362	-16
	10 mm top aperture	1342	1365	-23
	4 mm top aperture	1342	1363	-21
	closed top aperture	1343	1363	-20
	Average difference			-21

6. CONCLUSION

In this study, wire antennas inside missile bulkheads are simulated and measured. Mock missile structure is made up of brass. Using 2 different monopole antennas, 2 different bulkheads, 5 different nose apertures, 4 different antenna positions atotal of 70 different cases are studied. A simple deembedding of antenna pigtail cabşe is performed to extract wire antenna impedance from measurements. The conductance and susceptance values for 70 different cases are compared to simulations results, which are carried out using FEKO. Mainly, resonances of the wire antennas are studied as conductance and susceptance values largely disagree because of substractive cancellation. However, it was observed that susceptance measurements were more close to their simulated counterparts. Also 5 cm antenna measurements were more close to its simulation values only with the exception where it was too close to the edge of the bulkhead enclosure.

Once again, it is verified that simulations differ with measurements for missile-like structure with small apertures on the body. Accurate characterization of fields inside cavities with small apertures still presents a challenge for numerical solvers because of subtractive cancellation.

REFERENCES

1. Shumpert JD, Butler CM. Penetration through slots in conducting cylinders. 1. TE case. *IEEE Transactions on Antennas and Propagation.* 1998; 46(11): 1612-1621.

2. Shumpert JD, Butler CM. Penetration through slots in conducting cylinders. Part 2: TM case. *IEEE Transactions on Antennas and Propagation.* 1998; 46(11): 1622-1628.

3. Schelkunoff SA. Kirchhoof's formula, its vector analogue, and other field equivalence theorems. *Communications on Pure and Applied Mathematics.* 1951; 4(1): 43-59.

4. Schuman H, Strait B, Warren D. Aperture coupling in bodies of revolution. *Antennas and Propagation Society International Symposium*. 1976; 14: 507-510. IEEE.

5. Glisson A, Wilton D. A simple approach to the problem of coupling through azimuthally symmetric apertures in bodies of revolution. *Antennas and Propagation Society International Symposium.* 1978; 16: 215-218. IEEE.

6. Yegin K. Optimization of Wire Antennas via Genetic Algorithms and Simplified Real Frequency Technique, and Penetration through Apertures in Axi-Symmetric Structures, *Ph.D. dissertation, Clemson University*, SC, 1999.

7. Richmond J. A reaction theorem and its application to antenna impedance calculations. *IRE Transactions on Antennas and Propagation.* 1961; 9(6): 515-520.

8. de Hoop AT. Reciprocity, Discretization, and the Numerical Solution of Direct and Inverse Acoustic Radiation and Scattering Problems. *Inverse Methods in Action.* Berlin: Springer; 1990.

9. Baum CE, Kritikos HN. *Electromagnetic symmetry*. New York: CRC Press; 1995.

10. Yegin K. Application of electromagnetic reciprocity principle to the computation of signal coupling to missile-like structures. *Progress In Electromagnetics Research.* 2012; 23: 79-91.

11. Yegin K. Weak penetration and radiation through apertures in conducting bodies of revolution. *Turkish Journal of Electrical Engineering Computer Sciences*. 2009; 17(3), 231-240.

12. FEKO, Altair, [cited 2019 10 May]. Available from: https://altairhyperworks.com/product/FEKO

13. Rubin HL, Manuel JP, Cristian CB. *Computational Physics: Problem Solving with Computers*. Wiley-VCH; 2007.

APPENDIX A: MATLAB CODE FOR CONDUCTANCE AND SUSCEPTANCE TRANSFORMATION

```
load('cm3ya_t4p3admc.mat')   %loading admittance values for the
corresponding measurement
load('cm3ya_t4p3empc.mat')   %loading impedance values for the
corresponding measurement
load('S3E.mat')              %loading Shorted antenna measurements
freq=S3E(:,1);               %frequency
realS=S3E(:,2);              % Real part of the Z_short or Z_o depending
on the notation
imgS=S3E(:,3);               % Imaginary part of Z_short or Z_o depending
on the notation
realA=cm3ya_t4p3empc(:,2);   % Real part of Z_antenna
imgA=cm3ya_t4p3empc(:,3);    % Imaginary part of Z_antenna
Zat=[(realA-50)+imgA*1i];    % Numerator of Zat gamma= (zant-
Zo)/(zant+Zo) equation written in complex form for calculations  (t
denotes top)
Zab=[(realA+50)+imgA*1i];    % Denumerator of Zab gamma= (zant-
Zo)/(zant+Zo) equation written in complex form for calculations( b
denotes bottom)
Zst=[(realS-50)+imgS*1i];    % Numerator of Zst  gamma_short= (z_short-
Zo)/(Z_short+Zo)equation written in complex form for calculations  (t
denotes top)
Zsb=[(realS+50)+imgS*1i];    % Denumerator of Zst  gamma_short= (z_short-
Zo)/(Z_short+Zo)equation written in complex form for calculations( b
denotes bottom)
ZatM=abs(Zat);               % Magnitude of Zat, to divide the values
easier changed the complex Zat to phasor domain.
ZatP=angle(Zat);             % Angle of Zat,to divide the values easier
changed the complex Zat to phasor domain.
ZabM=abs(Zab);               % Magnitude of Zab, to divide the values
easier changed the complex Zat to phasor domain.
ZabP=angle(Zab);             % Angle of Zat,to divide the values easier
changed the complex Zat to phasor domain.
GA_M=ZatM./ZabM;             % Magnitude of Gamma_antenna
GA_P=(ZatP-ZabP);            % Phase of Gamma_antenna
GA_R=GA_M.*cos(GA_P);        % Real part of Gamma_antenna, Changing
Gamma_antenna from phasor domain to complex domain
GA_I=GA_M.*sin(GA_P);        % Imaginary part of Gamma_antenna, Changing
Gamma_antenna from phasor domain to complex domain
ZstM=abs(Zst);               % Magnitude of Zst, to divide the values
easier changed the complex Zat to phasor domain.
ZstP=angle(Zst);             % Angle of Zst,to divide the values easier
changed the complex Zat to phasor domain.
ZsbM=abs(Zsb);               % Magnitude of Zsb, to divide the values
easier changed the complex Zat to phasor domain.
ZsbP=angle(Zsb);             % Angle of Zsb,to divide the values easier
changed the complex Zat to phasor domain.
GS_M=ZstM./ZsbM;             % Magnitude of Gamma_short
GS_P=(ZstP-ZsbP);            % Phase of Gamma_short
GS_R=GS_M.*cos(GS_P);        % phasör  domainden  complex hale
dönüþtürdüm
GS_I=GS_M.*sin(GS_P);        % phasör  domainden  complex hale
dönüþtürdüm
```

```
YantT=((GS_R+GA_R)+(GS_I+GA_I)*1i); % numerator of Yant = Yo *
(Gamma_Short +Gamma_Antenna)/(Gamma_Short-Gamma_Antenna)
YantB=((GS_R-GA_R)+(GS_I-GA_I)*1i);% denumerator of Yant = Yo *
(Gamma_Short +Gamma_Antenna)/(Gamma_Short-Gamma_Antenna)
YantT_M=(abs(YantT));         % Magnitude of YantT, to divide the values
easier changed the complex Zat to phasor domain.
YantT_P=(angle(YantT));       % Angle of of YantT, to divide the values
easier changed the complex Zat to phasor domain.
YantB_M=(abs(YantB));         % Magnitude of YantB, to divide the values
easier changed the complex Zat to phasor domain.
YantB_P=(angle(YantB));       % Angle of of YantB, to divide the values
easier changed the complex Zat to phasor domain.
YF_M=((YantT_M./YantB_M)*0.02); % Magnitude of Y_ant
YF_P=(YantT_P-YantB_P);       % Phase of Y_ant
YA_R=YF_M.*cos(YF_P);         % Real part of Y_ant
YA_I=YF_M.*sin(YF_P);         % Imaginary Part of Y_ant
adm_R=cm3ya_t4p3admc(:,2);    % real part of admittance of corresponding
measurement
adm_I=cm3ya_t4p3admc(:,3);    % imaginary part of admittance of
corresponding measurement
subplot(1,2,1)
plot(freq,adm_R, 'g');        % Conductance value plot of direct
measurement
hold on
plot(freq,YA_R, 'r');         % Conductance value plot of calculated
transformed value
xlabel('frequency  , r is YA, g is meas');
ylabel('Admittance Real ');
subplot(1,2,2)
plot(freq,adm_I,'c');         % Susceptance value plot of direct
measurement
hold on
plot(freq,YA_I,'m');          % Susceptance value plot of calculated
transformed value
xlabel('frequency  , magenta is YA, cyan is meas');
ylabel('Admittance Img');
M3yata4_p3i=[freq YA_I];
save M3yata4_p3i.dat M3yata4_p3i -ascii % saving files for later to use
with Stanford Graphics
```